博士学位論文

Study on elucidation of the roundness improvement mechanism of the inner surface of a tube by magnetic abrasive finishing process

磁気研磨法による円管内面の真円度改善メカニズム解明に関する研究

劉　江楠

2023 年 2 月

Contents

Chapter I Introduction

1.1 Research background

Recently, advanced cleaning technologies are required in various fields such as semiconductor related industries, nuclear related industries, and aircraft related industries, and it is especially important that the surface finishing of high purity fluid storage bombs and transportation piping systems. When the internal surface roughness value is large, contaminants are deposited on the internal surface, and causes corrosion and damage. Nuclear related industries will result in a catastrophe called radioactive leakage. Therefore, the high precision internal surface of the container and piping system is required to prevent contamination and deposition of contaminants.

The magnetic field-assisted finishing process has been proposed for finishing high precision internal surfaces that are difficult to finish with ordinary tools and labor [101–104]. Utilizing the penetrability of magnetic field lines, the application of magnetic force has great advantages for the finishing of internal surfaces. Therefore, there have been many studies on the internal surface finishing process using the finishing force generated by magnetic field. Shinmura et al. developed an internal finishing process based on the application of magnetic abrasive finishing, and it was confirmed that this process is applicable to the internal finishing of the bottom of a clean gas bomb with a narrow opening which is hard to finish by the conventional finishing process [105]. In addition, Shinmura et al. developed an internal magnetic abrasive finishing process for nonferromagnetic complex-shaped tubes consisting of bent and straight sections and achieved the nearly uniform internal finishing of bent tubes

by a single processing iteration Development of an internal magnetic abrasive finishing process for nonferromagnetic complex shaped tubes [106]. Yamaguchi et al. proposed the magnetic abrasive finishing process using multiple pole tip systems to finish the entire internal surface of capillary tubes and a method to define a pole tip feed length that can achieve a uniform surface roughness on the entire target surface by calculating the pole-tip coverage time over the target surface. Moreover, they clarified the finishing characteristic and mechanism and showed the effects of the tool's magnetic properties on the tool and abrasive motion and the interior finishing characteristic of capillary tubes [107,108]. Jain et al. developed a precision finishing process for complex internal geometries using a smart magnetorheological polishing fluid and discussed the process performance in terms of surface roughness reduction, concluding that the reduction in surface roughness value increases with an increase in the current (A) and the number of finishing cycles [109–111]. Kim et al. developed an internal polishing system using magnetic force for the production of ultra clean tubes with average surface roughness ranging from 0.02 μm to 0.05 μm or less and the application of magnetic abrasives composed of WC/Co powder. They concluded that for highly efficient machining, large size particles #90 are appropriate because the magnetic abrasives must be attracted sufficiently by the magnetic force. Furthermore, the supplied amount of magnetic abrasives was a very important variable for the improvement of surface roughness [112]. In addition, the stochastic approach to experimental analysis of the cylindrical lapping process was studied and it was concluded that lapping pressure has a significant effect on the efficiency of cylindrical lapping [113]. Wang et al. studied a high-precision polishing method for magnetic gel abrasive finishing and developed a rotating cylinder based magnetic finishing setup to allow the gel abrasive and workpieces to tumble and rotate together during the

polishing process to finish the internal surface of the stainless tubes [114,115]. Zou et al. developed an internal magnetic abrasive finishing process using a magnetic machining tool to improve the roughness and the roundness of the internal surface of a thick tube [116]. They also developed a new internal finishing process for tubes which is the magnetic abrasive finishing process combined with electrochemical machining [117]. In other respects, regarding the abrasive machining, Pereira et al. studied the super abrasive machining of integral rotary components using grinding flank tools and concluded that super abrasive machining implies a suitable, controllable, and predictable process for improving the manufacture of aeronautical critical components, such as Integrally Bladed Rotors [118]. The authors studied the isotropic finishing of untampered iron casting cylindrical parts by roller burnishing and concluded that the technique greatly improves surface roughness and eliminates the kinematic driven roughness pattern of turning, leading to a more isotropic finishing [119].

1.2 Research purpose

Magnetic abrasive finishing process is a finishing technology that uses the magnetic force generated by magnetic particles [120,121]. For the inner surface finishing such as the bomb for the gas storage, the entrance is narrow, the insertion of the usual polishing tool is difficult resulting the precision finishing is not allowed, and the magnetic abrasive finishing process is considered to be effective. In other words, the magnetic abrasives can be easily supplied to the inside of the container, and the finishing pressure of the magnetic particles can be easily generated by permanent magnets installed outside the container, and the relative motion necessary for the processing is given by the container and the permanent magnets rotate opposite to each other, so it is realized that the internal

surface of the container can be finished.

Initially, the precision machining of an inner surface occurs by magnetic abrasive finishing process, which relies on the magnetic force generated by magnetic particles put inside the tube and magnetic poles outside, two-dimensional schematic as shown in Fig.1.1. It has been proven that this process is effective for finishing the tubes with a thickness less than 5 mm [122]. However, when the thickness of the tube increases, the magnetic force (finishing force) is also weakened, which makes it impossible to process. In order to solve this problem, the process of magnetic abrasive finishing using a magnetic machining tool was proposed [123], two-dimensional schematic as shown in Fig.1.2. In this process, the magnetic force (finishing force) can be enhanced by placing a magnetic machining tool inside the tube, which consists of four permanent magnets (Nd-Fe-B magnet) and a yoke, and it is dozens of times higher than the process using magnetic particles. It has been proved that this process is effective for finishing the inner surface of the tubes with a thickness from 5 mm to 30 mm. And it has been concluded that this process can improve roundness while improving roughness [124]. However, the mechanism of improving the roundness is unclear, so it is necessary to study it theoretically. Therefore, this research mainly studies the mechanism of roundness improvement and clarifies the factors influencing the roundness improvement of inner surfaces.

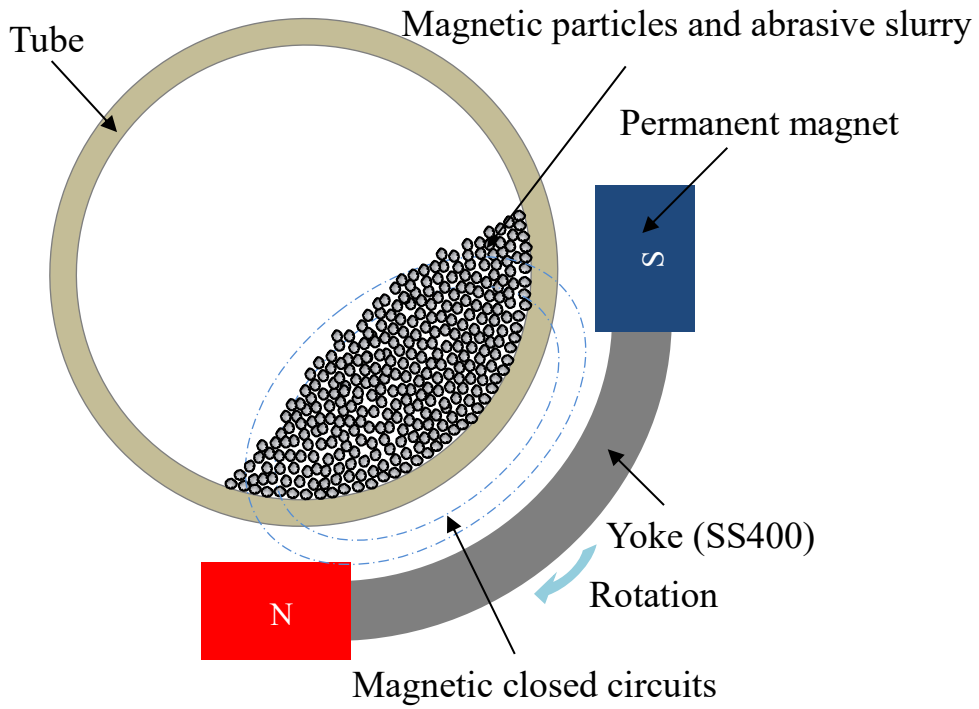

Fig.1.1 Two-dimensional schematic of internal magnetic abrasive finishing process using magnetic abrasives

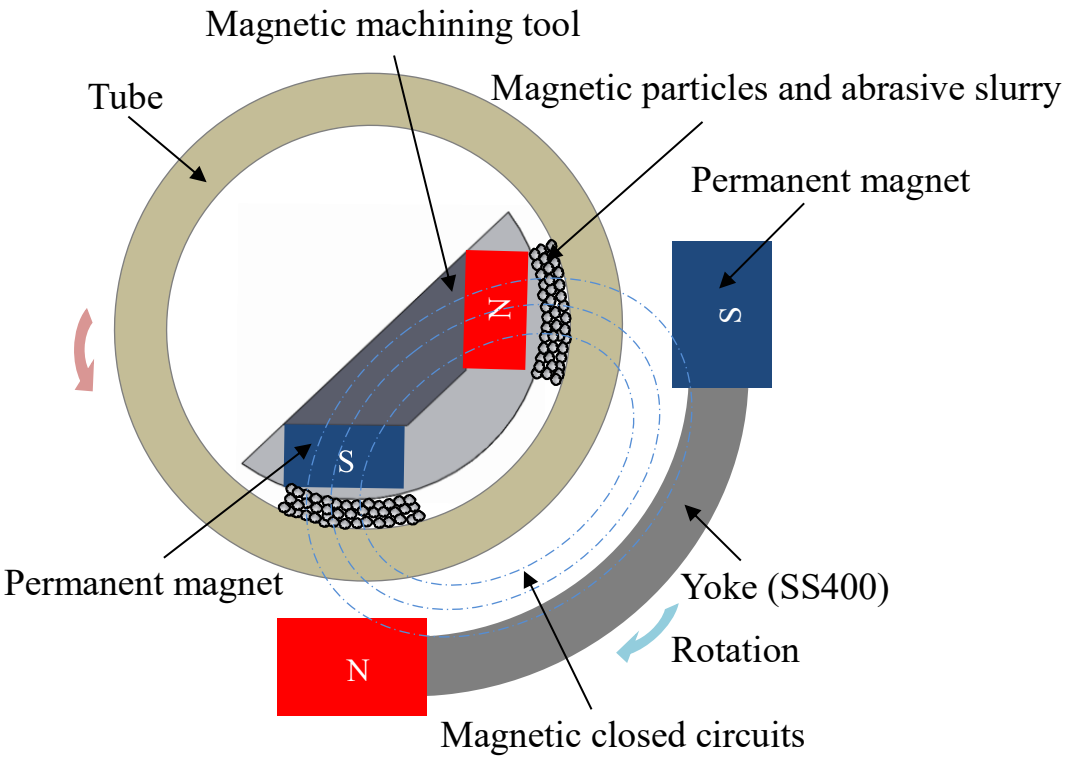

Fig.1.2 Two-dimensional schematic of internal magnetic abrasive finishing process using magnetic machining tool

1.3 Overview of thesis

This thesis studies the mechanism of roundness improvement by internal magnetic abrasive finishing. The overview of each chapter of the thesis is as follows:

In chapter 1, the research background and some research on internal magnetic abrasive finishing process are introduced. In addition, the research purpose of this thesis is explained and the content of each chapter is summarized.

In chapter 2, the processing principle and experimental setup of the internal magnetic abrasive finishing using magnetic machining tool are explained. Moreover, in order to clarify the force that affects the roundness improvement, the finishing force is analyzed. In addition, in this process, the magnetic machining tool also rotates in the opposite direction to the workpiece, so its force is analyzed.

In chapter 3, mainly studies the roundness improvement theoretically and discusses the factors influencing the roundness improvement of internal surfaces. Firstly, the roundness curve expression is derived using the principle of roundness measurement by the assumed center method, and the expression of roundness curve expanded by the Fourier series was obtained. Secondly, the process of roundness change is analyzed, and then the factors influencing the roundness improvement are discussed. Finally, the experiments were carried out on SUS304 stainless steel tube and by setting the distance between the magnetic machining tool and the magnetic pole of finishing unit, the thickness of the tube is equivalent to 10 mm, 20 mm and 30 mm, respectively.

In chapter 4, mainly discussing the influence of finishing characteristics on internal surface roundness improvement. Firstly, the roundness improvement of the inner surface of SUS304 stainless steel tube with the

thickness more than 5 mm was discussed through the dynamic and trajectory analysis. Because the roundness improvement is related to the material removal, and the material removal is related to the finishing force during finishing. The finishing characteristics affecting the internal roundness improvement is investigated by discussing the reciprocating velocity of magnetic pole unit. Secondly, in order to discuss the influence of different structures of magnetic particles on roundness improvement, comparative experiments were carried out. Each experiment carried out five stages of processing, and in the first-stage, two different kinds of magnetic particles were used, the electrolytic iron particles (1680 μm in mean dia.) and the KMX magnetic particles (1000 ~ 1680 μm in mean dia.) respectively. Furthermore, in order to further clarify the influence of finishing characteristics on roundness improvement in this process, due to the magnetic machining tool and tube rotate in opposite directions, so discussing the influence of rotational speed of the magnetic machining tool by analyzing the finishing force and the influence of rotational speed of the workpiece on roundness improvement. And the influence of rotational speed is discussed comprehensively.

In chapter 5, according to the distribution of magnetic force lines, the magnetic machining tool is divided into three areas, which are left area, middle area and right area, and the magnetic particles on the left area and right area of the magnetic machining tool form magnetic brushes in the direction of the magnetic force line before finishing. And after finishing, the pressure exerted by some magnetic particles on the magnetic force of the magnetic machining tool and the magnetic pole unit forms a fixed magnetic brush, so mainly discusses the influence of the circumferential length of fixed magnetic brush on roundness improvement.

In chapter 6, investigating the industrial applicability of the inner surface

magnetic abrasive finishing process using a magnetic machining tool, and conducted detailed verification experiments. By adjusting the distance between the magnetic processing tool and the permanent magnet of the magnetic pole unit, the SUS304 stainless steel tube with a thickness of 10mm was used as the workpiece. Rough machining, semi-precision finishing, and precision finishing process were performed by selecting the size of the magnetic particles and abrasive particles, and the initial surface roughness of Ra 4.9 μm can be finished to a mirror surface of Ra 0.01 μm. And the roundness can be improved from 206 μm to 13 μm. It is hope for industrial application by this process.

In chapter 7, the main conclusions of this study are summarized.

Chapter II Processing principle and experimental setup

2.1 Processing principle

Fig.2.1 shows a schematic of the internal magnetic abrasive finishing process using a magnetic machining tool. Fig.2.2 shows the structure of magnetic machining tool. The magnetic machining tool is composed of two pairs of permanent magnets and a yoke and wrapped with epoxy putty to conform to the shape of the tube's internal surface. Furthermore, in order to prevent a collision, the magnetic machining tool is wrapped with non-woven fabric during processing. The magnetic particles are magnetically attracted to the surface of the magnetic machining tool. The magnetic machining tool inside the tube is attracted by the permanent magnets outside the tube, forming magnetic closed circuits that generating high magnetic force as a finishing force. When the magnetic machining tool rotates with the rotation of the permanent magnets, this results in relative movement between the workpiece and the magnetic particles. In order to achieve a high-quality surface, abrasive slurry that mixing with abrasive particles and water-soluble abrasive solution in a certain proportion is used. Therefore, the relative movement is indirectly transferred from the magnetic particles to the abrasive particles. Moreover, when the permanent magnets outside the tube are driven in the direction of the tube axis while rotating, that the high precision finishing of the entire internal surface of the tube can be achieved.

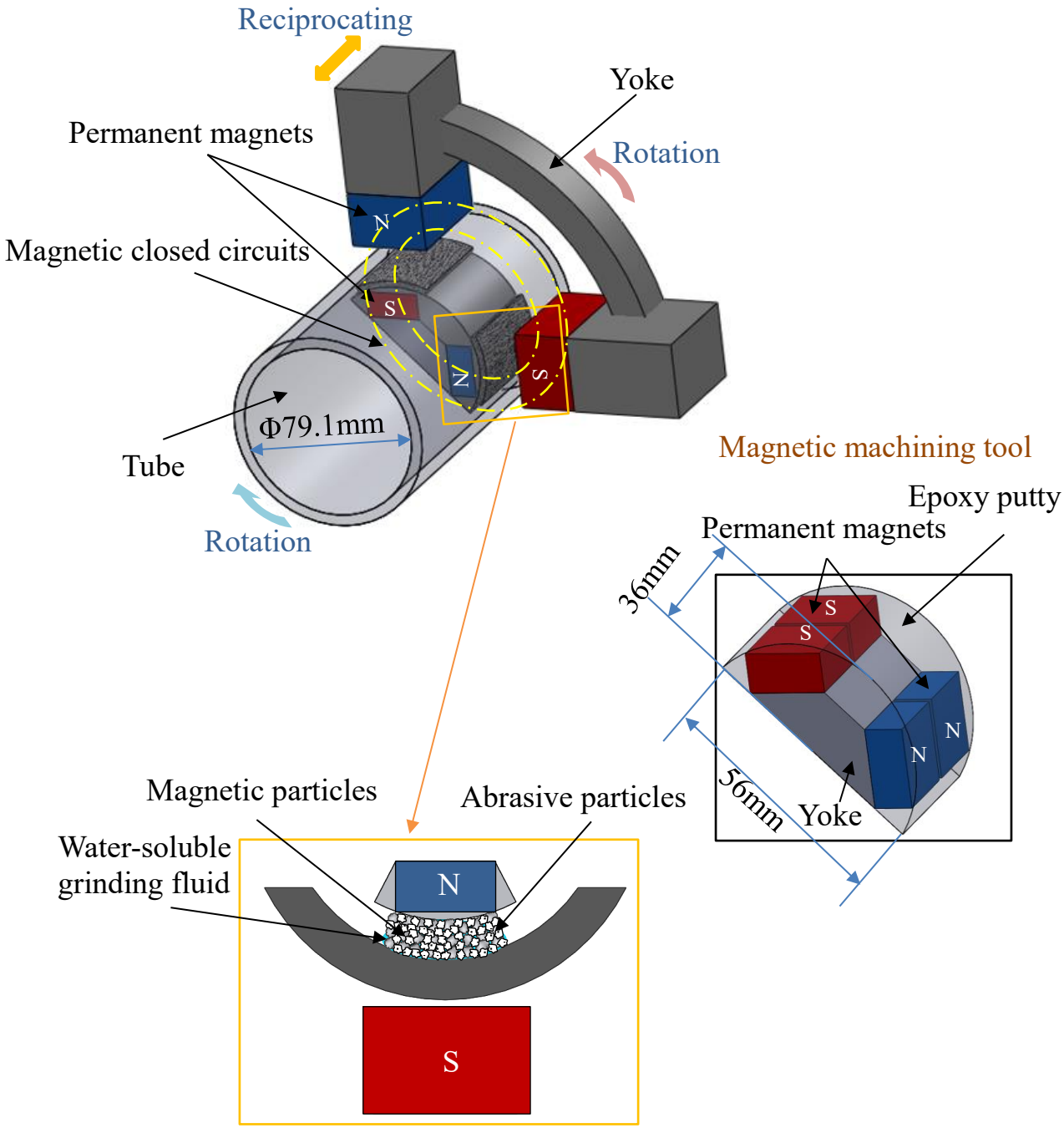

Fig.2.1 Schematic of the internal magnetic abrasive finishing process using magnetic machining tool

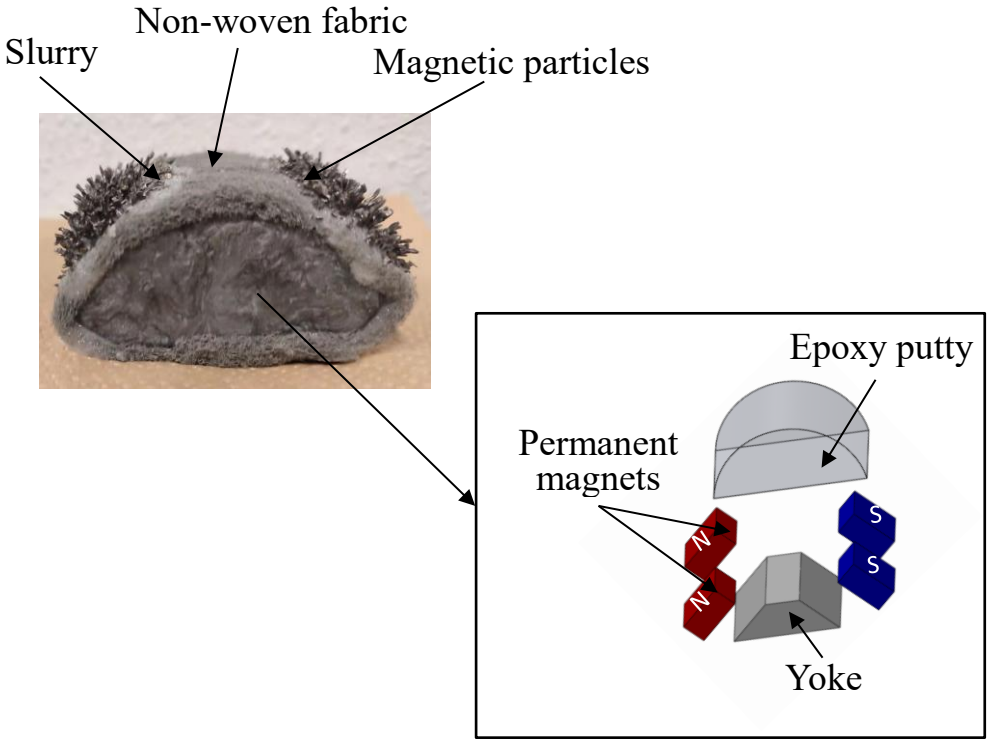

Fig.2.2 Structure of the magnetic machining tool

This process is realized by the magnetic particles attracted by the magnetic force on the surface of the magnetic machining tool, so the magnetic machining tool and the magnetic particles are regarded as a whole for force analysis. In addition, the magnetic machining tool and the magnetic poles outside the tube also generate magnetic attraction force. Fig.2.3 shows the force analysis model diagram of the magnetic machining tool. $\boldsymbol{F}_y$ is the magnetic attraction force generated by the magnetic machining tool and the permanent magnetics outside the tube. $\boldsymbol{F}_x$ is the magnetic force generated by the magnetic machining tool and permanent magnetics outside the tube in the direction of the equipotential line. $\boldsymbol{F}_c$ is the centrifugal force generated by the rotation of the magnetic machining tool. G is the gravity including the gravity of magnetic machining tool and

magnetic particles. F_f is the frictional resistance.

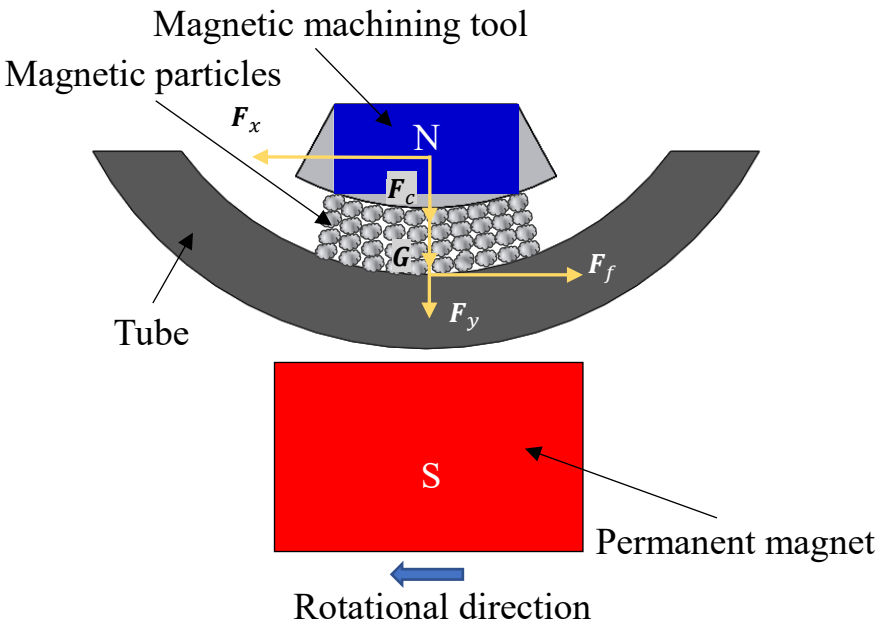

Fig.2.3 Force analysis model diagram of the magnetic machining tool

2.2 Experimental setup

Fig.2.4 shows an external view of the experimental setup for the internal magnetic abrasive finishing process using the magnetic machining tool. SUS304 stainless steel tube, as a workpiece, is clamped in the chuck and the other side is fixed with the tailstock and the top. The finishing unit, consisting of four ferrite permanent magnets (50 × 35 × 26 mm) attached inside a yoke, is set up on the reciprocating table. The permanent magnets are arranged N-S-S-N at a 90° interval toward the tube center, and the magnets' distribution is flexible for various tube diameters. An adequate finishing force can be obtained because of the placement of the magnetic machining tool inside the tube. Moreover, the finishing unit can be driven in the direction of the tube axis during rotation. At the same time, the workpiece also rotated to generate relative movement and then realize the finishing of the internal surface of the tube.

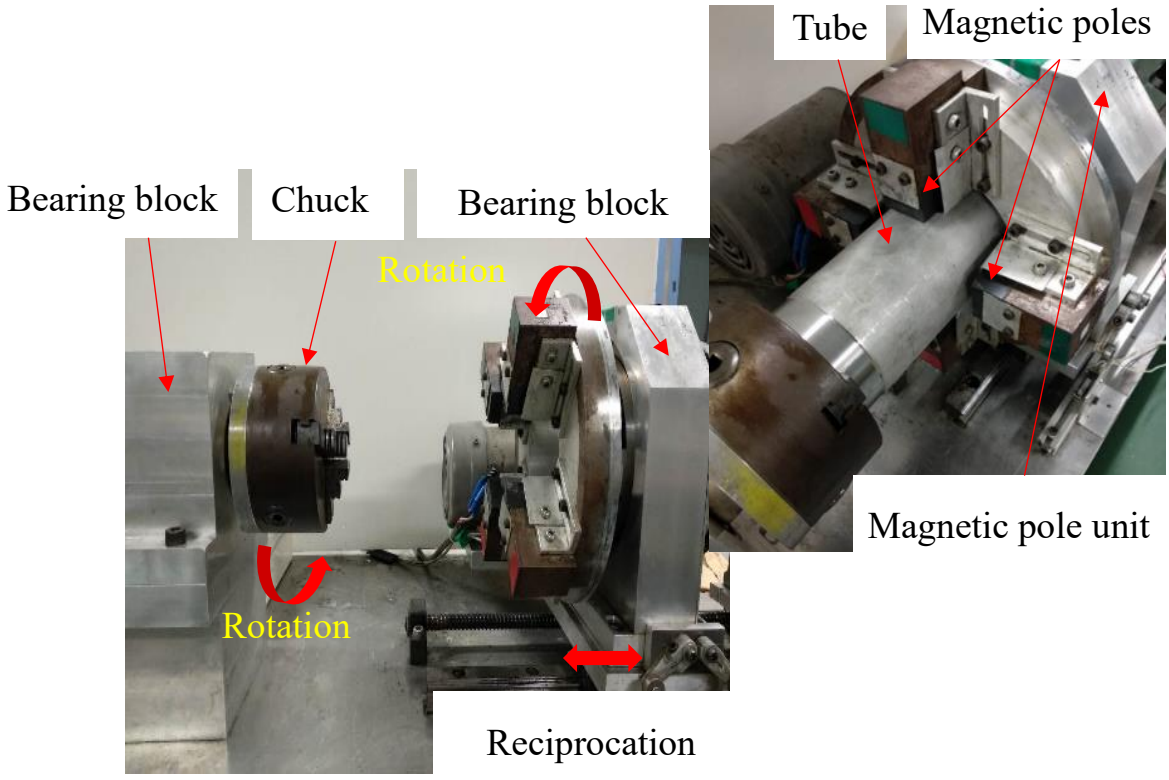

Fig.2.4 External view of the experimental setup

2.3 Finishing force analysis

In the process of internal magnetic abrasive finishing using magnetic machining tool, the magnetic force generated by two sources acts together to realize the finishing process. One is that magnetic particles are attracted to the surface of the magnetic machining tool through magnetic force, and the other is that the magnetic machining tool is magnetically attracted by the magnets of the magnetic pole unit, exerting pressure on the magnetic machining tool in the normal direction, and then exerting pressure on the magnetic particles. Therefore, the using of the magnetic machining tool can not only enhance the finishing force, but also prevent the scattering of magnetic particles, resulting in a sufficient number of abrasive particles for

finishing. Fig.2.5 shows a diagram of finishing force analysis. This process is a finishing process in which the workpiece is removed in the form of micro-chips with the resultant force of finishing force $\boldsymbol{F}$ to overcome the finishing resistance. And through the three actions that rotation and reciprocating motion of magnetic machining tool, and rotation of the workpiece, resulting in relative motion between the magnetic machining tool and the workpiece, and then generating the finishing force to overcome the finishing resistance. The components of finishing force in x, y and z directions are the normal component of finishing force $\boldsymbol{F}_n$, the tangential component of finishing force $\boldsymbol{F}_t$ and the axial component of finishing force $\boldsymbol{F}_a$ respectively. Furthermore, it is considered that the resultant force $\boldsymbol{F}_{xy}$ is a force related to the roundness improvement and the resultant force $\boldsymbol{F}_{xz}$ is a force related to the roughness improvement, as shown in Equation (2.1) and Equation (2.2).

$$F_{xy} = \sqrt{F_n^2 + F_t^2} \tag{2.1}$$

$$F_{xz} = \sqrt{F_n^2 + F_a^2} \tag{2.2}$$

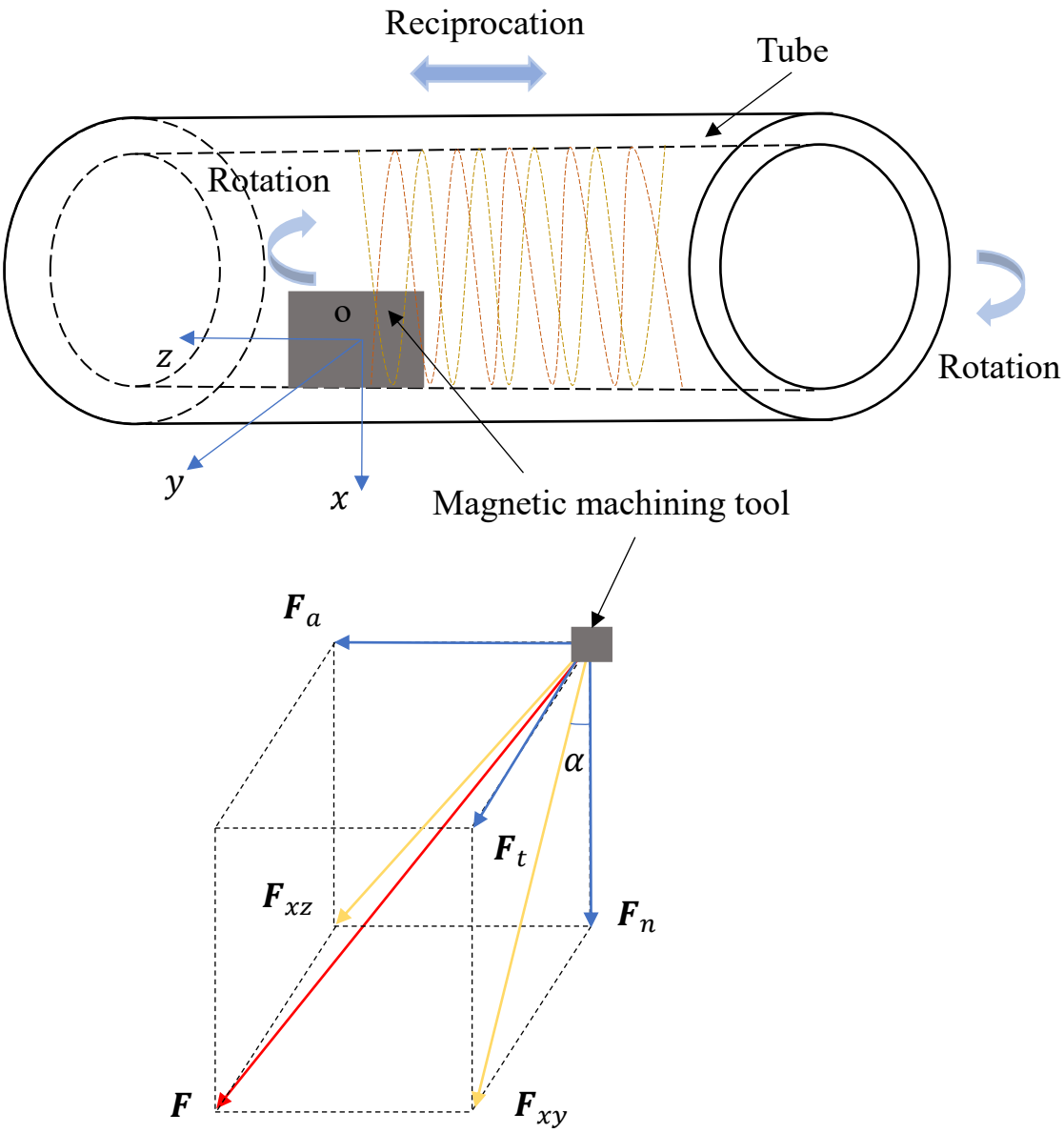

Fig.2.5 Diagram of finishing force analysis

2.4 Conclusions

In this chapter, the processing principle and experimental setup of the internal magnetic abrasive finishing using magnetic machining tool are explained. Moreover, in order to clarify the force that affects the roundness improvement, the finishing force is analyzed. In addition, in this process,

in order to enhance the magnetic force (finishing force), a magnetic machining tool was placed on the internal surface of the tube, so its force is analyzed. The main content can be summarized as follows.

1. The processing principle and experimental setup of the internal magnetic abrasive finishing using magnetic machining tool are introduced.

2. This process is a finishing process in which the workpiece is removed in the form of micro-chips with the resultant force of finishing force to overcome the finishing resistance. It is necessary to understand the composition of the finishing force, so the finishing force analysis is carried out.

Chapter III Investigation on roundness improvement theoretically

3.1 Introduction

The former internal magnetic abrasive method uses magnetic particles to generate finishing force. It has been proven that this process is effective for finishing the tubes with a thickness less than 5 mm [301]. However, when the thickness of the tube increases, the magnetic force (finishing force) is also weakened, which makes it impossible to process. In order to solve this problem, the process of magnetic abrasive finishing using a magnetic machining tool was proposed [302]. And it has been concluded that this process can improve roundness while improving roughness [303]. However, the mechanism of improving the roundness is not clear, so it is necessary to study it theoretically. Therefore, this chapter mainly studies the mechanism of roundness improvement and clarifies the factors influencing the roundness improvement of internal surfaces. Firstly, the roundness curve expression was derived using the principle of roundness measurement by the assumed center method, and the expression of roundness curve expanded by the Fourier series was obtained. Secondly, the process of roundness change was analyzed, and then the factors influencing the roundness improvement were discussed. Finally, the thickness of the tube was adjusted to 10 mm, 20 mm, and 30 mm, respectively, and then experiments on a SUS304 stainless steel tube were carried out.

3.2 Fourier series expression of roundness curve

In this research, the roundness curve expression was derived using the principle of roundness measurement by the assumed center method [304]. Fig.3.1 shows the schematic of the internal surface roundness measurement by the assumed center method. Point o is the assumed center, that is, the center of rotation during measurement and the detector is in contact with the internal surface of the tube. Vibration values of various angles are obtained during rotation, resulting in the roundness value including the influence of eccentricity. As shown in Fig.3.1 (a), θ is the angle of rotation, and $r(\theta)$ is the variable about angle θ. M is the roundness curve. Relative to the reference circle, the vibration value of each angle is positive when it is inside the reference circle and negative when it is outside. In the case of measuring the roundness of the reference circle, as shown in Fig.3.1 (b), the eccentricity between the center o' and the measuring center o is c_1, angle φ_1 is the phase, the radius of the reference circle is a_0, and the radius variable $r'(\theta)$ is expressed as:

$$r'(\theta) = a_0 - c_1\cos(\theta + \varphi_1) \tag{3.1}$$

Setting the position when the indicator value y_c of the detector is 0 as B-B, the distance to the measuring center is expressed by E. Then, the pointer reading $\mathrm{y_c}(\theta)$ about angle θ was described by the cosine curve can be obtained by:

$$\mathrm{y}_c(\theta) = \mathrm{E} - r'(\theta) = (\mathrm{E} - a_0) + c_1\cos(\theta + \varphi_1) \tag{3.2}$$

Moreover, as shown in Fig.3.1 (a), r(θ) is a periodic function with a period of 2π and the Fourier series expansion is given by:

$$\begin{aligned} \mathrm{r}(\theta) &= a_0 + a_1\cos\theta + a_2\cos 2\theta + a_3\cos 3\theta + \cdots\cdots + a_n\cos n\theta + \cdots\cdots \\ &\quad + b_1\sin\theta + b_2\sin 2\theta + b_3\sin 3\theta + \cdots\cdots + b_n\sin n\theta + \cdots\cdots \\ &= a_0 + c_1\cos(\theta+\varphi_1) + c_2\cos(2\theta+\varphi_2) + \cdots \\ &\quad + c_n\cos(n\theta+\varphi_n) + \cdots \end{aligned} \tag{3.3}$$

where, a_n and b_n are constants.

Then, the value y for the detector is expressed as:

$$\mathrm{y}(\theta) = \mathrm{E} - \mathrm{r}(\theta) = (\mathrm{E} - a_0) - c_1\cos(\theta+\varphi_1) - \sum_{n=2}^{\infty} c_n\cos(n\theta+\varphi_n) \tag{3.4}$$

Comparing Equation (3.2) with Equation (3.4), the first term $(\mathrm{E} - a_0)$ on the right is a constant which represents the size of the reference circle. The second term is the eccentricity of the assumed center from the reference circle.

Substituting Equation (3.3) into Equation (3.4) to obtain indicated value $\mathrm{y}(\theta)$ is achieved by:

$$\begin{aligned} \mathrm{y}(\theta) = (\mathrm{E} - a_0) - a_1\cos\theta - (a_2\cos 2\theta + \cdots\cdots + a_n\cos n\theta + \cdots\cdots) \\ - b_1\sin\theta - (b_2\sin 2\theta + \cdots\cdots + b_n\sin n\theta + \cdots\cdots) \end{aligned} \tag{3.5}$$

where $(\mathrm{E} - a_0)$ is a constant, $(a_1\cos\theta + b_1\sin\theta)$ is the eccentricity of the assumed center from the reference circle, and $(a_2\cos 2\theta + b_2\sin 2\theta + \cdots\cdots + a_n\cos n\theta + b_n\sin n\theta + \cdots\cdots)$ is the expression of roundness. Therefore, the roundness expression expanded by Fourier series is obtained by:

$$R(\theta) = a_2 \cos 2\theta + b_2 \sin 2\theta + \cdots\cdots + a_n \cos n\theta + b_n \sin n\theta + \cdots\cdots$$

$$= \sum_{n=2}^{\infty} c_n \cos(n\theta + \varphi_n) \tag{3.6}$$

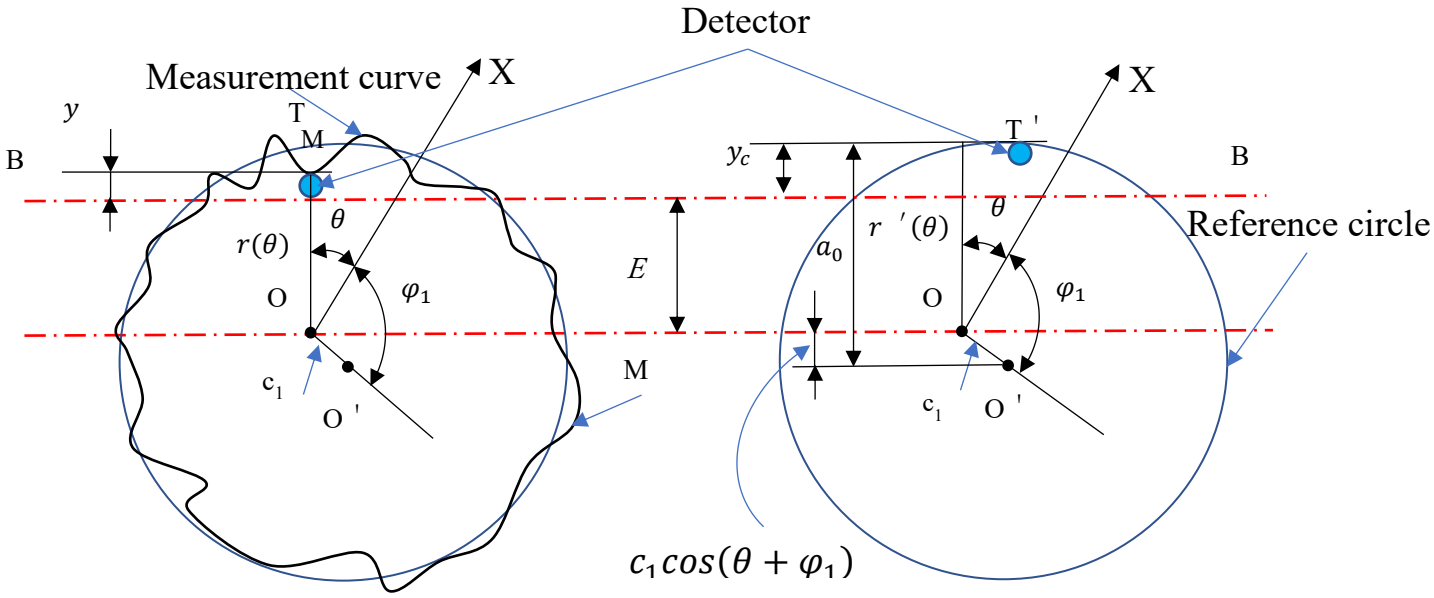

(a) By the measured roundness curve (b) By the reference circle

Fig.3.1 Schematic of internal surface roundness measurement by the assumed center method

3.3 The changing process of roundness improvement

In this study, we mainly consider the roundness to be changed by the finishing force and eccentricity during clamping. As shown in Fig.3.2, the roundness curve and the vibration curve caused by the eccentricity of the internal surface of the tube are $\Delta R_0(\theta)$ and $\Delta S_0(\theta)$, respectively, and given by [305,306]:

$$\left.\begin{aligned} \Delta R_0(\theta) &= \sum_{n=2}^{\infty} A_n \cos(n\theta + \varphi_n) \\ \Delta S_0(\theta) &= \sum_{m=1}^{\infty} B_m \cos(m\theta + \beta_m) + \Delta S(\theta) \end{aligned}\right\} \quad (3.7)$$

where A_n and B_m are amplitude, φ_n and β_m are phase angle, $\Delta S_0(\theta)$ is the random variation of the rotation axis, and θ is the angle of rotation.

The sum of Equation (3.7) plus the eccentricity $A_1 \cos(\theta + \varphi_1)$ when the tube is clamped, A_1 is amplitude, and φ_1 is the phase angle, the vibration amount $\varepsilon(\theta)$ of the internal surface of the tube can be expressed as:

$$\varepsilon(\theta) = \sum_{n=2}^{\infty} A_n \cos(n\theta + \varphi_n) + A_1 \cos(\theta + \varphi_1) + \sum_{m=1}^{\infty} B_m \cos(m\theta + \beta_m) + \Delta S(\theta) \quad (3.8)$$

Moreover, the vibration removal $\varepsilon_w(\theta)$ after processing at point Q on the internal surface of the tube is given by:

$$\varepsilon_w(\theta) = C_m[K\varepsilon(\theta) + P] \quad (3.9)$$

The value of $\varepsilon_w(\theta)$ is positive on the inside of the tube and negative on the outside. When P is the standard setting of finishing force, K is the proportional coefficient between the finishing force and the change of roundness in internal surface of the tube, and C_m is the processing quantity coefficient (which is related to the type and size of magnetic particles and

abrasive materials, the presence and type of abrasive fluid, and the material of the workpiece, etc.).

When the tube and the magnetic machining tool relative rotate one circle, the change in the internal surface is calculated by:

$$\varepsilon(\varphi + 2\pi) = \varepsilon(\varphi) - C_m K\varepsilon(\varphi) = (1 - C_m K)\varepsilon(\varphi) \quad (0 \le \varphi \le 2\pi) \tag{3.10}$$

Then, the roundness curve $\Delta R_N(\theta)(\theta = \varphi + 2N\pi)$ after N turns is given by:

$$\begin{aligned} \Delta R_N(\theta) &= \Delta R_N(\varphi + 2N\pi) \\ &= \Delta R_N(\varphi) \\ &= \Delta R_{N-1}(\varphi) - C_m[K\,\varepsilon\{\varphi + 2(N-1)\pi\} + P] + L_N \end{aligned} \tag{3.11}$$

where L_N is the correction value of the reference circle (zero value) and $N = 1, 2, 3, \cdots\cdots$ The roundness $\Delta R_N(\varphi)$ after N rotations is obtained by arranging the left and right sides of the above Equation in the form:

$$\Delta R_N(\varphi) = \Delta R_0(\varphi) - C_m K \sum_{i=1}^{N} \varepsilon[\varphi + 2(i-1)\pi] - C_m\, N\, P + \sum_{i=1}^{N} L_i \tag{3.12}$$

where $C_m\, N\, P$ and $\sum_{i=1}^{N} L_i$ are the reference circle position of the specified roundness curve, which has no direct relationship with roundness, so the roundness curve $\Delta R_N(\varphi)$ can be calculated thus:

$$\Delta R_N(\varphi) = \Delta R_0(\varphi) - C_m K \sum_{i=1}^{N} \varepsilon[\varphi + 2(i-1)\pi] \tag{3.13}$$

Moreover, substituting Equation (3.8) into Equation (3.13) to obtain the roundness $\Delta R_N(\varphi)$ is expressed as:

$$\Delta R_N(\varphi) = (1 - C_m K)^N \sum_{n=2}^{\infty} A_n \cos(n\varphi + \varphi_n) - C_m K \sum_{i=0}^{N-1} (1 - C_m K)^{N-i-1} \left[A_1 \cos(\varphi + \varphi_1) + \sum_{m=1}^{\infty} B_m \cos(m\varphi + \beta_m) + \Delta S(\varphi + 2i\pi) \right] \quad (3.14)$$

As shown in Equation (3.14), the first item is the influence of the roundness curve before finishing, the second term concerns the influence of eccentricity during clamping, the third term is the influence of periodic variations due to eccentricity, and the fourth term is the effect of the randomness of eccentricity.

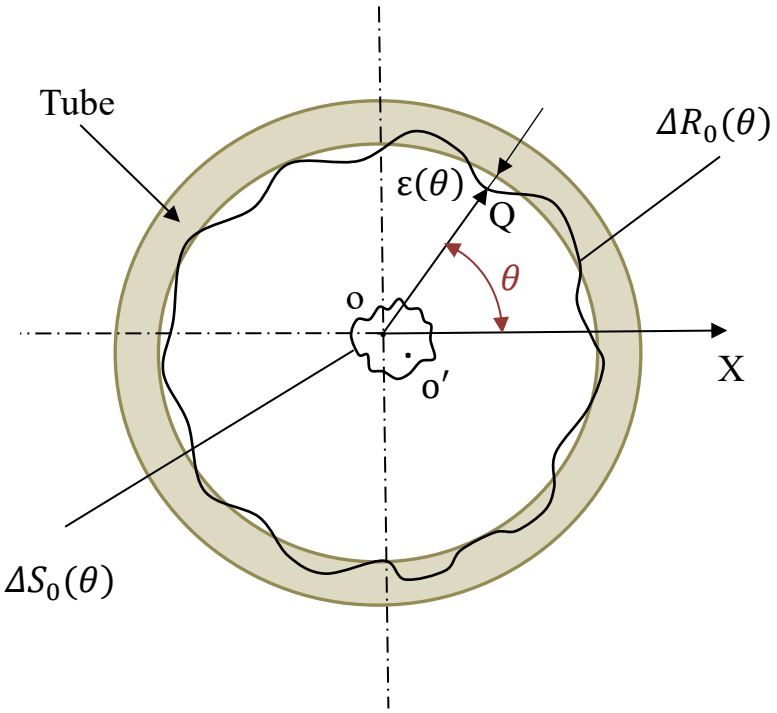

Fig.3.2 Analysis of the changing process of roundness curve

3.4 Analysis of the influencing factors of roundness improvement

3.4.1. Discussion on the influence of eccentricity

If the parameters in Equation (3.14) are determined, the roundness value can be calculated. However, this is difficult because the process involves the repeated processing of the same point to achieve the purpose of finishing, so it can be analyzed by considering N to be infinite. That is, each parameter can be analyzed by $\Delta R_\infty(\varphi)$.

We know that $|1 - C_m K| < 1$, that is $[(1 - C_m K)^N]_{N\to\infty} = 0$. This is obtained by:

$$\left[C_m K \sum_{i=0}^{N-1} (1 - C_m K)^{N-i-1}\right]_{N\to\infty} = 1 \tag{3.15}$$

When $N \to \infty$, it is obtained by:

$$(1 - C_m K)^N \sum_{n=2}^{\infty} A_n \cos(n\varphi + \varphi_n) = 0 \tag{3.16}$$

Therefore, in this case, the influence of the roundness curve before machining can be ignored. Then, the equipment is expressed as:

$$-C_m K \sum_{i=0}^{N-1} (1 - C_m K)^{N-i-1} \left[A_1 \cos(\varphi + \varphi_1) + \sum_{m=1}^{\infty} B_m \cos(m\varphi + \beta_m)\right]$$
$$= -A_1 \cos(\varphi + \varphi_1) - \sum_{m=1}^{\infty} B_m \cos(m\varphi + \beta_m) \tag{3.17}$$

From Equation (3.17), it can be seen that the influence of the eccentricity during clamping and the periodic variation caused by the eccentricity is proportional. If $A_1 = 0$, the influence of eccentricity can be eliminated, and then $B_m = 0$, which can be achieved by clamping at both ends.

Moreover, for random item $\Delta S(\varphi + 2i\pi)$, if the maximum absolute value is assumed to be ΔS_m, then it is obtained by:

$$\left| C_m K \sum_{i=0}^{N-1} (1 - C_m K)^{N-i-1} \Delta S(\varphi + 2i\pi) \right| < C_m K \sum_{i=0}^{N-1} (1 - C_m K)^{N-i-1} \Delta S_m = [1 - (1 - C_m K)^N] \Delta S_m \quad (3.18)$$

when $N \to \infty$, the right side of the above formula gradually approaches ΔS_m, but does not exceed ΔS_m. The value of ΔS_m is very small. If we assume a value of 0.1, then the effect of the random variable is less than 0.1. Therefore, the influence of eccentricity can be ignored.

3.4.2. Discussion on the influence of finishing force

Furthermore, it can be seen from Equation (3.9) that the change in vibration is proportional to K, that is, it is also proportional to the finishing force. Figure 3.3 shows the analysis of the roundness improvement. Fig. 3.3 (a) is a straight-line expansion of the roundness curve. According to the evaluation method of roundness [307], it can be seen that when the $\varepsilon_A(\theta)$ becomes smaller, it is beneficial to improve the roundness, while when the absolute value of $\varepsilon_B(\theta)$ becomes larger, it is unfavorable to improve the roundness. Therefore, as shown in Fig.3.3 (b), in the case of internal magnetic abrasive finishing process using the magnetic machining tool,

because the magnetic particles are attracted to the surface of the magnetic machining tool by the magnetic force and the magnetic machining tool and the magnetic pole outside the tube produce pressure on the magnetic particles, the magnetic particles form a fixed magnetic brush, resulting in the finishing force mainly being concentrated at point A and little finishing force acting on point B, which can improve the roundness. As shown in Fig.3.3 (c), in the case of using magnetic particles, point B is closer to the permanent magnet than point A, and the magnetic force (finishing force) is concentrated at point B that this process is unfavorable for roundness improvement [308]. It is clarified why the internal magnetic abrasive finishing process using the magnetic machining tool is effective in the roundness improvement theoretically.

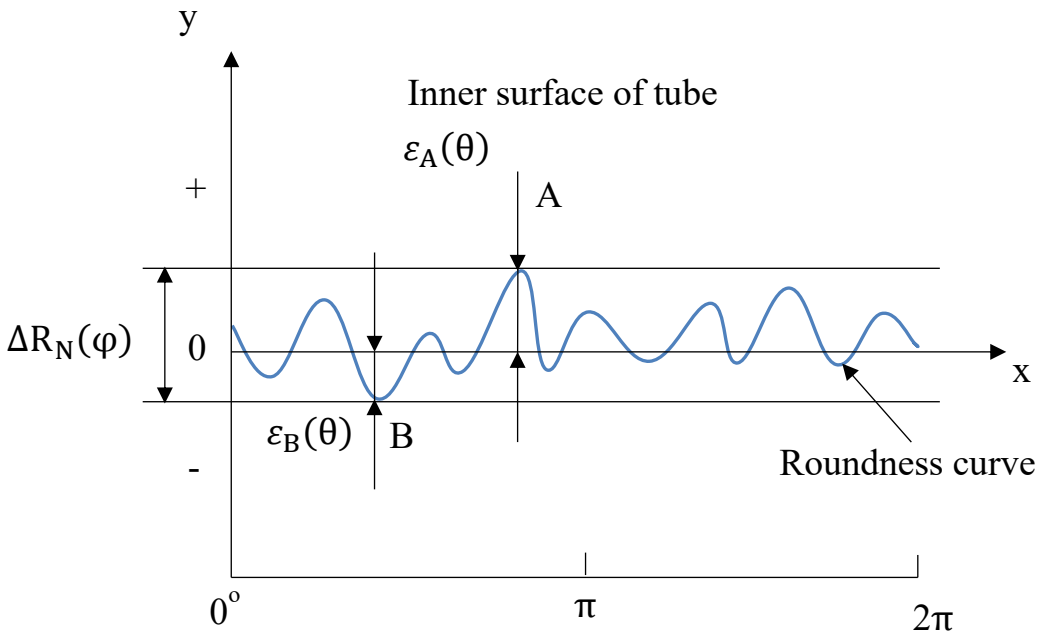

(a) Straight-line expansion of the roundness curve

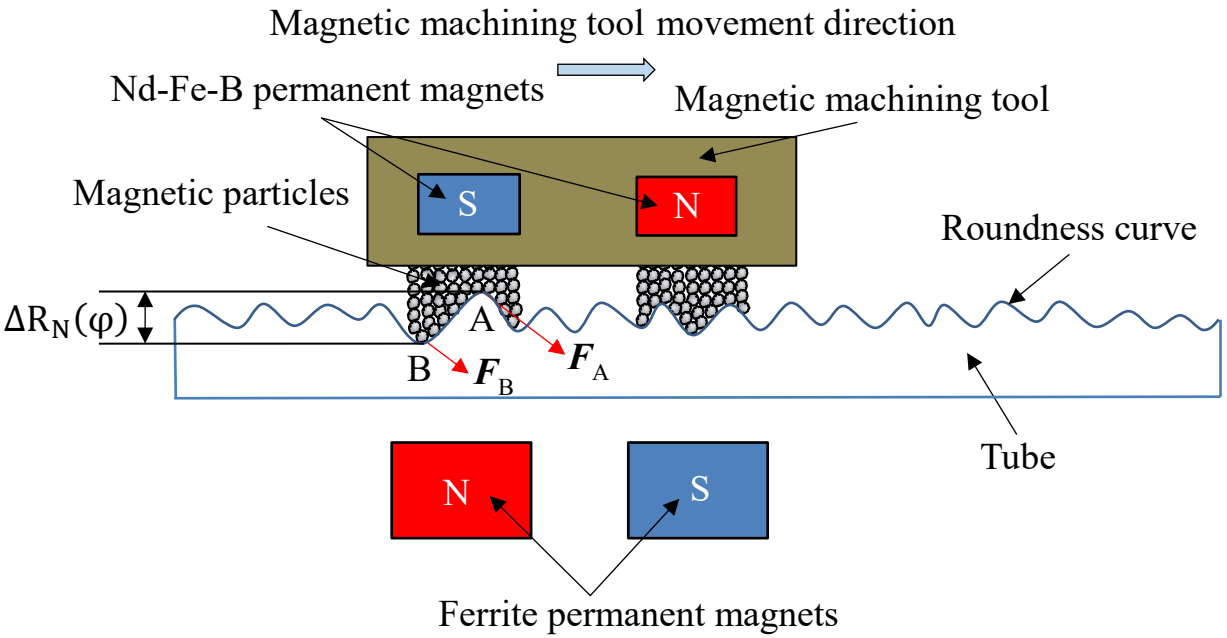

(b) Internal magnetic abrasive finishing process using the magnetic machining tool

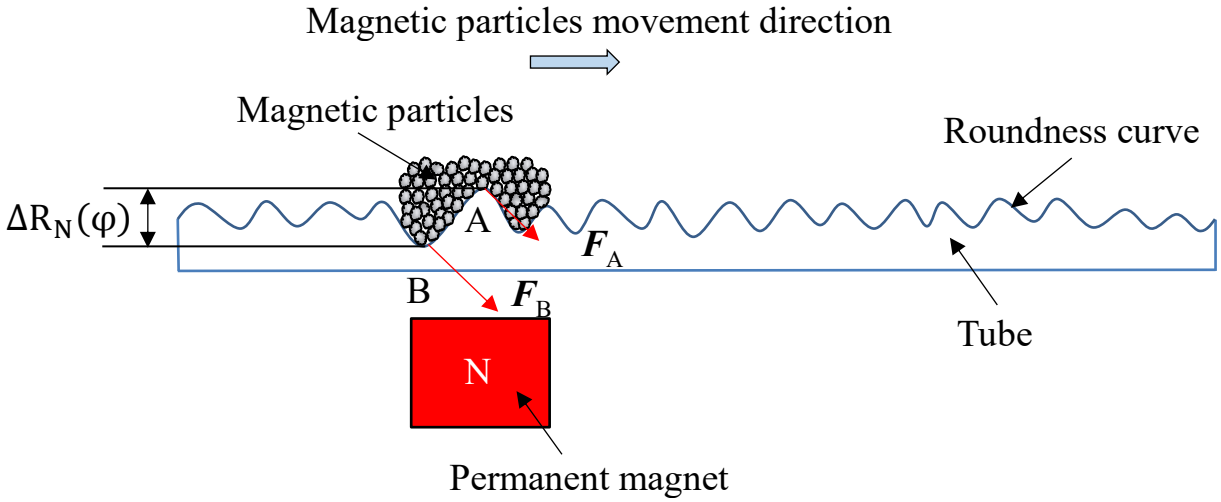

(c) Internal magnetic abrasive finishing process using magnetic particles

Fig.3.3 Analysis of roundness improvement

3.5 The experimental verification of SUS304 stainless steel tube

3.5.1 Experimental conditions

The experimental conditions are shown in Table 3.1. The conditions of each experiment included the rotational speed of the tube and finishing unit. The reciprocating speed of the finishing units were the same, and the magnetic particles were all electrolytic iron particles 1680 μm in mean diameter. The roughness of the internal surface was improved by using abrasive particles with a gradually reduced particle size. The length of the tube axis direction in the finishing area is 80mm. After each stage of processing (15 min), the roughness, roundness, and weight of the tube were measured. Among these, the roughness was measured by a surface roughness meter (SURFPAK-PRO produced by Mitutoyo, Japan), the roundness measurement model is shown in the Fig.3.4. The inner surface roundness was measured in the axial direction of the tube by a roundness measuring instrument (RONDCOM 40C produced by TOKYO SEIMITSU, Japan), the roughness measurement model is shown in the Fig.3.5. And the weight of the workpiece was measured using the balance PR8001 (SHIMADZU, Japan, minimum weighing unit: 0.1 g). Furthermore, as shown in Fig.3.6, in the experiment the distance L between the tube and the permanent magnet of the magnetic pole unit was adjusted to 7 mm, 17 mm, and 27 mm, respectively. If the finishing gap (the distance between the permanent magnet of the finishing unit and the tube) is assumed to be 2 mm, the thickness of tube D will be equivalent to 10 mm, 20 mm, and 30 mm, respectively.

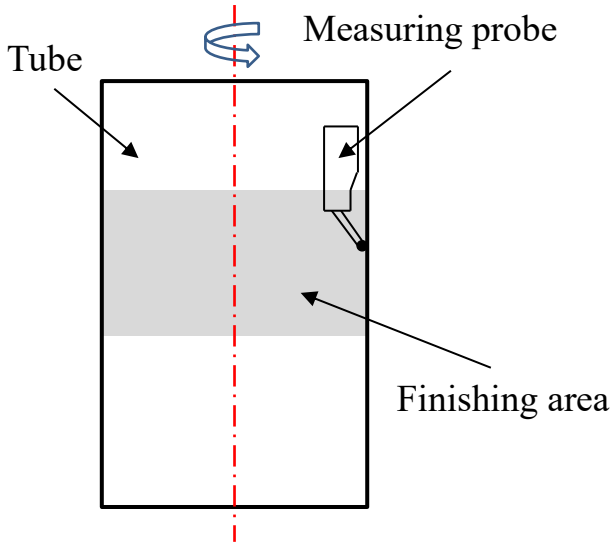

Fig.3.4 The roundness measurement model

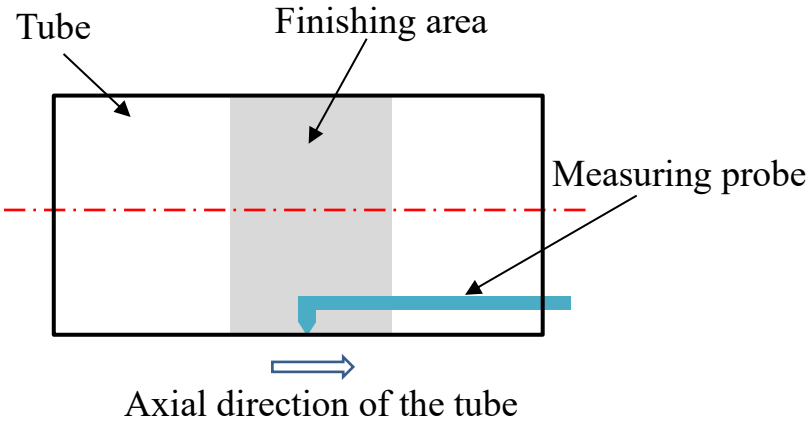

Fig.3.5 The roughness measurement model

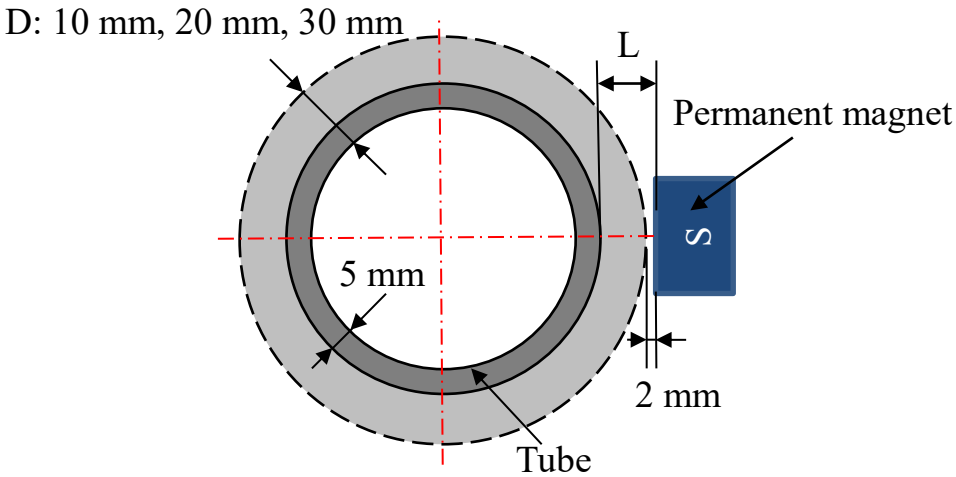

Fig.3.6 The relationship between the distance between the poles and the thickness of the tube

Table 3.1 Experimental conditions

Workpiece	SUS304 stainless steel tube Ø89.1×79.1×200 mm Rotational speed: 162 rpm
Magnetic machining tool	Magnet: Nd-Fe-B permanent magnet, Yoke: SS400 steel Molding material: Polymer
Magnetic pole unit	Magnet: Ferrite permanent magnet 50×35×26 mm Yoke: SS400 steel Rotational speed: 186 rpm Reciprocating speed: 25 mm/s
Magnetic particles	Electrolytic iron particles: 1680 μm in mean dia., 24 g
Abrasive particles	1^{st}-stage to 6^{th}-stage: WA #400, 2.5 g 7^{th}-stage: WA #3000, 2.5 g 8^{th}-stage: WA #6000, 2.5 g 9^{th}-stage: WA #10000, 2.5 g
Grinding fluid	Water-soluble grinding fluid (SCP-23): 30 g
Thickness of the tube	10 mm, 20 mm, 30 mm
Finishing time	135 min (Single 15 min)

3.5.2 Experimental results and discussion

Fig.3.7 shows the changes in surface roughness and material removal with finishing time. It can be seen that, due to the diameters of the magnetic particles and the abrasives used in the experiment were the same, the surface roughness after finishing was almost the same. As the thickness of the tube increased, the finishing force decreased, meaning that the amount of material removed decreased. For different tube thicknesses, the amount of material removed was 14.2 g in the case of 10 mm, 8.4 g in the case of

20 mm, and 5.4 g in the case of 30 mm. In addition, it was concluded that the internal magnetic abrasive finishing process using the magnetic machining tool process could finish thick tubes with thicknesses ranging from 10 mm to 30 mm.

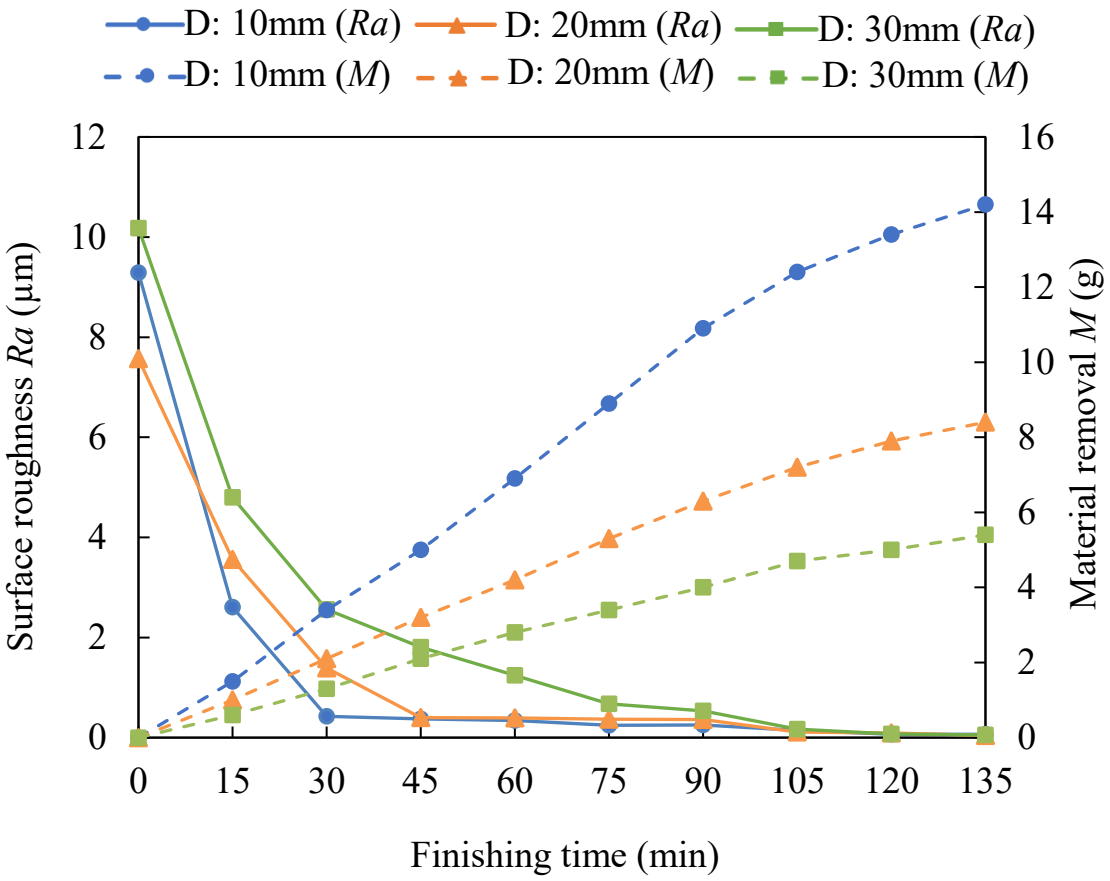

Fig.3.7 Changes in material removal and surface roughness with finishing time

Fig.3.8 shows the changes in roundness with finishing time. It can be seen that this process can improve the roundness of thick tubes whose thickness is from 10 mm to 30 mm. As the thickness of the tube increased, the value of the roundness improvement decreased. For different tube thicknesses, the value of roundness improvement was 150 μm in the case of 10 mm, 127 μm in the case of 20 mm, and 98 μm in the case of 30 mm.

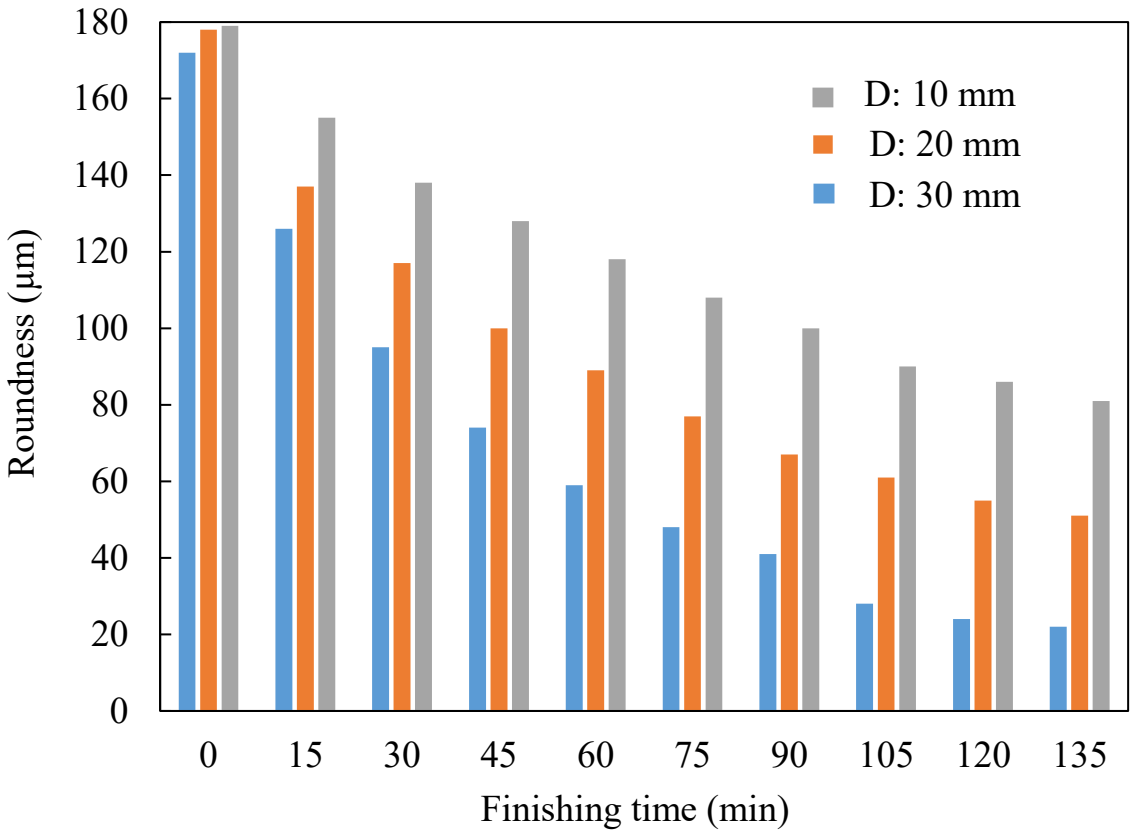

Fig.3.8 Changes in roundness with finishing time

Fig.3.9 shows the roundness profiles of the internal surface of the tube before and after finishing. For different tube thicknesses, the roundness was improved from 172 μm to 22 μm in the case of 10 mm, from 178 μm to 51 μm in the case of 20 mm, and from 179 μm to 81 μm in the case of 30 mm. It can be seen from the experimental results that as the thickness of the tube decreased, the finishing force of the radial direction of the tube increased. Consequently, it was concluded that the internal magnetic abrasive finishing process using the magnetic machining tool was effective for improving the roundness of thick tubes with thicknesses from 10 mm to 30 mm.

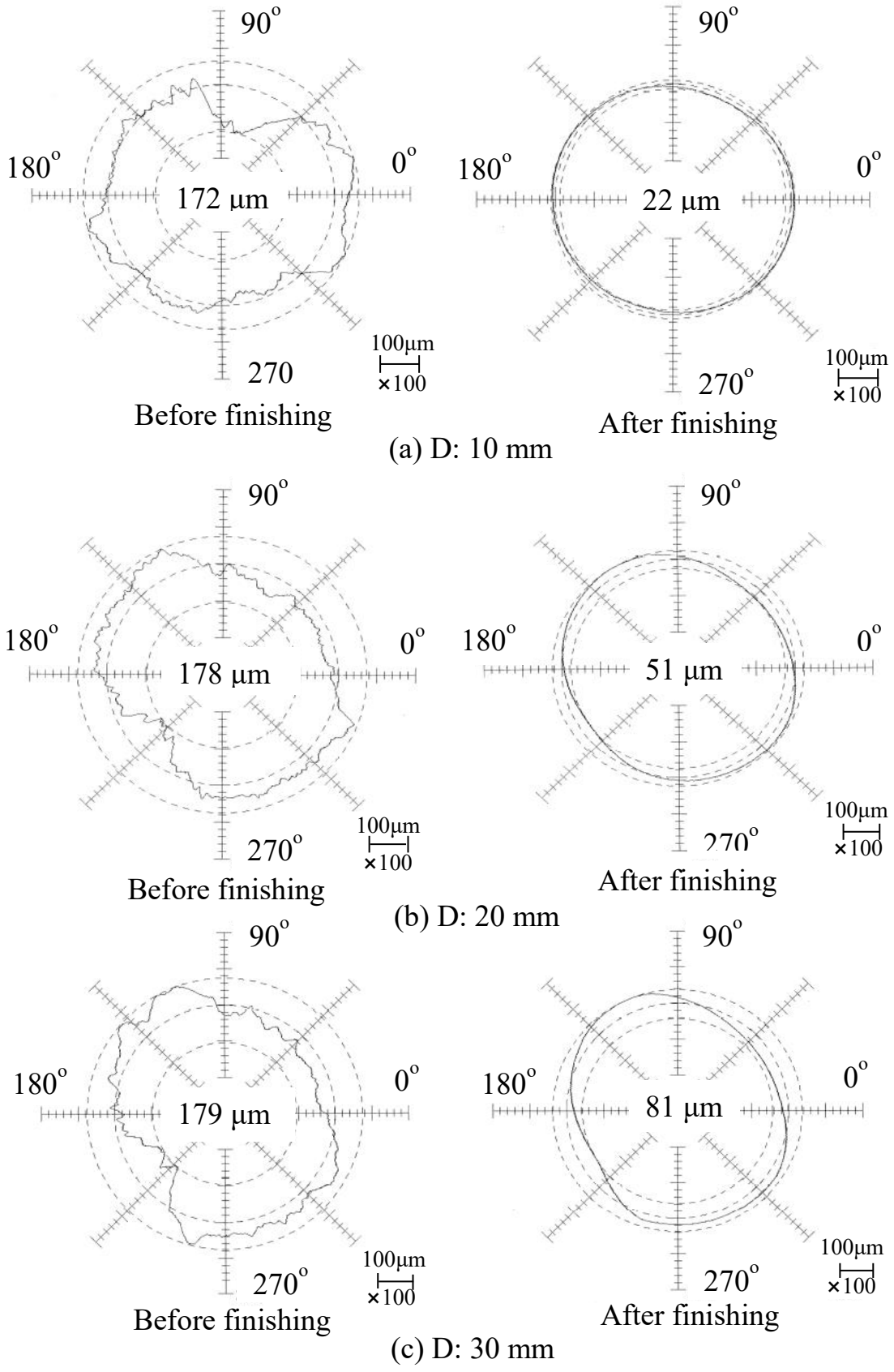

Fig.3.9 Roundness profiles of the internal surface of the tube before and after finishing

3.5.3 Simulation of magnetic induction intensity

In this study, Magnet Version 7 software is used to simulate the magnetic induction intensity. Because in the experiment, the tube thickness of 5 mm is used to equal the thickness of 10 mm, 20 mm and 30 mm, simulating the magnetic induction intensity using a model with only two permanent magnets. And in order to clarify the variety rule of magnetic induction intensity on the finishing area with the three thicknesses, simulating the magnetic induction intensity on line O_1O_2. Fig.3.10 shows the simulation analysis results of the magnetic induction intensity. In the case of the thickness of the tube is 10 mm, when the actual thickness of the tube is 10 mm, the average value of the magnetic induction intensity of the line O_1O_2 is 0.5195 T, when the equivalent thickness of the tube is 10 mm, the average value of the magnetic induction intensity of the line O_1O_2 is 0.5104 T. It can be seen that the average value of the magnetic induction intensity of the line O_1O_2 is basically the same. In the case of the thickness of the tube is 20 mm, when the actual thickness of the tube is 20 mm, the average value of the magnetic induction intensity of the line O_1O_2 is 0.4355 T, when the equivalent thickness of the tube is 20 mm, the average value of the magnetic induction intensity of the line O_1O_2 is 0.4356 T. It can be seen that the average value of the magnetic induction intensity of the line O_1O_2 is basically the same. In the case of the thickness of the tube is 30 mm, when the actual thickness of the tube is 30 mm, the average value of the magnetic induction intensity of the line O_1O_2 is 0.3947 T, when the equivalent thickness of the tube is 30 mm, the average value of the magnetic induction intensity of the line O_1O_2 is 0.3939 T. It can be seen that the average value of the magnetic induction intensity of the line O_1O_2 is basically the same.

It also can be seen that the magnetic force decreases as the thickness of the tube increases.

The actual thickness of the tube: 10 mm

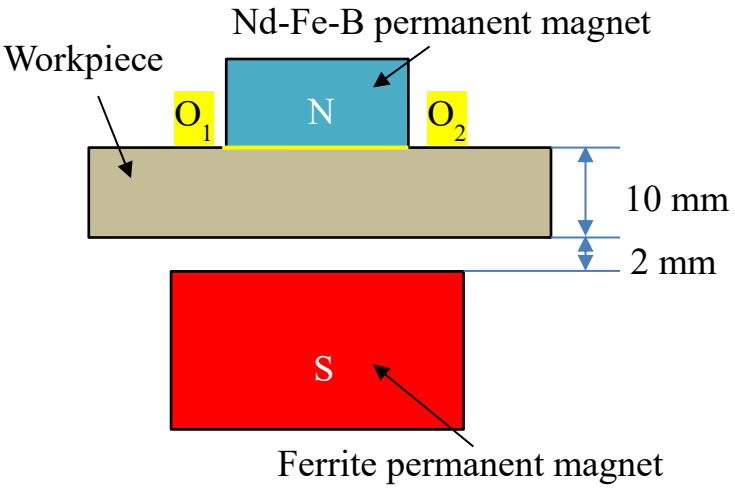

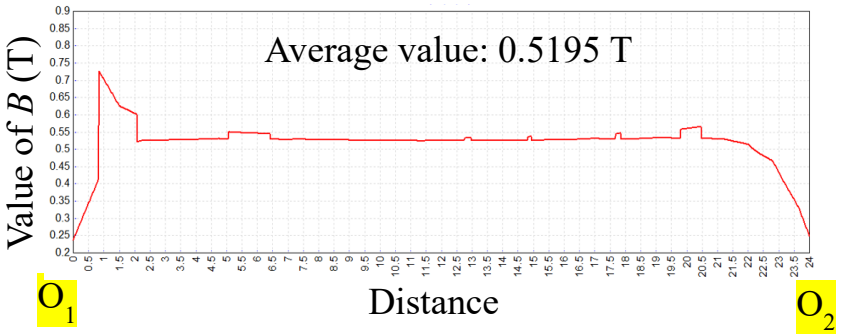

The equivalent thickness of the tube: 10 mm

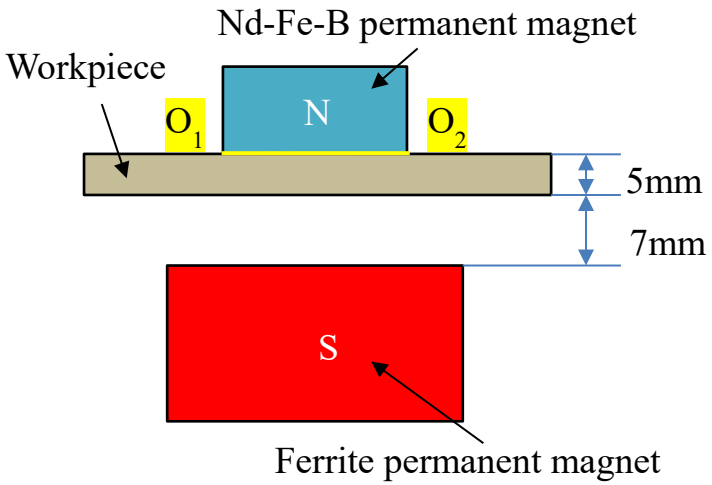

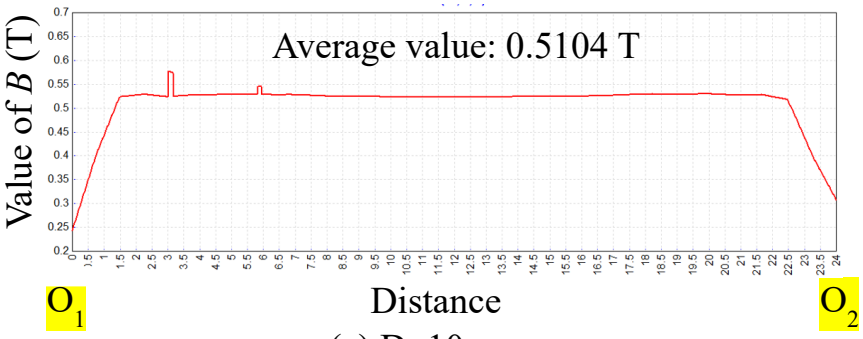

(a) D: 10 mm

The actual thickness of the tube: 20 mm

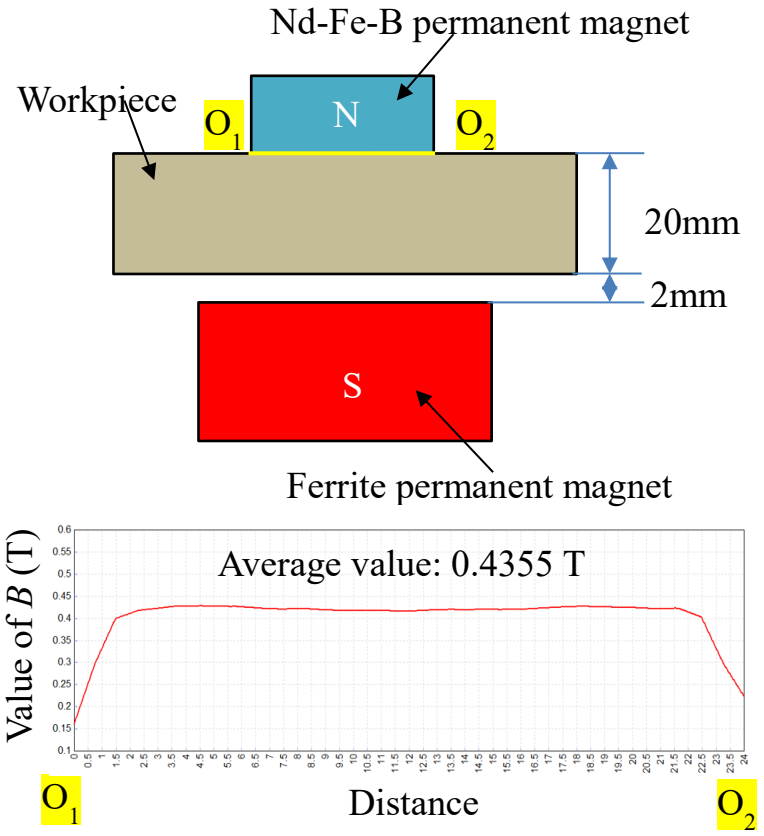

The equivalent thickness of the tube: 20 mm

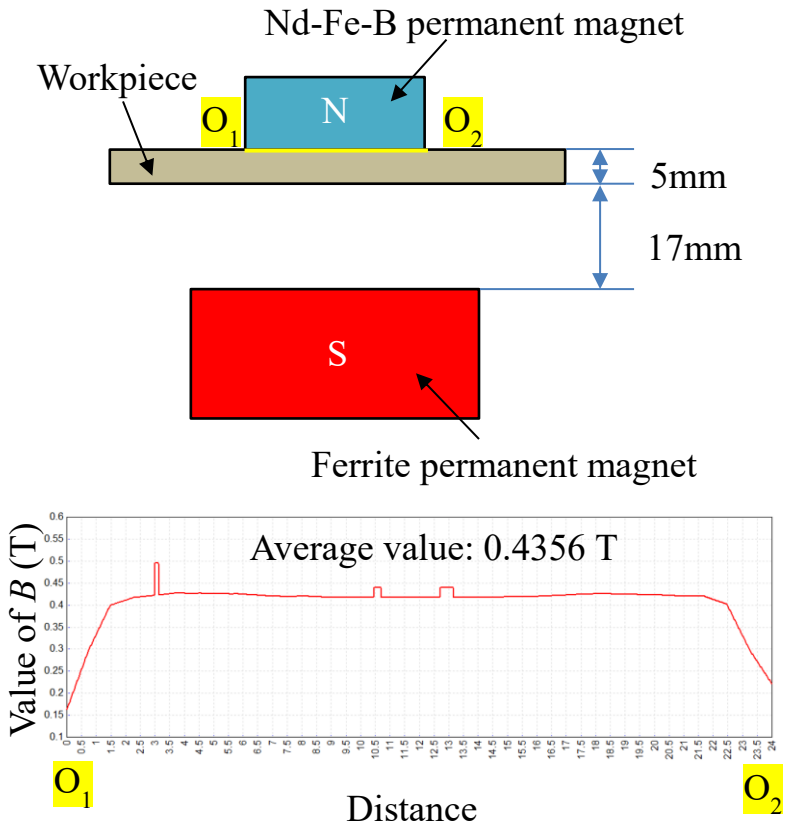

(b) D: 20 mm

The actual thickness of the tube: 30 mm

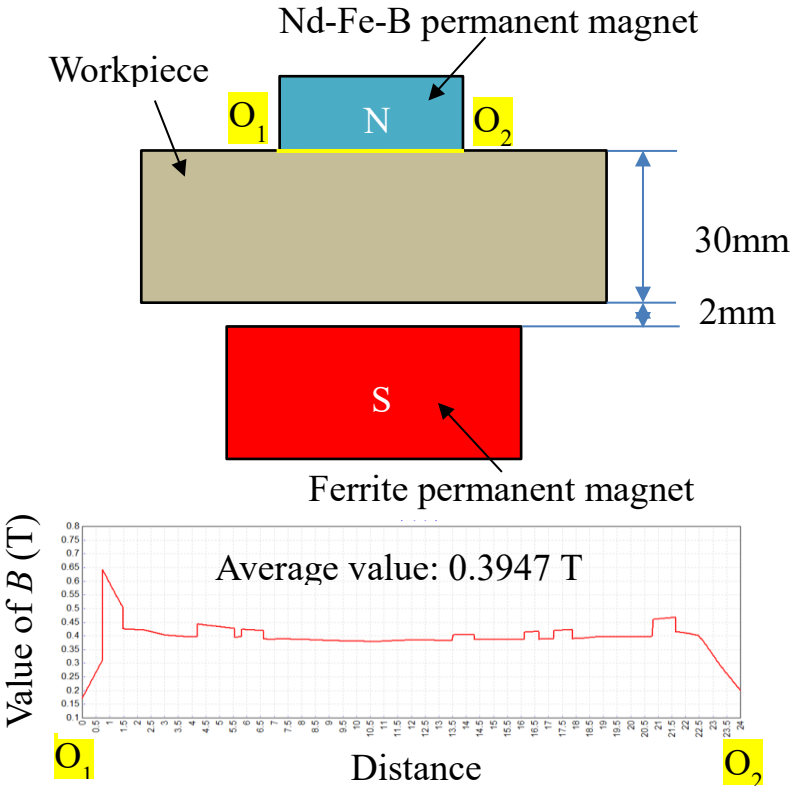

The equivalent thickness of the tube: 30 mm

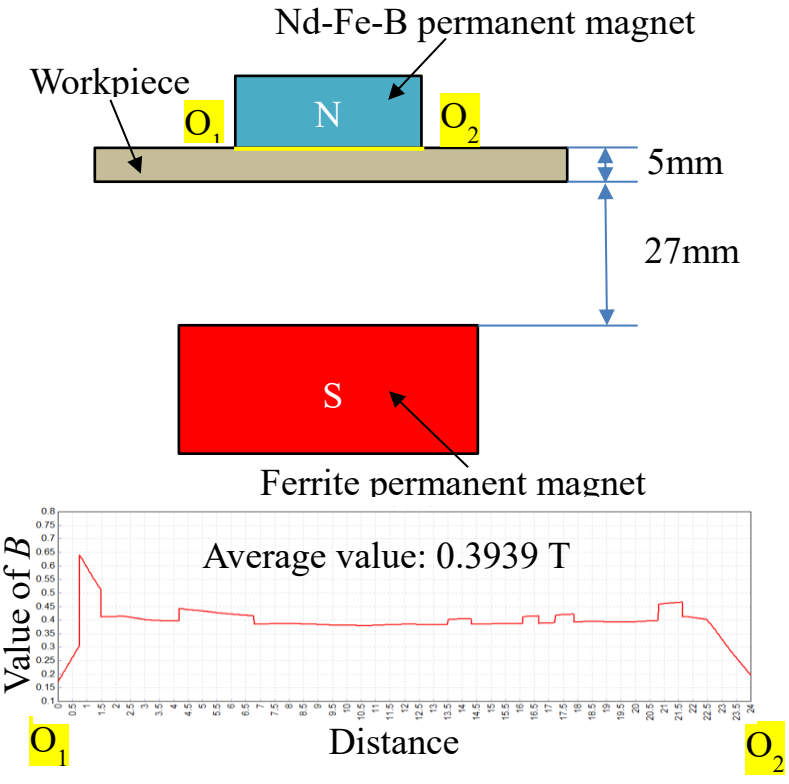

(c) D: 30mm

Fig.3.10 Simulation analysis results of the magnetic induction intensity

3.6 Experimental verification of theoretical analysis results

When the influence of eccentricity during clamping and random items on the roundness curve is ignored, Equation (3.14) can be written as:

$$\Delta R_N(\varphi) = (1 - C_m K)^N \sum_{n=2}^{\infty} A_n \cos(n\varphi + \varphi_n) \tag{3.19}$$

This is obtained by:

$$\Delta R_{46980}(\varphi)/\Delta R_0(\varphi) = (1 - C_m K)^{46980} \tag{3.20}$$

In the case of thickness of the tube being 10 mm, $\Delta R_{46980}(\varphi)/\Delta R_0(\varphi)$ is 0.1279. In the case of thickness of the tube is 20 mm, $\Delta R_{46980}(\varphi)/\Delta R_0(\varphi)$ is 0.2865. Furthermore, in the case of the thickness of the tube being 30 mm, $\Delta R_{46980}(\varphi)/\Delta R_0(\varphi)$ is 0.4525. It can be seen from the calculation results that as the thickness of the tube increased, the value of K decreased, that is, the finishing force decreased. Therefore, it can be concluded that as the thickness of the tube increased, the roundness improvement decreased.

Fig.3.11 shows the changes in finishing depth per revolution. When the thickness of the tube became smaller, the processing depth per revolution became larger. As the finishing time became longer, the changes in finishing depth per revolution became smaller. For the processing interval of 0~15 min, in the case of a tube thickness of 10 mm, the change in the finishing depth per revolution is 0.008812 μm; in the case of a tube thickness of 20 mm, the change in the finishing depth per revolution is 0.007854 μm and in the case of a tube thickness of 30 mm, the change in

the finishing depth per revolution is 0.004598 μm. In the processing interval of 120~135 min, in the case of a tube thickness of 10 mm, the change in the finishing depth per revolution is 0.000383 μm; in the case of a tube thickness of 20 mm, the change in the finishing depth per revolution is 0.000383 μm and in the case of a tube thickness of 30 mm, the change in the finishing depth per revolution is 0.000575 μm.

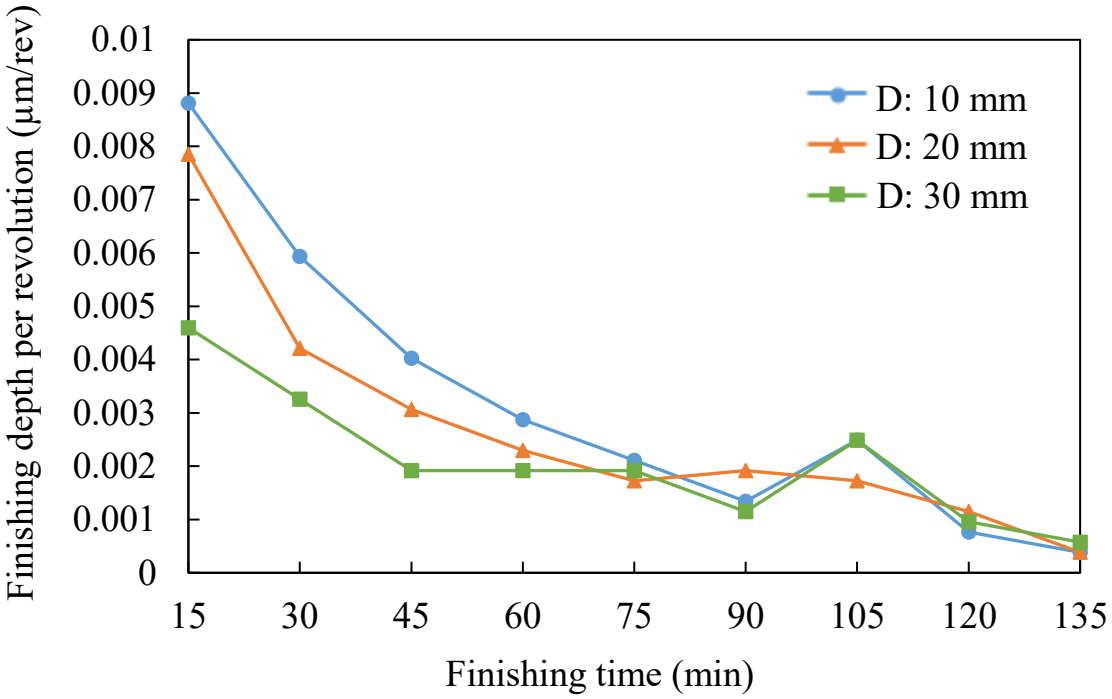

Fig.3.11 Changes in finishing depth per revolution with finishing time

3.7 Conclusions

1.The mechanism of roundness improvement was analyzed theoretically. The roundness curve expression was derived using the principle of roundness measurement by assumed center method and the expression of the roundness curve expanded by Fourier series was obtained.

2.The factors influencing roundness improvement eccentricity and finishing force were discussed. When the workpiece is clamped at both ends, the influence of eccentricity can be ignored. Moreover, it is clear that

the magnetic abrasive finishing process using the magnetic machining tool was effective in improving the roundness of the inner surface of the tubes with thickness more than 5 mm.

3.Confirming the mechanism analysis results and the experimental results, it can be concluded that the internal magnetic abrasive finishing process using the magnetic machining tool was effective for improving the roundness of thick tubes with a thickness from 10 mm to 30 mm. As the thickness of the tube increased, the finishing force decreased, causing the roundness improvement to decrease. For different tube thicknesses, the roundness was improved from 172 μm to 22 μm in the case of 10 mm, from 178 μm to 51 μm in the case of 20 mm, and from 179 μm to 81 μm in the case of 30 mm.

Chapter IV Discussion on the influence of finishing parameters on inner surface roundness improvement

4.1 Introduction

Clean gas cylinders and transport gas piping systems used in semiconductor manufacturing and aerospace-related industries that required high internal surface accuracy to prevent the adhesion of contaminants. Among them, when the diameter becomes larger that the inner surface of the tubes with the thickness of 5 mm or more, the previous process using magnetic particles is unable to finishing due to insufficient magnetic force (finishing force) [401,402]. In order to increase the finishing force, the process using a magnetic machining tool has been proposed. It has been confirmed that the magnetic force can be several tens of times higher than that of the process using magnetic particles, and this process enables finishing inner surface of the tube (5~30 mm in thickness). It also clarified that form accuracy (roundness) can be improved while improving surface roughness [403-405].

In this chapter, firstly, the improvement of roundness is discussed through the experiments on the SUS304 stainless steel tube. Each experiment carried out five stages of processing, and in the first-stage, two different kinds of magnetic particles were used, the electrolytic iron particles (1680 μm in mean dia.) and the KMX magnetic particles (1000~1680 μm in mean dia.) respectively. And then, researches the improvement of internal roundness of the thick SUS304 stainless steel tube through the velocity analysis. Due to the roundness improvement is related

to the material removal, and the material removal is related to the finishing force during processing. The factors affecting the improvement of internal roundness of the thick tube was investigated by studying the reciprocating velocity of magnetic pole unit. Furthermore, in order to further clarify the mechanism of roundness improvement in this process, the influence of rotational speed is discussed. Discussing the influence of rotational speed of magnetic machining tool on roundness improvement by analyzing the finishing force and the influence of rotational speed of workpiece on roundness improvement. And the influence of rotational speed is discussed comprehensively.

4.2 Influence of reciprocating velocity of magnetic pole unit

4.2.1 Velocity analysis of the magnetic machining tool

Fig.4.1 shows the motion model of the magnetic machining tool. First, the machining model was established. The tube is assumed to be stationary, but the magnetic abrasive tool relative to the tube rotation and linear motion. In this process, there are three kinds of motion: the rotation of tube, the rotation and the reciprocating motion of magnetic pole unit. The two rotations produce the relative rotation of the tube and the magnetic machining tool. The reciprocating motion of the magnetic pole unit drives the magnetic machining tool to move in a straight line. These two motions combine to make the magnetic machining tool move along the spiral of the tube. Where, $s(t)$ is the trajectory, P is the pitch of the trajectory.

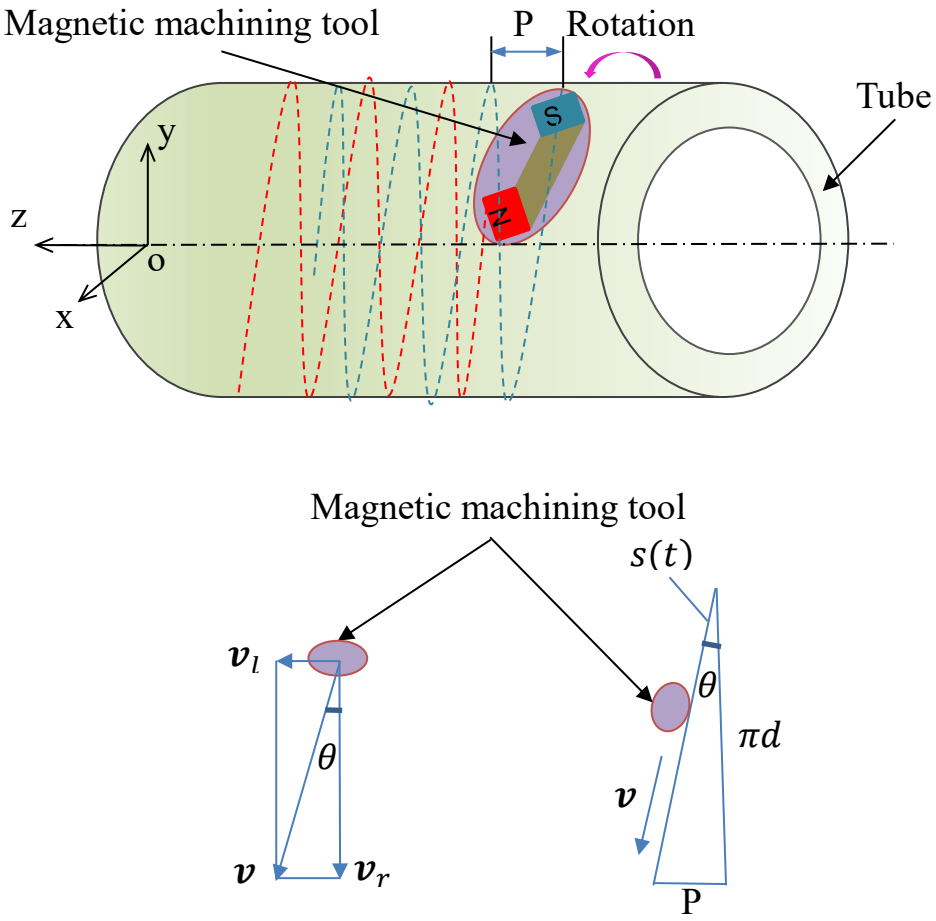

(a) Velocity analysis (b) Track unfolding

Fig.4.1 Motion model of the magnetic machining tool

Because magnetic abrasive tool does two motions: rotation and linear motion. Therefore, the magnetic machining tool produces the tangential velocity of rotation $\boldsymbol{v}_r$ and the velocity of linear motion $\boldsymbol{v}_l$ on the inner surface of the workpiece, as shown in Fig.4.1 (a). The two velocities are combined at a velocity of $\boldsymbol{v}$ which is the speed along the spiral. With respect to Angle θ, there are $\tan\theta = v_l/v_r$.The velocity relation can be derived as shown in Equation (4.1).

$$v_r = (v^2 - v_l^2)^{1/2} \tag{4.1}$$

Moreover, as shown in Fig.4.1 (b), unfolding the track which the magnetic machining tool rotating 360° obtain the trajectory $s(t)$ along spiral with velocity v. The Angle between $s(t)$ and πd is θ, there $\tan\theta = p/\pi d$. Finally, it is shown in Equation (4.2).

$$\tan\theta = v_l/v_r = p/\pi d \tag{4.2}$$

It follows that the linear velocity of the magnetic machining tool and the pitch of the spiral are directly proportional. The rotation frequency is faster per unit time with a short pitch. It corresponds to the high rotation speed of the magnetic machining tool, so the improvement in roundness is beneficial.

4.2.2 Experimental conditions

Table 4.1 shows the experimental conditions. The three reciprocating velocities that 27 mm/s, 38 mm/s and 58 mm/s were compared in the experiments. The rotational speed of the tube and the magnetic pole unit are 88 rpm and 254 rpm, so the relative rotational speed of the magnetic machining tool and the workpiece is 342 rpm.

Table 4.1 Experimental conditions

Workpiece	SUS304 stainless steel tube Ø89.1×79.1×200 mm, Rotational speed:88 rpm	
Magnetic machining tool	Magnet: Nd-Fe-B permanent magnet, Yoke: SS400 steel, Molding material: Polymer	
Magnetic pole unit	Magnet: Ferrite magnet 50×35×26 mm, Yoke: SS400 steel, Rotational speed of pole:254 rpm Reciprocating speed: 27 mm/s, 38 mm/s and 58 mm/s	
Processing (The concentration of the abrasive slurry:7.5%wt, SCP-23, 40 mL)	1st-stage (30 min)	Magnet particles: Electrolytic iron particles (1680 μm in mean dia.), Abrasive: WA #400
	2nd-stage (15 min)	Magnet particles: Electrolytic iron particles (510 μm in mean dia.), Abrasive: WA #1200
	3rd-stage (15 min)	Magnet particles: Electrolytic iron particles (330 μm in mean dia.), Abrasive: WA #2000
	4th-stage (15 min)	Magnet particles: Electrolytic iron particles (149 μm in mean dia.), Abrasive: WA #4000
	5th-stage (15 min)	Magnet particles: Electrolytic iron particles (75 μm in mean dia.), Abrasive: WA #8000

4.2.3 Experimental results and discussion

Fig.4.2 shows the changes in material removal and surface roughness with finishing time. The result shows that due to the diameters of the magnetic particles and the abrasives used in the experiment were the same, the surface roughness after finishing was almost the same and low reciprocating velocity of magnetic pole unit is beneficial to the material removal.

Fig.4.3 shows the roundness improvement at each stage. As the reciprocating velocity of magnetic pole unit increases, the value of the roundness improvement of each stage decreases.

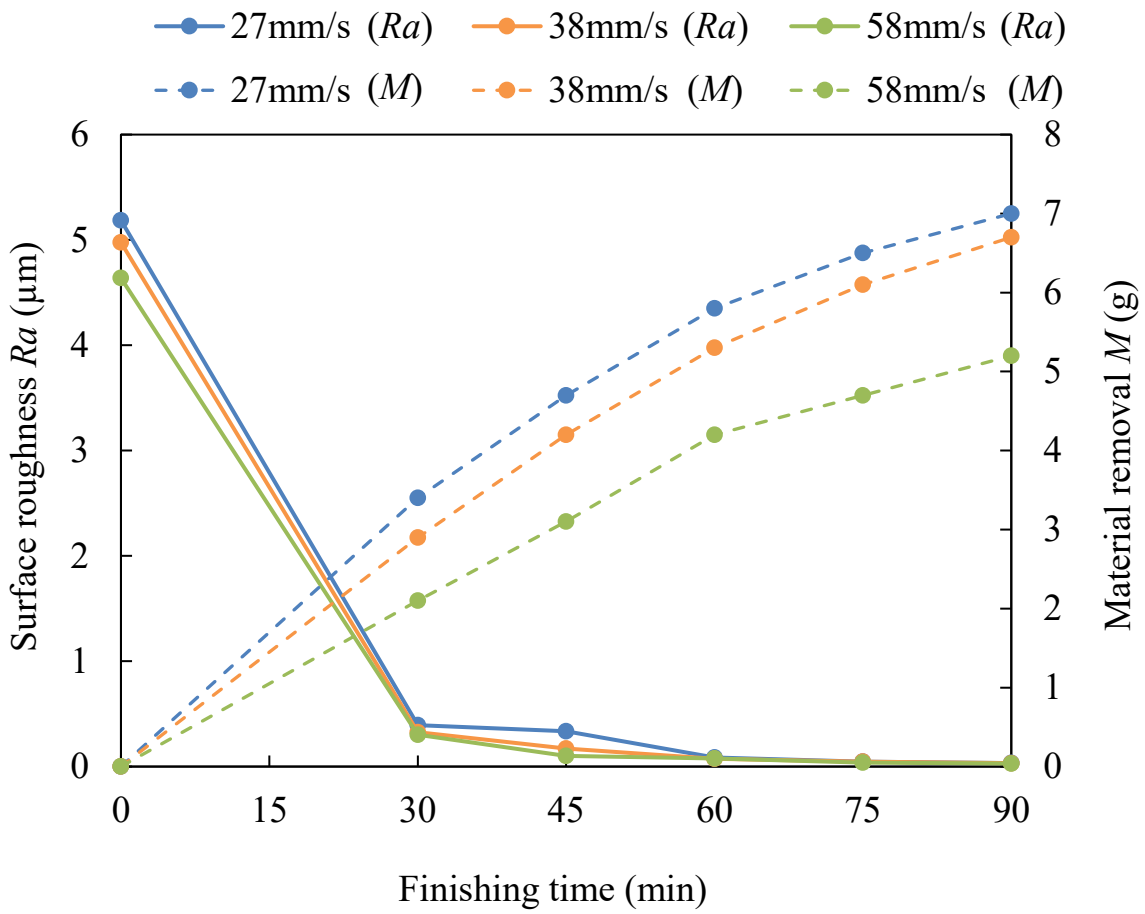

Fig.4.2 Changes in material removal and surface roughness with finishing time

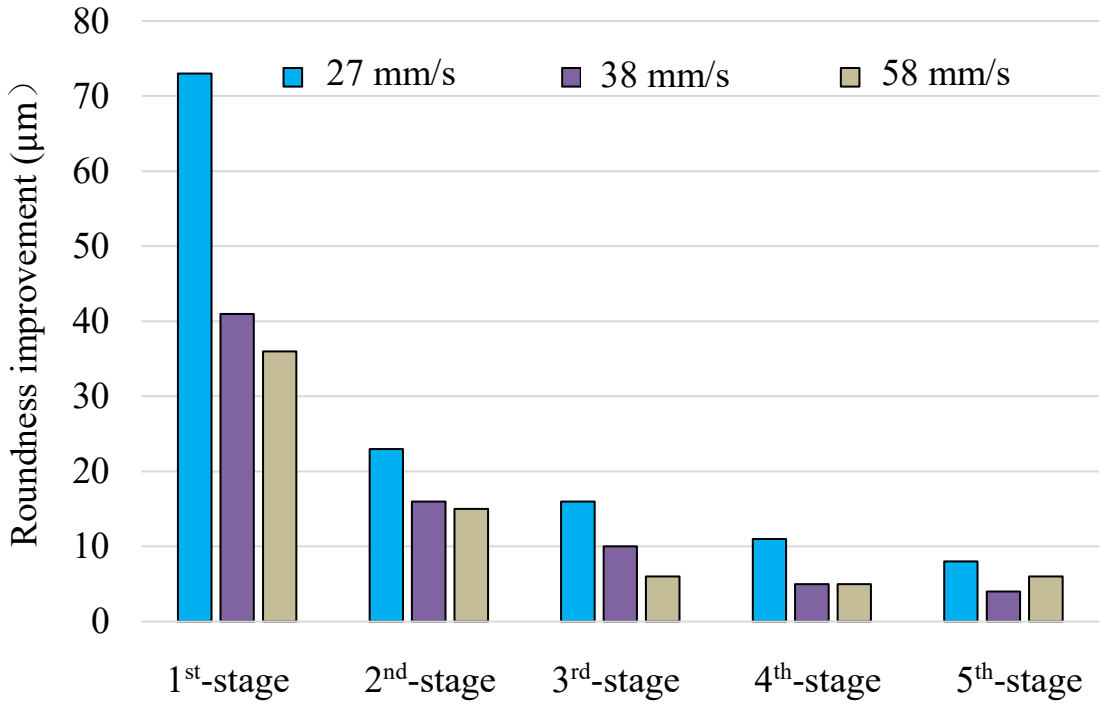

Fig.4.3 Roundness improvement at each stage

Fig.4.4 shows the trajectory simulation of the three reciprocating velocities. When the velocity is low the pitch of the trajectory is also low. The result shows that low reciprocating velocity of magnetic pole unit is beneficial to the improvement of internal roundness.

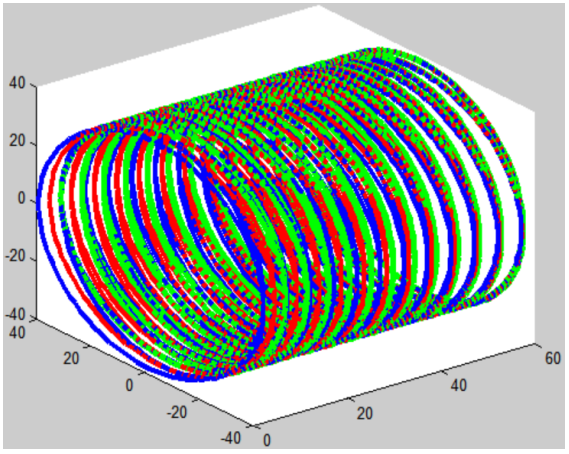

P: 4.68 mm

(a) 27 mm/s

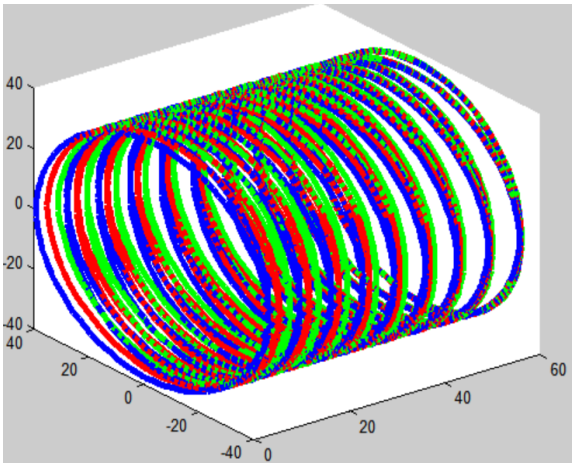

P: 6.73 mm

(b) 38 mm/s

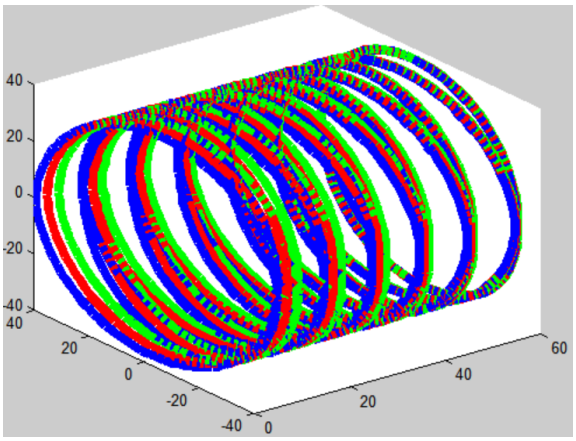

P: 10.23 mm

(c) 58 mm/s

Fig.4.4 The trajectory simulation of the three reciprocating velocities with finishing time

Fig.4.5 shows the roundness charts of before and after finishing. In the case of 27 mm/s, the change of roundness is the largest and the change is 58 μm. The roundness of tube is from 167 μm to 59 μm.

P-P:167 μm

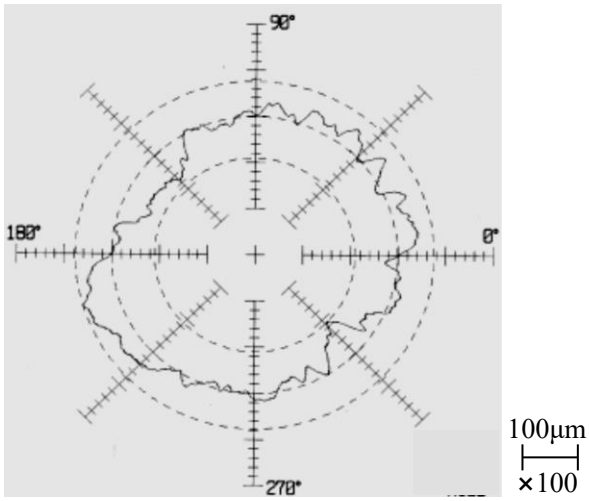

Before finishing

P-P: 59 μm

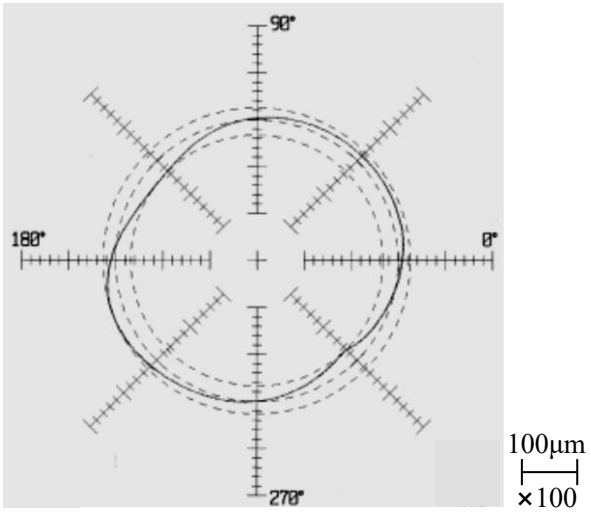

After finishing

Fig.4.5 Roundness charts of before and after finishing

4.3 Influence of different structures of magnetic particles on the improvement of inner surface roundness

4.3.1 Experimental conditions

The experimental conditions are shown in Table 4.2. A five stages of processing using magnetic particles and abrasive that gradually decrease in size was performed in the experiments. And in the first-stage, two different kinds of magnetic particles were used, the electrolytic iron particles (1680 μm in mean dia.) and the KMX magnetic particles (1000 ~ 1680 μm in mean dia.) respectively. Fig.4.6 shows the SEM photographs of the electrolytic iron particles and the KMX magnetic particles. It can be seen that the structure of the two kinds of magnetic particles is different. The electrolytic iron particles are the magnetic particles reduced by electrolysis and the KMX magnetic particles are the magnetic particles that made by sintering iron particles and abrasive.

Table 4.2 Experimental conditions

Workpiece	SUS304 stainless steel tube Ø89.1×79.1×200 mm, Rotational speed:88 rpm	
Magnetic machining tool	Magnet: Nd-Fe-B permanent magnet, Yoke: SS400 steel, Molding material: Polymer	
Magnetic pole unit	Magnet: Ferrite permanent magnet 50×35×26 mm, Yoke: SS400 steel, Rotational speed of pole: 254 rpm Velocity of linear motion: 38 mm/s	
Processing (The concentration of the abrasive slurry:7.5%wt, SCP-23, 40 mL)	1st-stage (30 min)	Magnetic particles: ①Electrolytic iron particles (1680 μm in mean dia., 12×2 g) ②KMX magnetic particles (1000～1680 μm in mean dia., 12×2 g) Abrasive: WA #400, 3.2 g
	2nd-stage (15 min)	Magnetic particles: Electrolytic iron particles (510 μm in mean dia., 10×2 g) Abrasive: WA #1200, 3.2 g
	3rd-stage (15 min)	Magnetic particles: Electrolytic iron particles (330 μm in mean dia., 10×2 g) Abrasive: WA #2000, 3.2 g
	4th-stage (15 min)	Magnetic particles: Electrolytic iron particles (149 μm in mean dia., 10×2 g) Abrasive: WA #4000, 3.2 g
	5th-stage (15 min)	Magnetic particles: Electrolytic iron particles (75 μm in mean dia., 10×2 g) Abrasive: WA #8000, 3.2 g

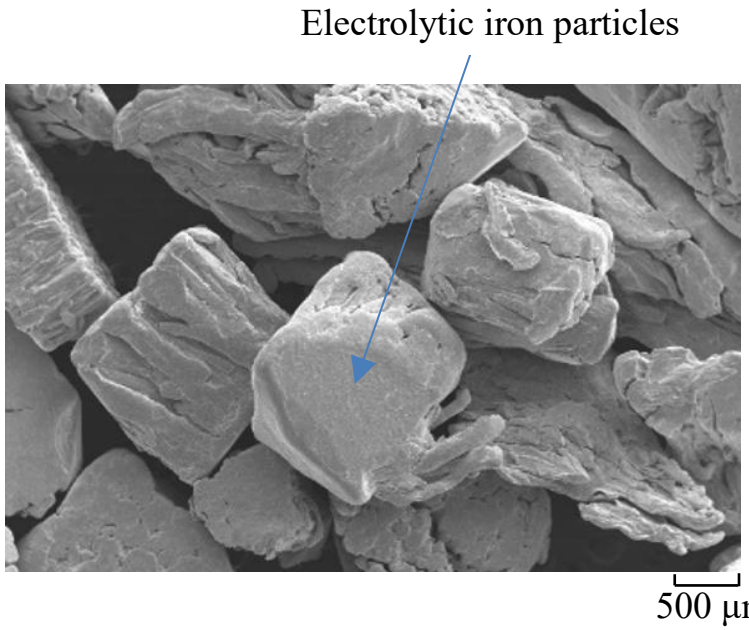

(a) The electrolytic iron particles (1680μm in mean dia.)

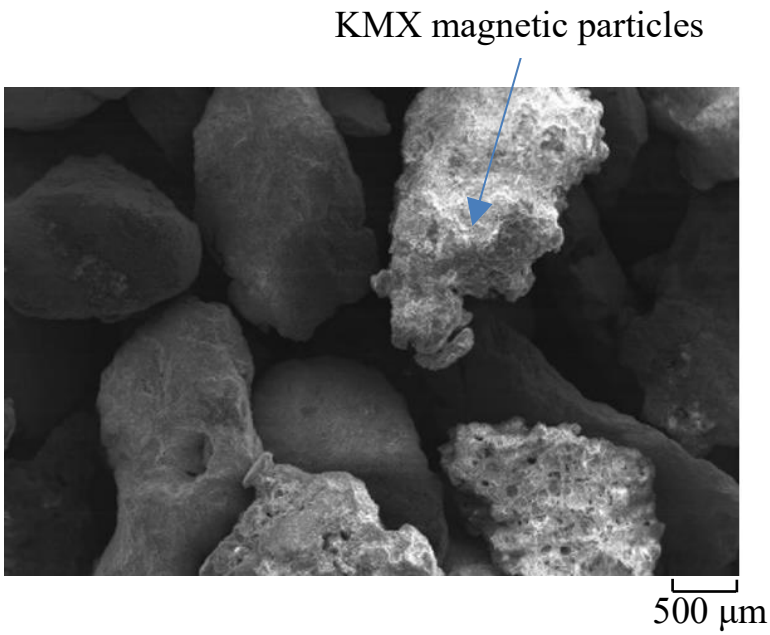

(b) The KMX magnetic particles (1000 ~ 1680 μm in mean dia.)

Fig.4.6 The SEM photographs of magnetic particles

4.3.2 Experimental results and discussion

Fig.4.7 shows the roundness profiles of the tube before and after finishing. The results show that the roundness of 149 μm was improved to 58 μm in the case of the first-stage using the electrolytic iron particles and 218 μm was improved to 92 μm in the case of the first-stage using the KMX magnetic particles. It was confirmed that the both kinds of magnetic particles can improve the roundness of the thick tube by magnetic abrasive finishing using a magnetic machining tool. Fig.4.8 shows the roundness improvement at each stage. It can be seen that the roundness of the inner surface of tube was improved at each stage of finishing. In particular, in the first-stage of finishing, the value of the roundness improvement is the largest due to the use of magnetic particles with large diameter, 61 μm in the case of using the electrolytic iron particles and 76 μm in the case of using the KMX magnetic particles. And the improvement is better by using the KMX magnetic particles because of the structure of the KMX magnetic particles that is equivalent to adding a lot of cutting edges in the process comparing with electrolytic iron particles.

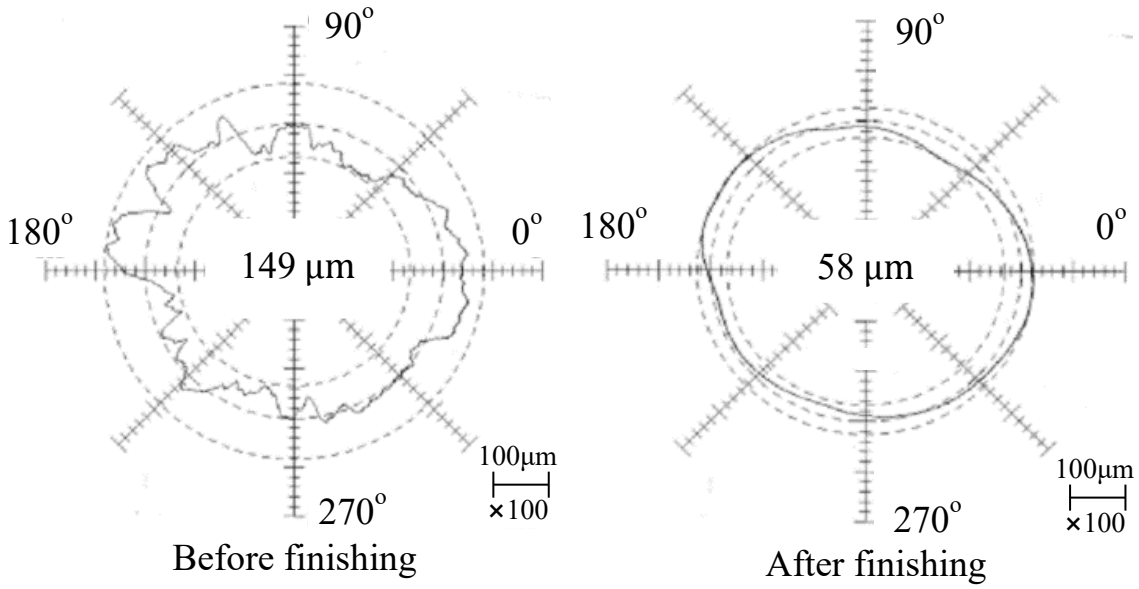

(a) The first-stage using the electrolytic iron particles

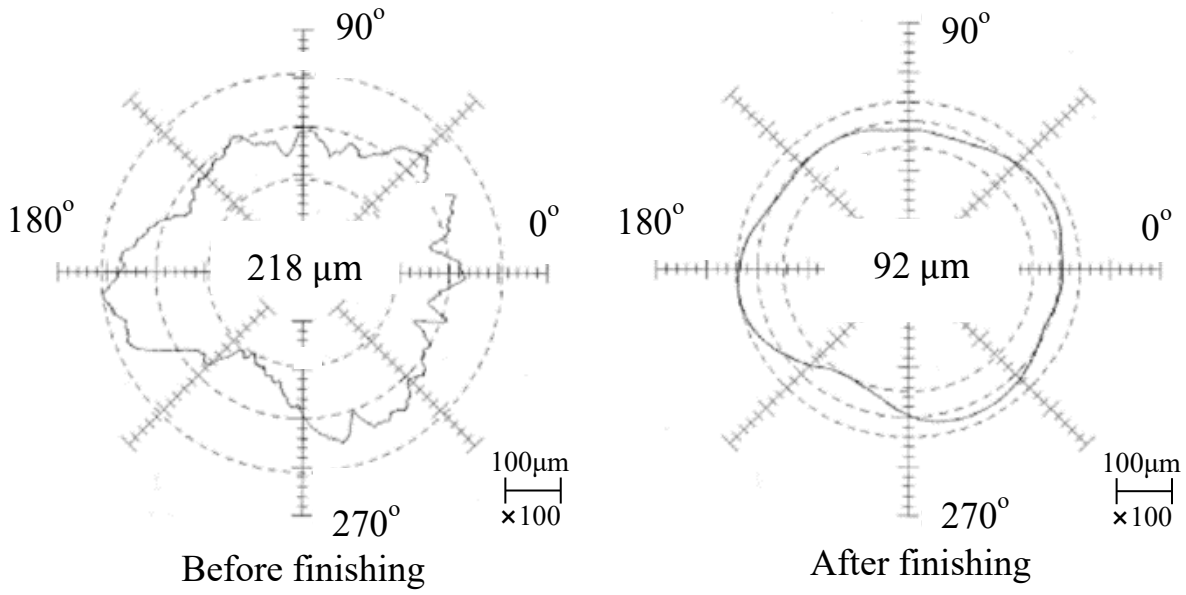

(b) The first-stage using the KMX magnetic particles

Fig.4.7 Roundness profiles of the tube before and after finishing

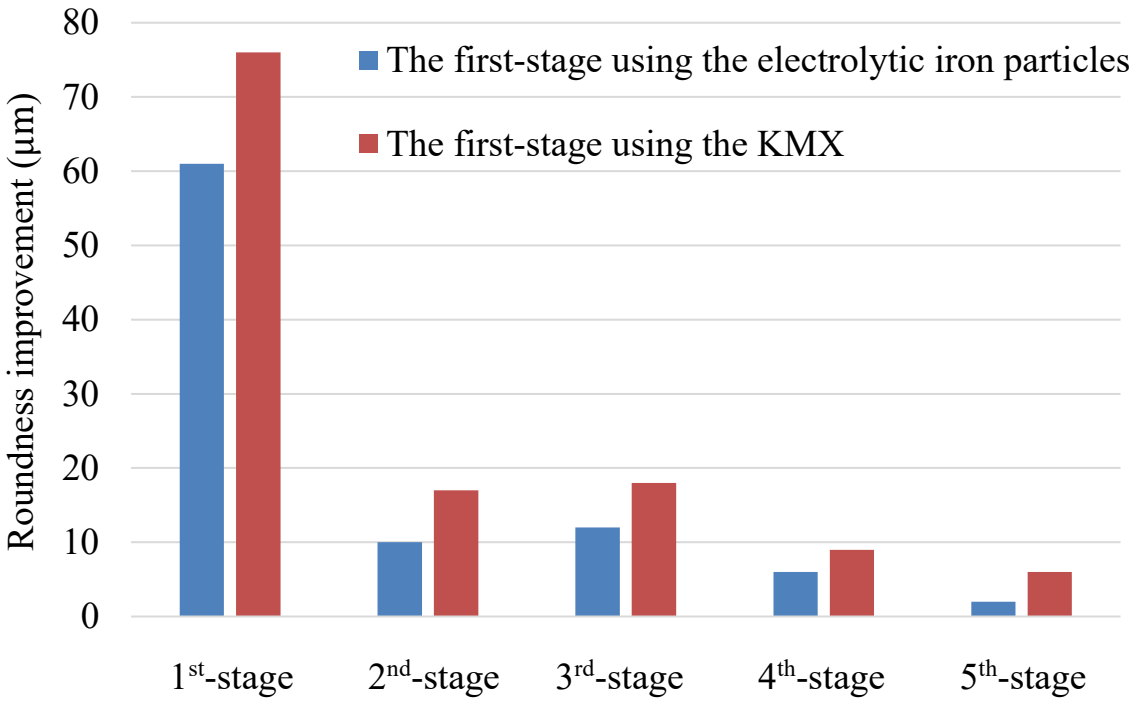

Fig.4.8 Roundness improvement at each stage

4.4 Influence of rotational speed on the improvement of inner surface roundness

4.4.1 Influence of rotational speed of the magnetic machining tool

In the internal magnetic abrasive finishing using magnetic machining tool process, not only the magnetic machining tool rotates, but also the workpiece rotates, and the rotation direction is opposite, so the tangential finishing force is generated by relative motion between magnetic machining tool and workpiece. In order to study the influence of rotational speed on roundness improvement, experiments were carried out under the conditions of different rotational speeds of magnetic machining tool, the same rotational speed of workpiece and different rotational speeds of workpiece, the same rotational speed of magnetic machining tool, respectively.

4.4.1.1 Experimental conditions

The experimental conditions are shown in Table 4.3. The nonferromagnetic SUS 304 stainless steel tube was used as the workpiece. In order to study the influence of the rotational speed of the magnetic machining tool (equal to the rotational speed of magnetic pole unit), the rotational speed of workpiece was the same (66 rpm), while the rotational speed of magnetic machining tool was 32 rpm, 123 rpm and 215 rpm, respectively. The finishing time was 100 min, to understand the changes of roundness, surface roughness and material removal, each stage finishing time was 20 min, and then the workpiece was cleaned with ultrasonic cleaner and measured with the surface roughness meter (SURFPAK-PRO

produced by Mitutoyo, Japan), the roundness measuring instrument (RONDCOM 40C produced by TOKYO SEIMITSU, Japan) and the balance PR8001 (SHIMADZU, Japan, minimum weighing unit: 0.1 g) respectively.

Table 4.3 Experimental conditions

Workpiece	SUS304 stainless steel tube Ø89.1×79.1×200 mm Clearance: 7 mm (Thickness of tube is equivalent to 10 mm.) Rotational speed: 66 rpm
Magnetic machining tool	Magnet: Nd-Fe-B rare earth permanent magnet Yoke: SS400 steel Molding material: Polymer
Magnetic pole unit	Magnet: Ferrite magnet 50×35×26 mm Yoke: SS400 steel Rotational speed: 32 rpm 122 rpm 212 rpm Reciprocating speed: 25 mm/s
Magnetic particles	Electrolytic iron particles: 1680 μm in mean dia., 24 g
Abrasive particles	WA #400, 2.5 g
Grinding fluid	Water-soluble grinding fluid (SCP-23): 30 g
Finishing width	80 mm
Finishing time	100 min (each stage 20 min)

4.4.1.2 Experimental results and discussion

Fig.4.9 shows the changes in surface roughness and material removal with finishing time. It can be seen that because of the diameter of the magnetic particles and the abrasive particles used in the experiments are the same, the final surface roughness after finishing is almost the same. And as the rotational speed of the magnetic machining tool increases, the amo

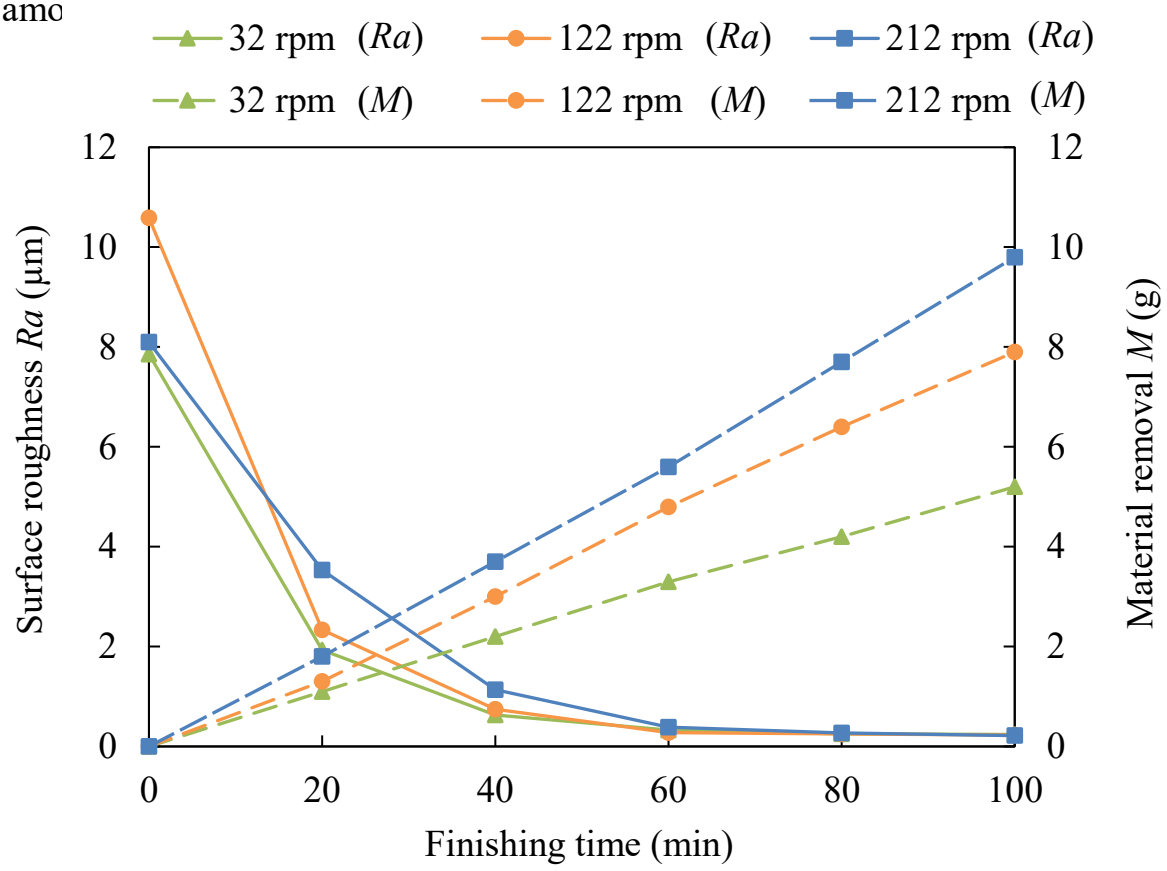

Fig.4.9 Changes in material removal and surface roughness with finishing time

Fig.4.10 shows the roundness improvement with finishing time. It can be seen that the roundness improvement increases with an increase in rotational speed of magnetic machining tool. This is because in this process, the internal surface finishing is realized by a magnetic machining tool

whose surface attracts magnetic particles magnetically. According to the force analysis of the magnetic machining tool, the magnetic machining tool has its own weight and rotates, the finishing force during processing also includes the centrifugal force of the magnetic machining tool. And it is that as the rotational speed of the magnetic machining tool increases, the finishing force increases, so the faster rotational speed of the magnetic machining tool is beneficial to roundness improvement.

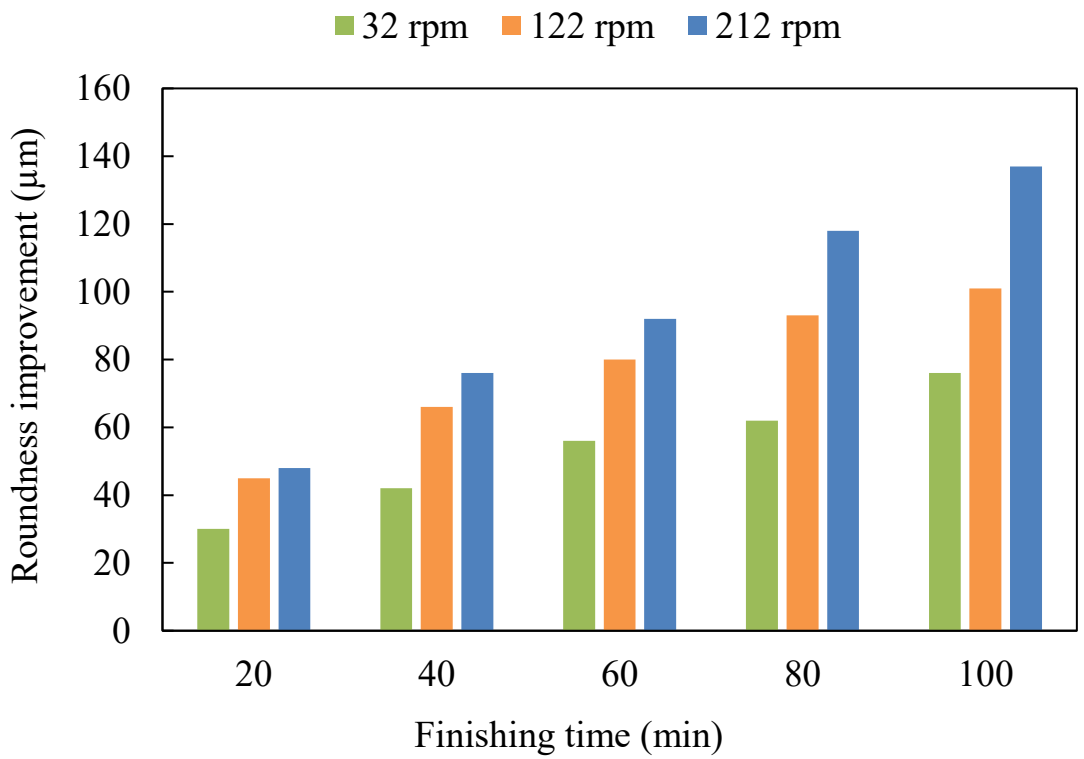

Fig.4.10 Roundness improvement with finishing time

Fig.4.11 shows the roundness profiles of the internal surface of the tube before and after finishing. For different rotational speeds of the magnetic machining tool, the roundness was improved from 205 μm to 129 μm in the case of 32 rpm, from 211 μm to 110 μm in the case of 122 rpm, and from 202 μm to 65 μm in the case of 212 rpm.

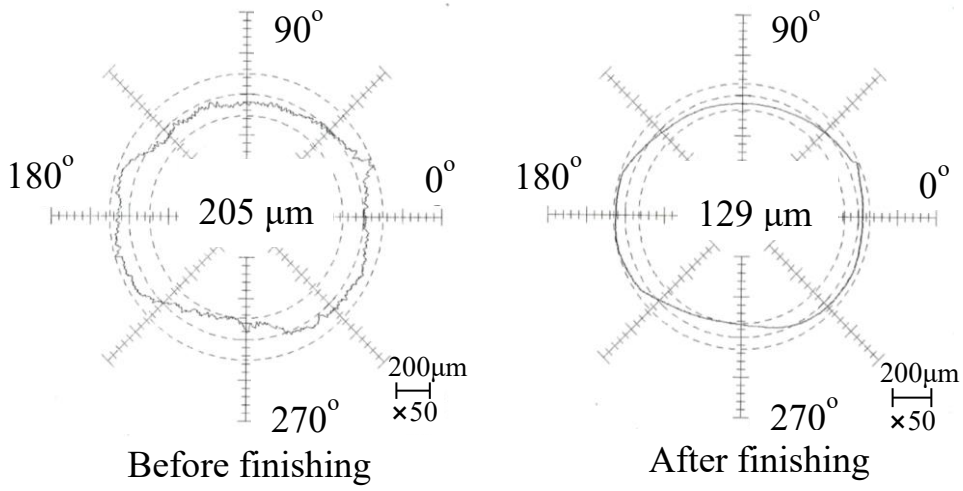

(a) 32 rpm

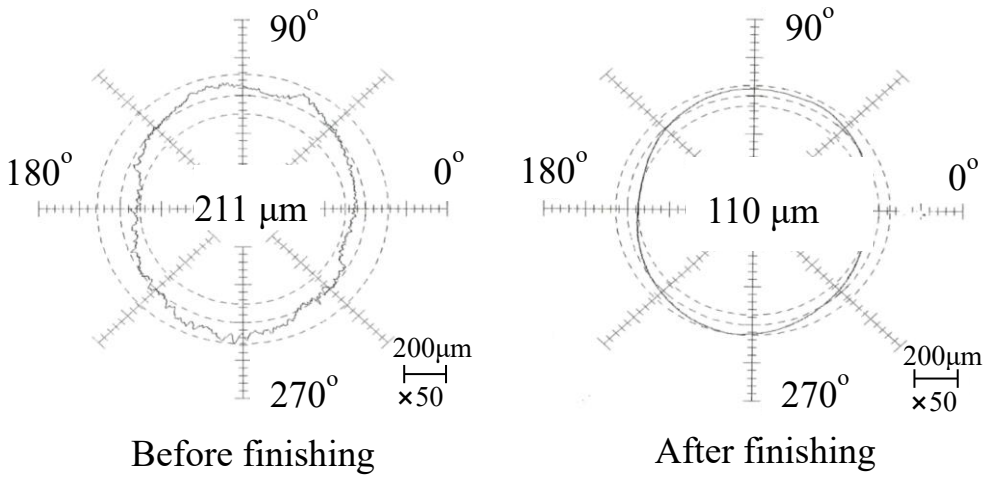

(b) 122 rpm

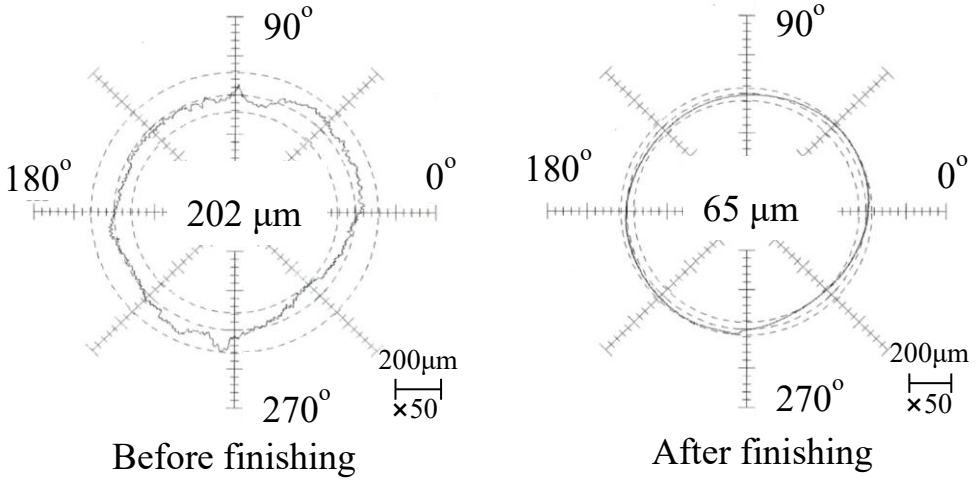

(c) 212 rpm

Fig.4.11 Roundness profiles of the internal surface of tube before and after finishing

The force of magnetic machining tools has been analyzed in section 2.1. In this process, due to the magnetic machining tool has its own weight and rotates, the finishing force includes the centrifugal force generated by the magnetic machining tool. According to the centrifugal force calculation formula, as shown in Equation (4.1).

$$F_C = m_T r\omega^2 = 4\pi^2 m_T n^2 r \tag{4.1}$$

Where, m_T is the weight of the magnetic machining tool, r is the rotational radius of the magnetic machining tool, ω is the angular speed of rotation of the magnetic machining tool and n is the rotational speed of the magnetic machining tool.

In this study, the weight of the magnetic machining tool is 522.4 g and the rotational radius of the magnetic machining tool is 39.55 mm. At three rotational speeds of magnetic machining tool that 32 rpm, 122 rpm and 212rpm, the centrifugal force generated by the magnetic machining tool was calculated, as shown in Table 4.4. It can be seen that as the rotational speed increases, the centrifugal force increases, so the roundness improvement also increases. This is consistent with the previous analysis results.

Table 4.4 Value of the centrifugal force

Rotational speed of the magnetic machining tool	Centrifugal force
32 rpm	0.228 N
122 rpm	3.358 N
212 rpm	10.153 N

Furthermore, the roundness improvement per revolution under the influence of centrifugal force was calculated, as shown in Table 4.5. It can be seen that as the rotational speed increases, the roundness improvement increases.

Table 4.5 Value of the Roundness improvement per revolution

Rotational speed of the magnetic machining tool	Roundness improvement per revolution
122 rpm	0.0028 μm
212 rpm	0.0046 μm

4.4.2 Influence of rotational speed of the workpiece

4.4.2.1 Experimental conditions

The experimental conditions are shown in Table 4.6. The nonferromagnetic SUS 304 stainless steel tube was used as the workpiece. In order to study the effect of the rotational speed of workpiece, setting the rotational speed of magnetic pole unit is the same (122 rpm), while the rotational speed of workpiece is 35 rpm, 115 rpm and 195 rpm, respectively. The finishing time is 100 min, to understand the changes of roundness, surface roughness and material removal, each stage finishing time is 20 min.

Table 4.6 Experimental conditions

Workpiece	SUS304 stainless steel tube Ø89.1×79.1×200 mm Clearance: 7 mm (Thickness of tube is equivalent to 10 mm.) Rotational speed: 35 rpm 115 rpm 195 rpm
Magnetic machining tool	Magnet: Nd-Fe-B permanent magnet Yoke: SS400 steel Molding material: Polymer
Magnetic pole unit	Magnet: Ferrite permanent magnet 50×35×26 mm Yoke: SS400 steel Rotational speed: 122 rpm Reciprocating speed: 25 mm/s
Magnetic particles	Electrolytic iron particles: 1680 μm in mean dia., 24 g
Abrasive particles	WA #400, 2.5 g
Grinding fluid	Water-soluble grinding fluid (SCP-23): 30 g
Finishing width	80 mm
Finishing time	100 min (each stage 20 min)

4.4.2.2 Experimental results and discussion

Fig.4.12 shows the changes in surface roughness and material removal with finishing time. It can be seen that because of the diameter of the magnetic particles and the abrasives used in the experiment are the same, the final surface roughness after finishing is almost the same. And as the rotational speed of the workpiece increases, the amount of material removal increases.

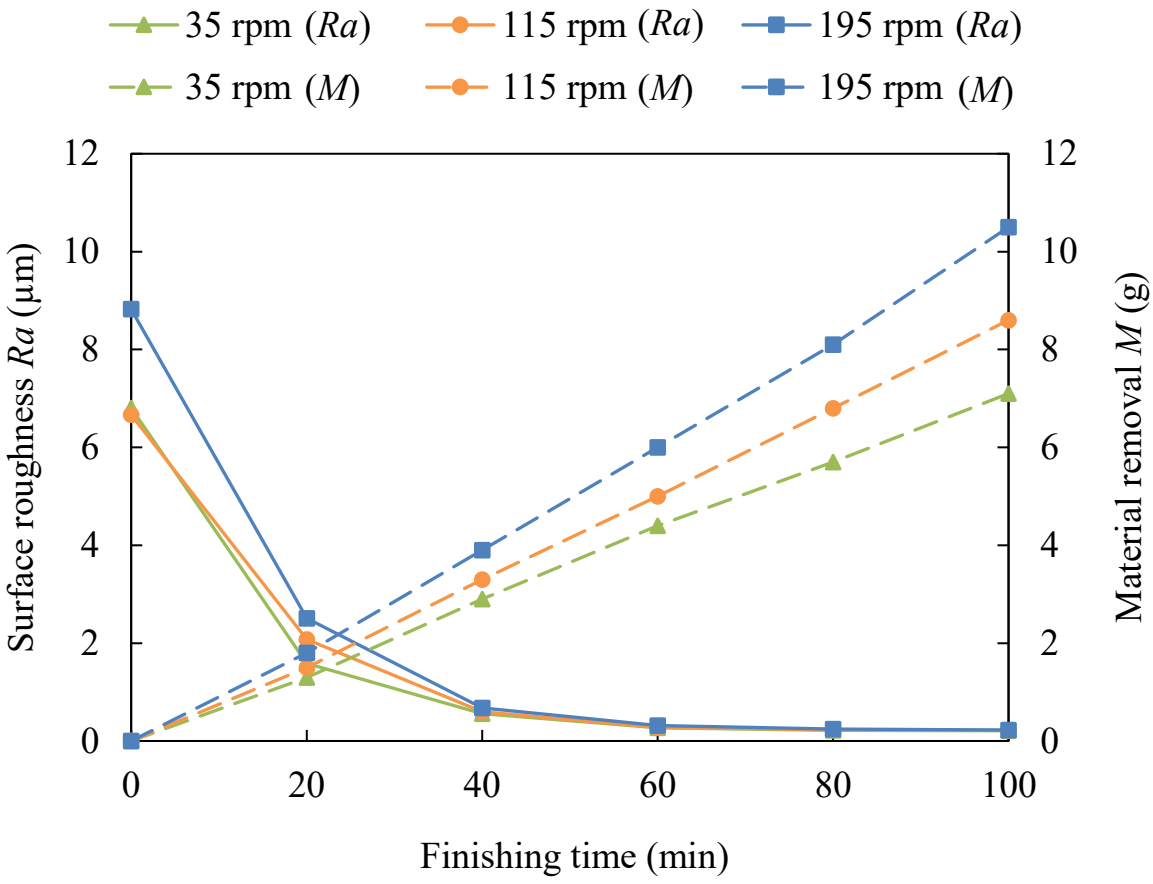

Fig.4.12 Changes in material removal and surface roughness with finishing time

Fig.4.13 shows the roundness improvement with finishing time. It can be seen that the roundness improvement increases with an increase in rotational speed of the workpiece.

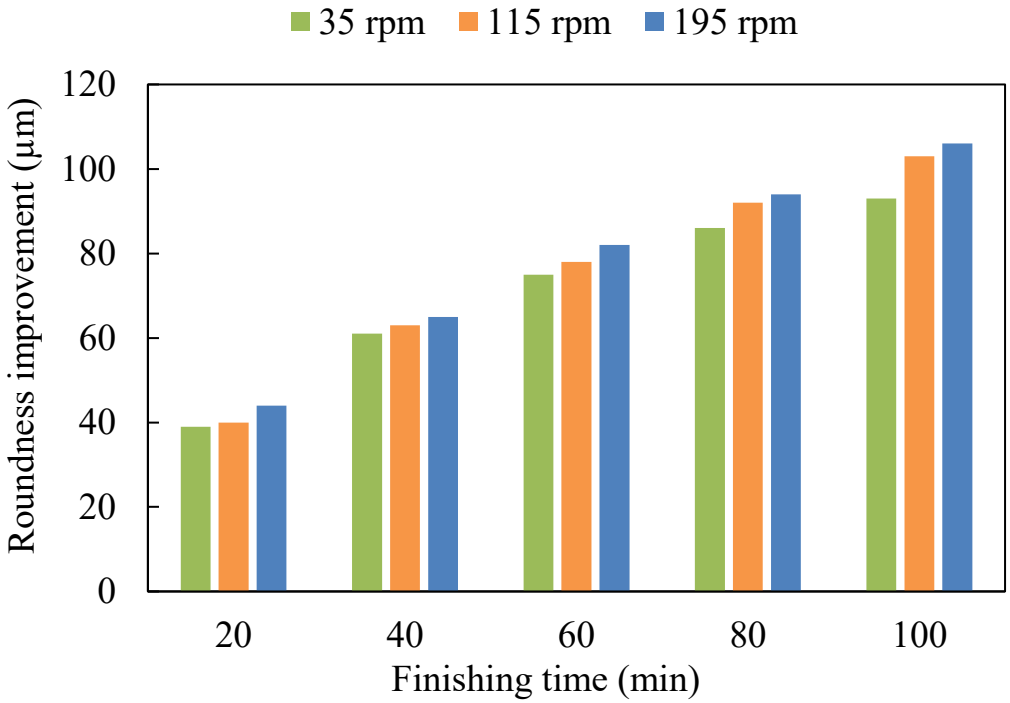

Fig.4.13 Roundness improvement with finishing time

Fig.4.14 shows the roundness profiles of the internal surface of the tube before and after finishing. For different rotational speeds of the workpiece, the roundness is improved from 166 μm to 73 μm in the case of 35 rpm, from 166 μm to 63 μm in the case of 115 rpm, and from 178 μm to 66 μm in the case of 195 rpm. It can be concluded that with the increase of the rotational speed of workpiece, the number of finishing times of workpiece increases, so the finishing results become better.

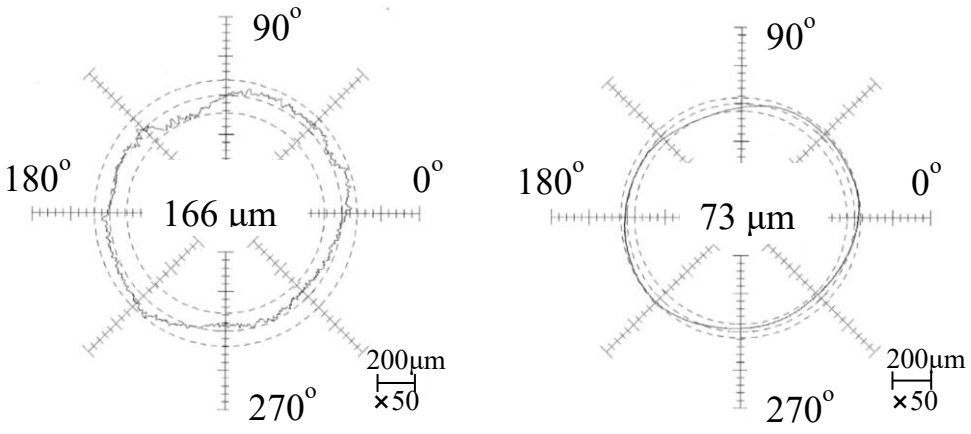

Before finishing

After finishing

(a) 35 rpm

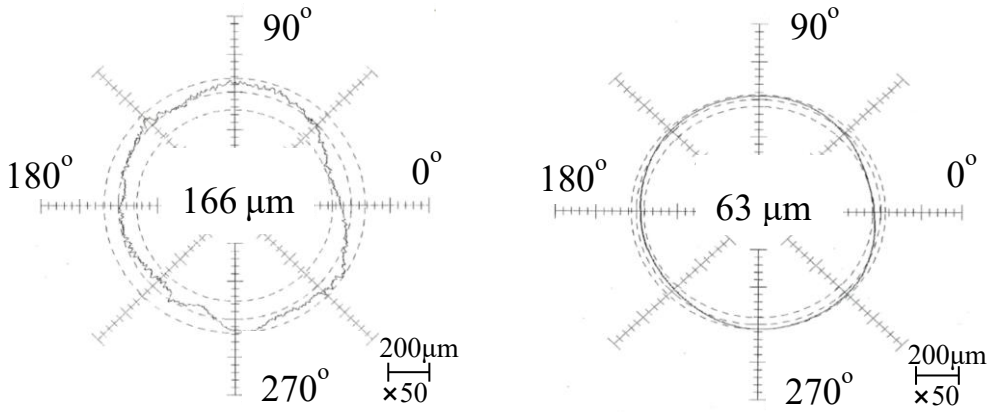

Before finishing　　After finishing

(b) 115 rpm

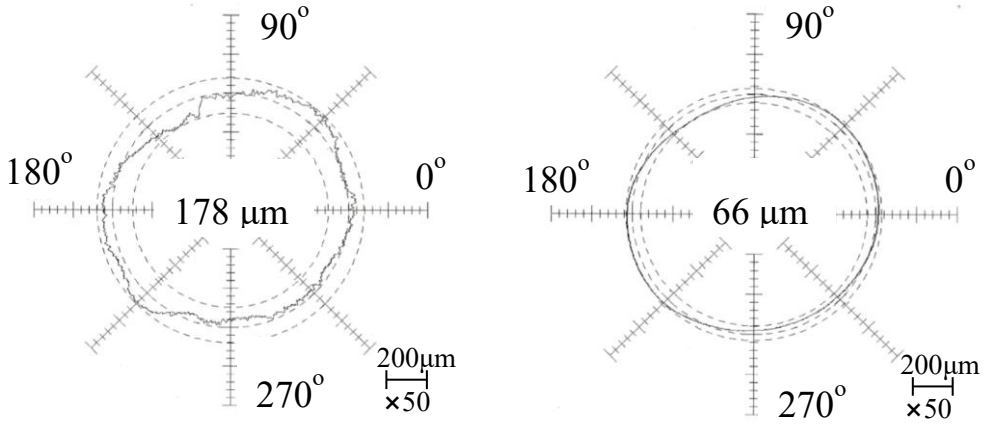

Before finishing　　After finishing

(c) 195 rpm

Fig.4.14 Roundness profiles of the internal surface of tube before and after finishing

4.4.3 Comprehensive discussion on influence of rotational speed

Through the above discussion, it is clear that when the rotational speed of the workpiece is the same, the roundness improvement increases with the increase of the rotational speed of the magnetic machining tool, and when the rotational speed of the magnetic machining tool is the same, the roundness improvement increases with the increase of the rotational speed of the workpiece. At the same time, it is necessary to clear which rotational

speed has a greater influence on the roundness improvement. At different rotational speeds, the difference in roundness improvement is caused. Therefore, it is discussed by compare the roundness improvement with relative motion for one circle under the influence of rotational speed difference. Fig.4.15 shows the roundness improvement with the magnetic machining tool and the workpiece rotate relative to each other for one circle. It can be seen that when the magnetic machining tool and the workpiece rotate relative for one circle, the rotation of the magnetic machining tool has a greater influence on the roundness improvement. Therefore, in this process, the rotational speed of magnetic processing tool is set to be greater than that of workpiece.

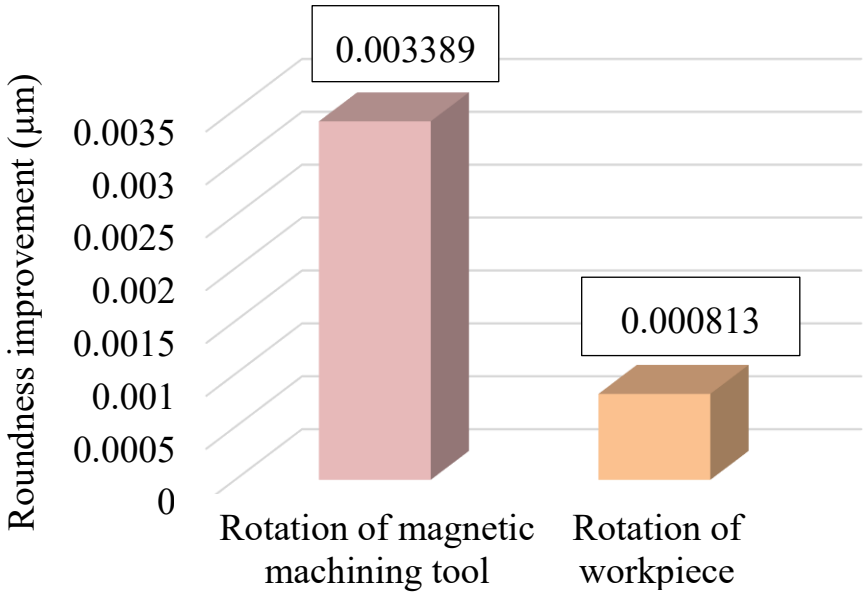

Fig.4.15 Roundness improvement with the magnetic machining tool and workpiece rotate relative for one circle

4.5 Conclusions

1. The force analysis diagram of the magnetic machining tool in the model doing uniform rotational motion was performed. And the dynamic

equation of magnetic abrasive tool was established. Three kinds of reciprocating velocity (27 mm/s, 38 mm/s and 58 mm/s) of magnetic pole unit were compared by the experiments. The experiments result shows that low reciprocating velocity of magnetic pole unit is beneficial to the material removal and also beneficial to the improvement of interior roundness of thick SUS304 stainless steel tube. In the case of the reciprocating velocity of the magnetic pole unit is 27 mm/s, the roundness of tube is from 167 μm to 59 μm and the decrease of roundness is 108 μm.

2.The improvement of form accuracy (roundness) of the thick tube by using two different kinds of magnetic particles in the first-stage of processing was discussed. In the first-stage of processing that both using the electrolytic iron particles (1680 μm in mean dia.) and the KMX magnetic particles (1000~1680 μm in mean dia.) can improve the roundness of the thick tube by magnetic abrasive finishing using a magnetic machining tool. And the improvement is better by using the KMX magnetic particles.

3.The mechanism of roundness improvement by the internal magnetic abrasive finishing process using magnetic machining tool and the experiments were carried out on nonferromagnetic SUS 304 stainless steel tube. Through analyzing the finishing force generated by magnetic machining tool, it is concluded that as the rotational speed of the magnetic machining tool increases, the tangential and normal finishing forces increase, and the resultant finishing force also increases, so the faster rotational speed of the magnetic machining tool is beneficial to roundness improvement when the rotational speed of workpiece is the same. And through discussion on different rotational speed of workpiece, it can be concluded that with the increase of the rotational speed of workpiece, the number of finishing times of workpiece increases, so the finishing results become better. Furthermore, according to compare the roundness

improvement with relative motion for one circle under the influence of rotational speed difference, when the magnetic machining tool and the workpiece rotate relative for one circle, the rotation of the magnetic machining tool has a greater influence on the roundness improvement. Therefore, in this process, the rotational speed of magnetic processing tool is set to be greater than that of workpiece.

Chapter V Discussion on the influence of magnetic particles distribution on magnetic machining tool

5.1 Introduction

Furthermore, the process of MAF also can realize the finishing of plane, cylindrical outer surface and deburring. Shinmura et al. studied the basic principle and finishing characteristics of MAF, and developed a plane magnetic finishing device using a stationary type electromagnet, it was verified that this process can achieve precision finishing of plane [501-503]. And also developed the magnetic abrasive finishing and its equipment by applying a rotating magnetic field to finish the outer surface of cylindrical workpiece [504]. Yamaguchi et al. proposed the magnetic abrasive finishing process using multiple pole tip systems to finish the entire internal surface of capillary tubes and a method to define a pole tip feed length that can achieve a uniform surface roughness on the entire target surface by calculating the pole tip coverage time over the target surface. And it has been clarified the finishing characteristic and mechanism and showed the effects of the tool's magnetic properties on the tool and abrasive motion and the interior finishing characteristic of capillary tubes [505-507]. Yin et al. studied the polishing characteristics and its mechanisms of three vibration modes in vibration assisted magnetic abrasive polishing and using this process to deburr for magnesium alloy and it has been concluded that deburring efficiency considerably increases with vibration assistance [508,509].

In this process, the magnetic force (finishing force) can be enhanced by

placing a magnetic machining tool inside the tube, which consists of four permanent magnets and a yoke. And the inner surface of the tube is finished by the magnetic particles that are magnetically adsorbed on the magnetic processing tool. According to the distribution of magnetic force lines, the magnetic machining tool is divided into three areas, which are left area, middle area and right area, as shown in Fig.5.1. In this paper, the distribution of four kinds of magnetic particles on magnetic processing tools is adopted, which is only distributed on the middle area, on the left and right areas, on the middle and right areas, and on the left, middle and right areas, as shown in Fig.5.2.

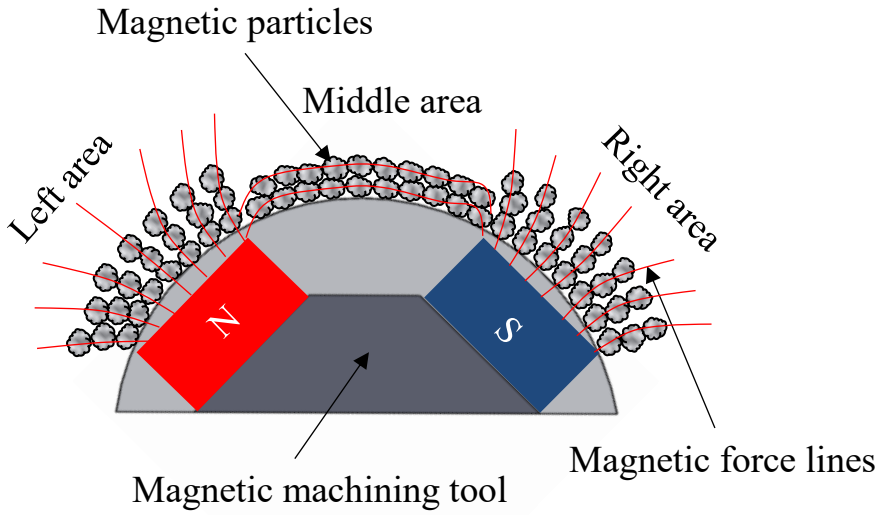

Fig.5.1 Distribution of magnetic force lines of magnetic machining tool

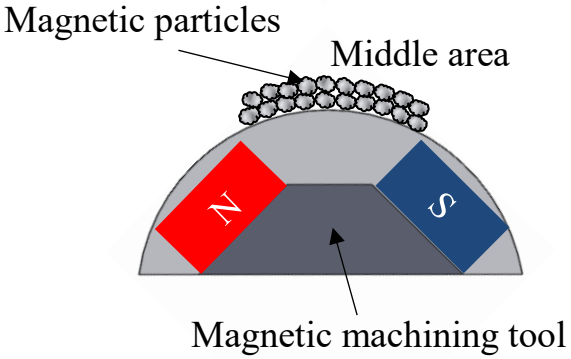

(a) Only placing magnetic particles on the middle area

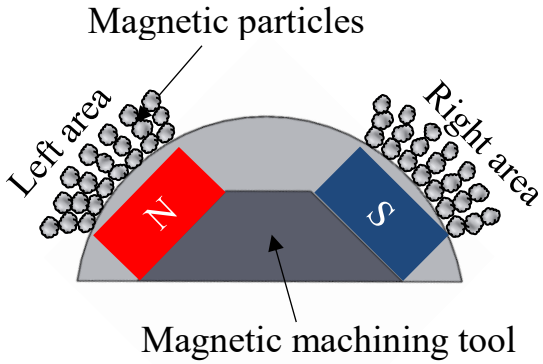

(b) Placing magnetic particles on the left and right areas

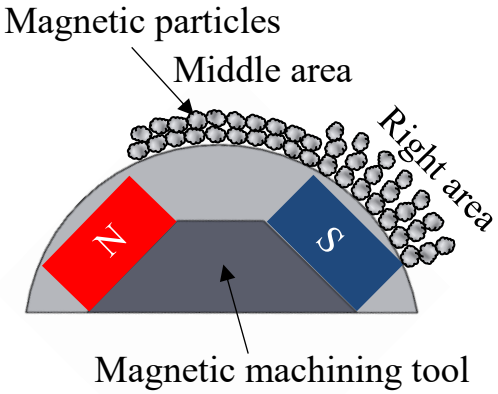

(c) Placing magnetic particles on the middle and right areas

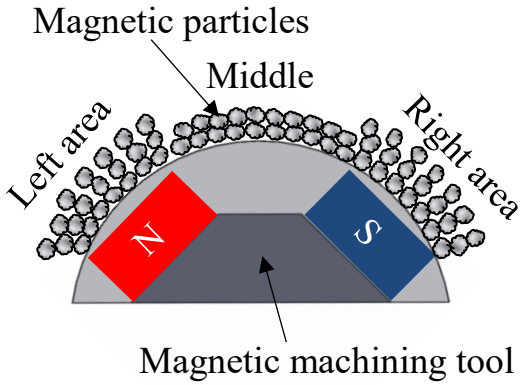

(d) Placing magnetic particles on the three areas

Fig.5.2 Models for the distribution of magnetic particles on magnetic machining tool

5.2 Analysis of roundness improvement by the shape change of roundness curve

Fig.5.3 shows the roundness curves before and after finishing. Seven peak points and eight trough points are selected from the roundness curve before finishing to form the peak polygon and trough polygon. From the roundness curves after finishing, it can be seen that the result of roundness improvement is that the peak polygon is close to the trough polygon, and the edge of the polygon is close to zero, that is, the polygon is improved to a circle. Fig.5.4 (a) shows the change of the polygon after finishing the peak point A, which reduces the number of sides of the polygon and makes the figure close to a circle. Fig.5.4 (b) shows the change of polygon after finishing the trough point B, which increases the number of sides of the polygon, and it is unfavorable for the figure to approach the circle. Therefore, it is concluded that removal of the peak of the roundness curve is beneficial to improvement of the roundness.

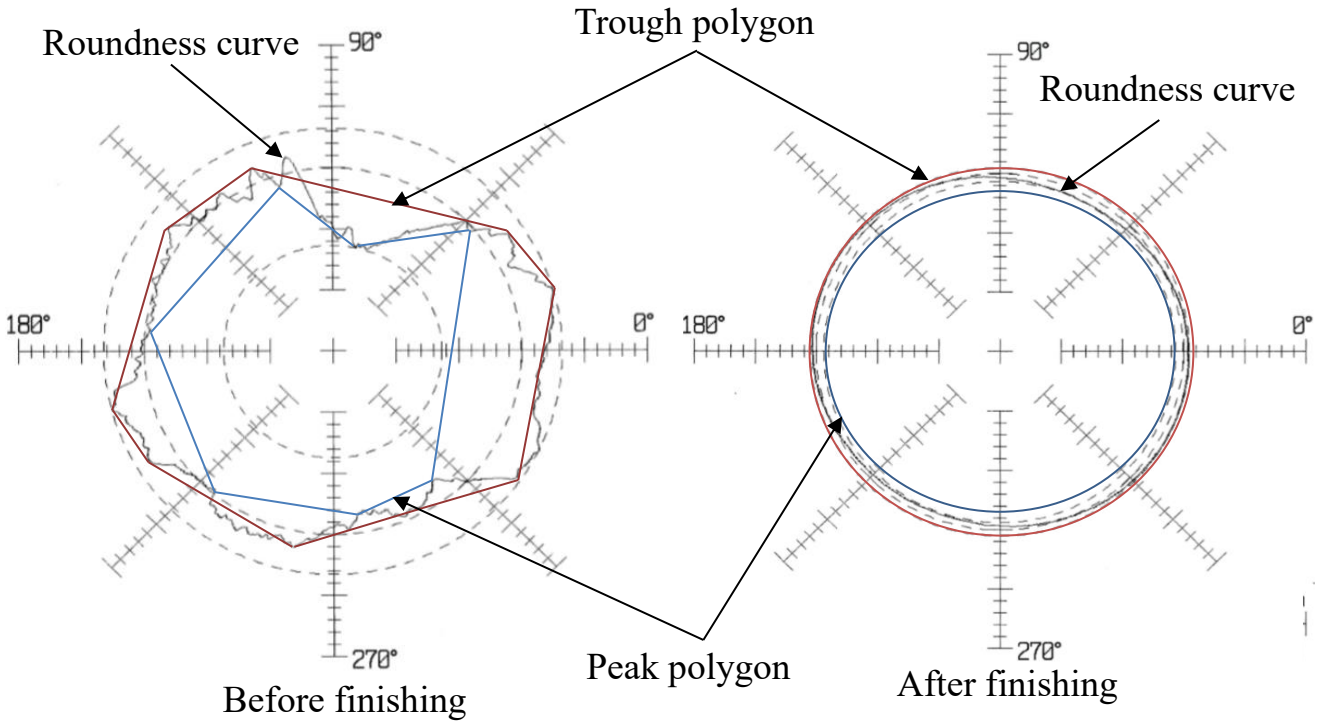

Fig.5.3 Roundness curves before and after finishing

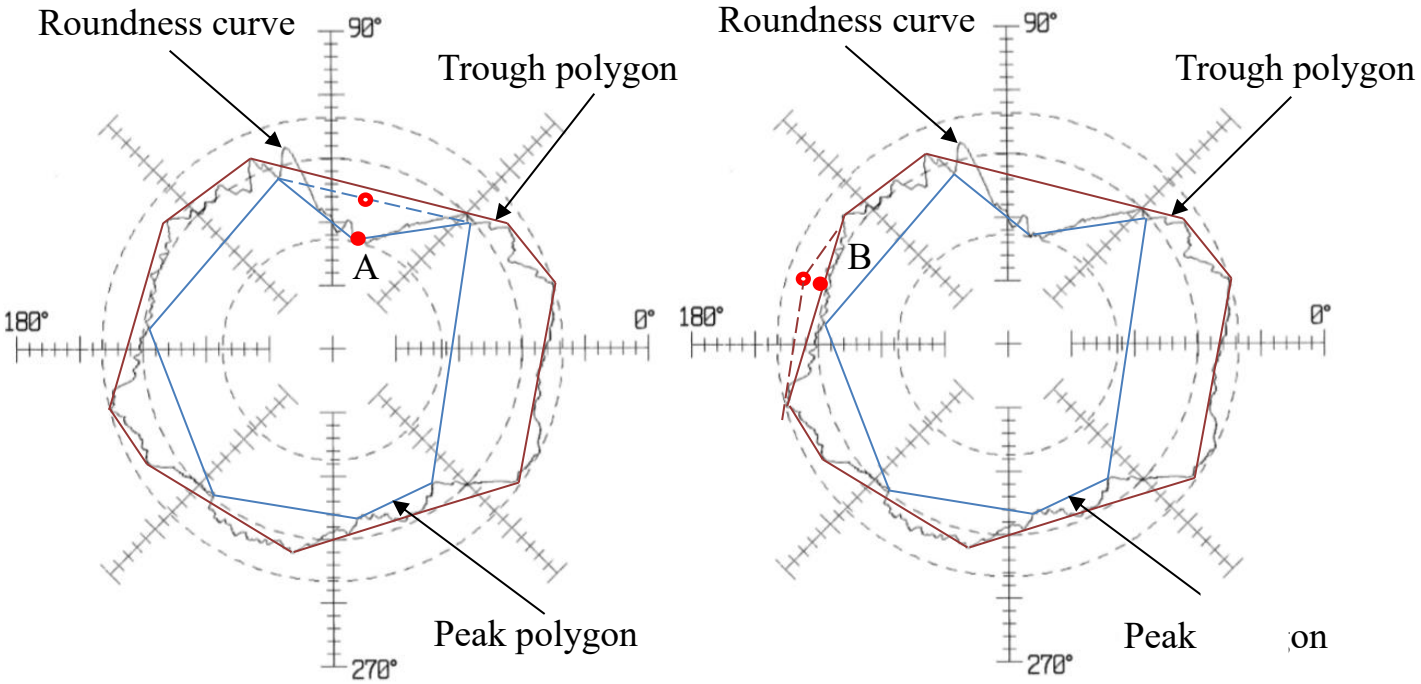

(a) At the peak point (b) At the trough point

Fig.5.4 Changes of the polygon after finishing

According to the analysis of the change of the roundness improvement by applying the Fourier series, it is also found that the removal of the peaks of the roundness curve is beneficial to the improvement of the roundness. When the initial roundness curve of the internal surface of the tube has n peaks, the curve wavelength λ is the circumference 2C/n.

In this process, after finishing, due to the magnetic force generated by the magnetic machining tool and the magnetic pole unit exerts pressure on the magnetic particles, a fixed magnetic brush is formed. In addition, due to the circumference length of the magnetic machining tool is about half of the circumference of the internal surface of the tube and the initial roundness curve of the internal surface of the tube has greater than 2 peaks, discussing the influence of the circumferential length of fixed magnetic brush. As shown in Fig.5.5 (a), in the case of the circumferential length of fixed magnetic brush L is less than the wavelength λ, the number of finishing times (the number of rotations) at the peak point is N.

As shown in Fig.5.5 (b), in the case of the circumferential length of fixed magnetic brush L is greater than the wavelength λ, the number of finishing times of the roundness curve peak is increased.

Then when the circumferential length of the fixed magnetic brush is x λ≤ L< (x+1/2) λ, where 1≤x≤C/λ , C is the perimeter of internal surface of tube, and then the number of finishing times at peak point is 2xN.

And when the circumferential length of the fixed magnetic brush is (x+1/2)λ≤ L< (x+1) λ, where 1≤x≤C/λ, C is the perimeter of internal surface of workpiece, and then the number of finishing times at peak point is (2x+1) N.

Therefore, it can be concluded that when the circumferential length of the fixed magnetic brush is long, the number of times of finishing the peak point increases, so it is beneficial to roundness improvement.

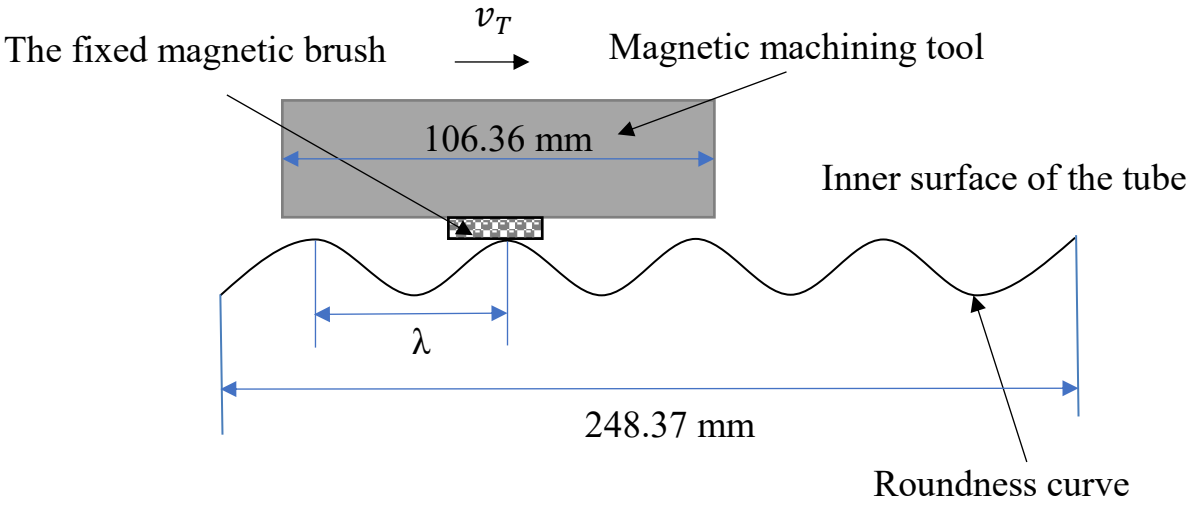

(a) L ＜ λ

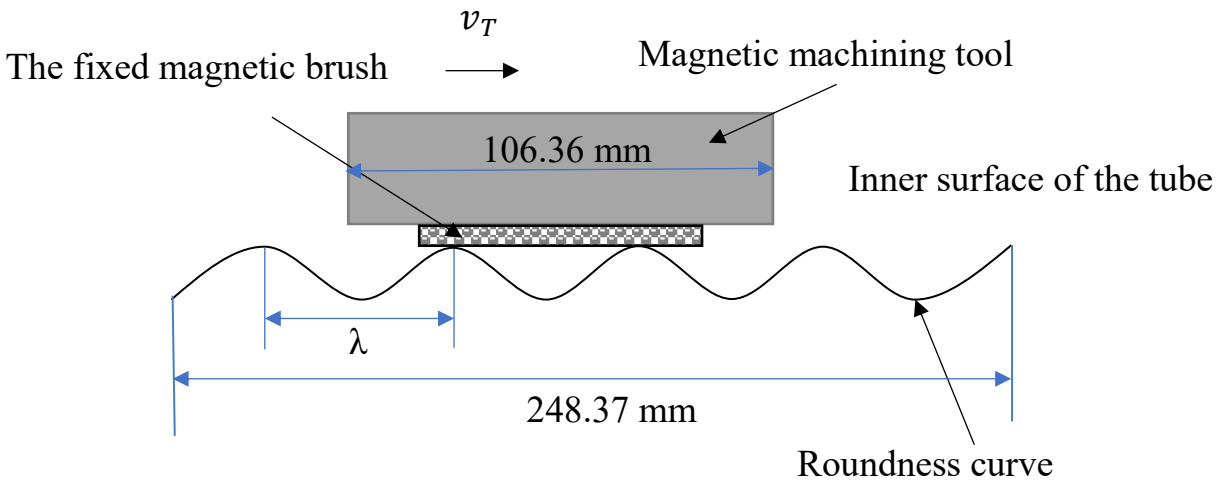

(b) L ≥ λ

Fig.5.5 Diagram of the relationship between the circumferential length of fixed magnetic brush and the wavelength of roundness curve

5.3 Only distributing magnetic particles on one area

5.3.1 Experimental conditions and method

The experimental conditions are shown in Table 5.1. In this part, only placing magnetic particles on the middle area, and the weight of magnetic particles is 12 g, 13 g and 14 g, respectively. Fig.5.6 (a) shows the photographs of distribution of magnetic particles on the magnetic machining tool before finishing. When the thickness of the magnetic brush formed by magnetic particles is 2.382 mm and the same length in the axial direction is 43 mm, the length of circumferential direction is 45 mm, 49 mm and 53 mm, respectively. The finishing time is 60 min, to understand the changes of roundness, surface roughness and material removal, each stage finishing time is 10 min.

Table 5.1 Experimental conditions

Workpiece	SUS304 stainless steel tube Ø89.1×79.1×200 mm Clearance: 7 mm (Thickness of tube is equivalent to 10 mm) Rotational speed: 80 rpm
Magnetic machining tool	Magnet: Nd-Fe-B permanent magnet Yoke: SS400 steel Molding material: Polymer
Magnetic pole unit	Magnet: Ferrite permanent magnet 50×35×26 mm Yoke: SS400 steel Rotational speed: 150 rpm Reciprocating speed: 25 mm/s
Magnetic particles	Electrolytic iron particles: 1680 μm in mean dia. Condition A1: On the middle area, 12 g Condition A2: On the middle area, 13 g Condition A3: On the middle area, 14 g
Abrasive particles	WA #400, 2.5 g
Grinding fluid	Water-soluble grinding fluid (SCP-23): 30 g
Finishing width	80 mm
Finishing time	60 min (each stage 10 min)

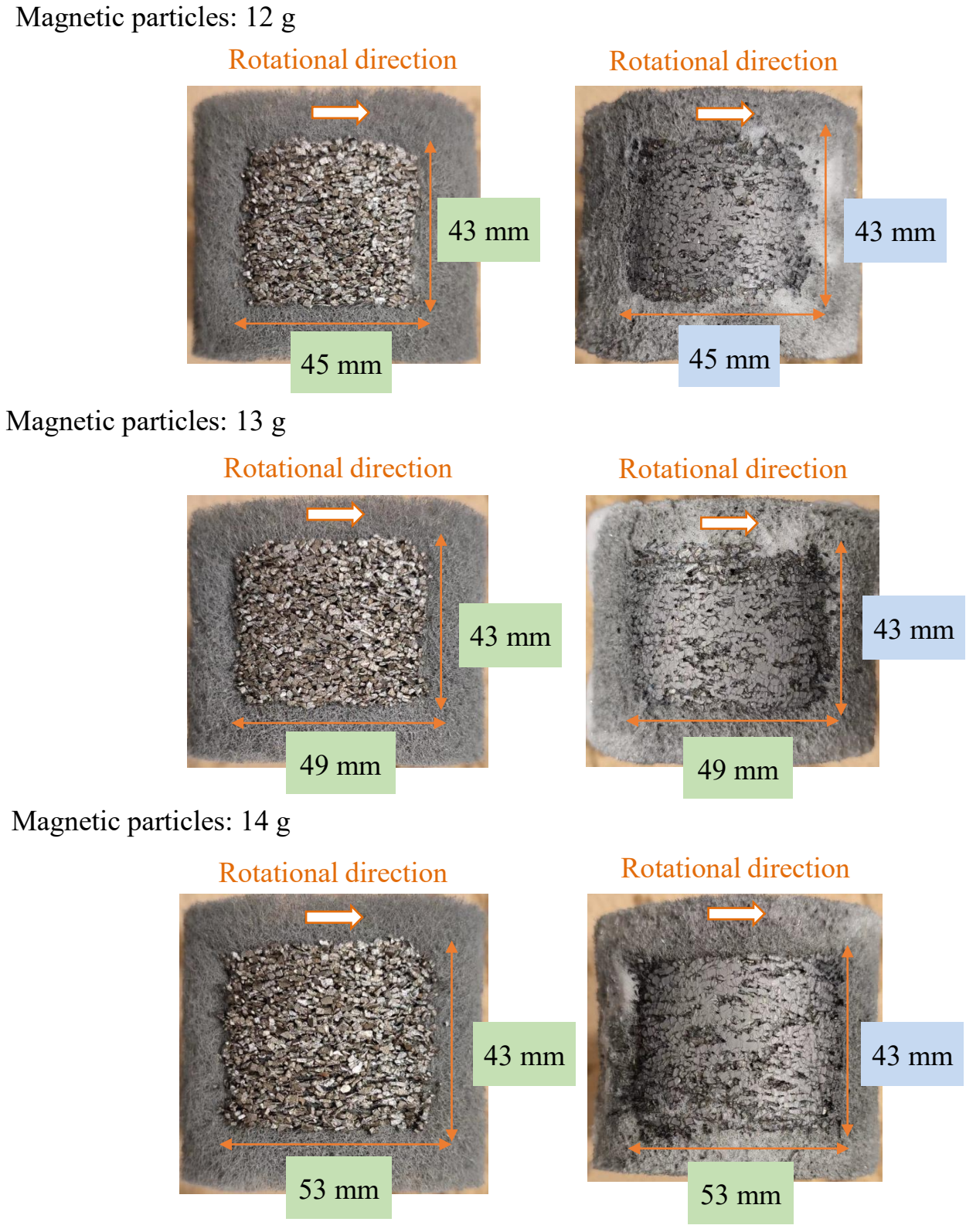

Fig.5.6 Photographs of magnetic machining tool before and after finishing

5.3.2 Experimental results and discussion

Fig.5.7 shows the changes in surface roughness and material removal with finishing time. It can be seen that the material removal increases and the final roughness decreases with the increase of the weight of magnetic particles.

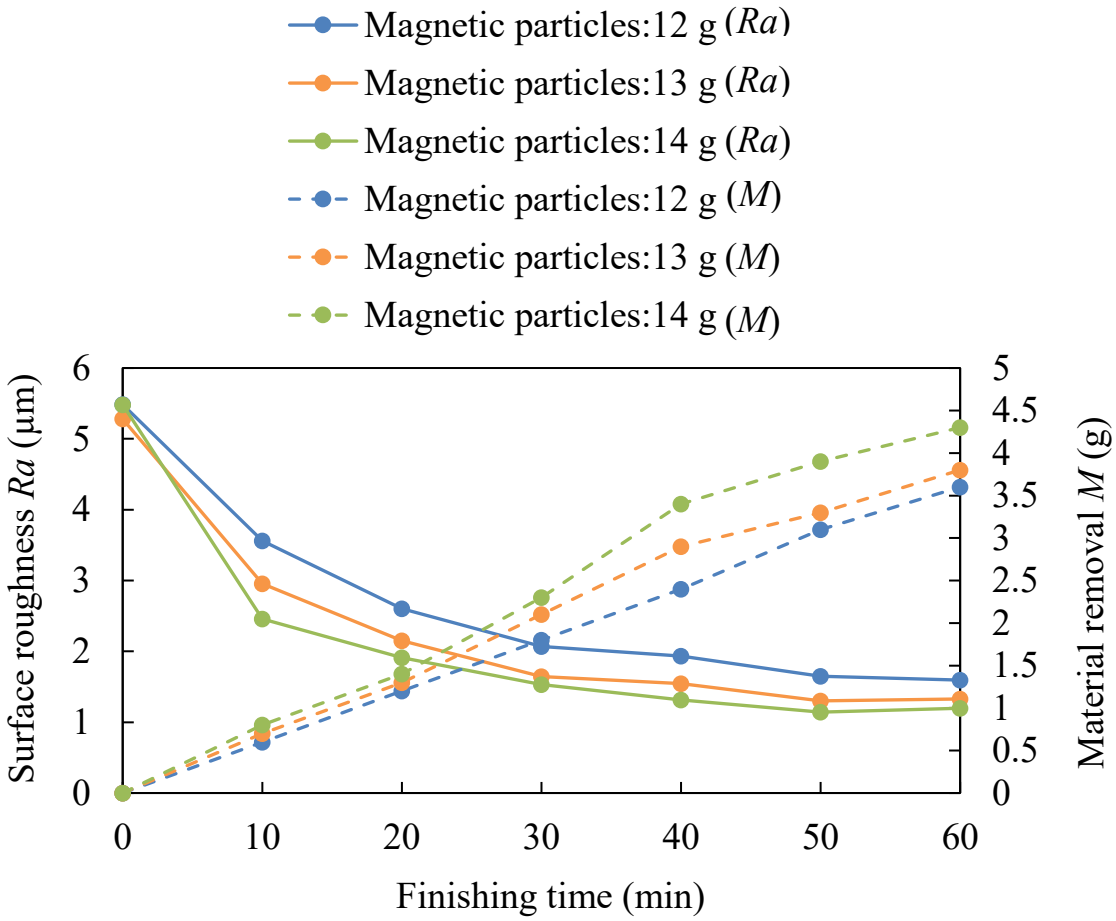

Fig.5.7 Changes in material removal and surface roughness with finishing time

Fig.5.8 shows the changes in roundness with finishing time. It can be seen that the roundness improvement increases with the increase of the weight of magnetic particles. Fig.5.6 (b) shows the photographs of the magnetic machining tool after finishing. It can be seen that the circumferential arc length of fixed magnetic brush increases with the increase of the weight of magnetic particles, 45 mm, 49 mm and 53 mm, respectively. This is because that when the circumferential length of fixed

magnetic brush is long, the removed value of roundness curve is large, so it is beneficial to roundness improvement.

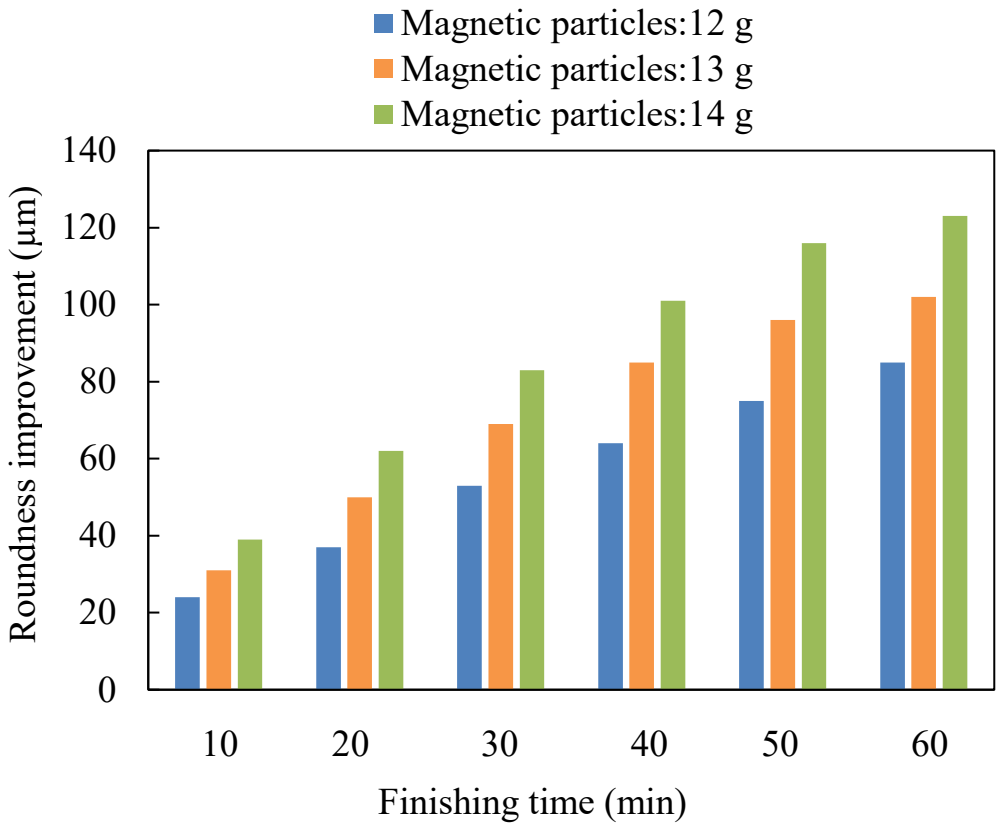

Fig.5.8 Roundness improvement with finishing time

Fig.5.9 shows the roundness profiles of the internal surface of the tube before and after finishing. For different weight of magnetic particles, the roundness is improved from 398 μm to 313 μm in the case of 12 g, from 403 μm to 301 μm in the case of 13 g, and from 396 μm to 273 μm in the case of 14 g.

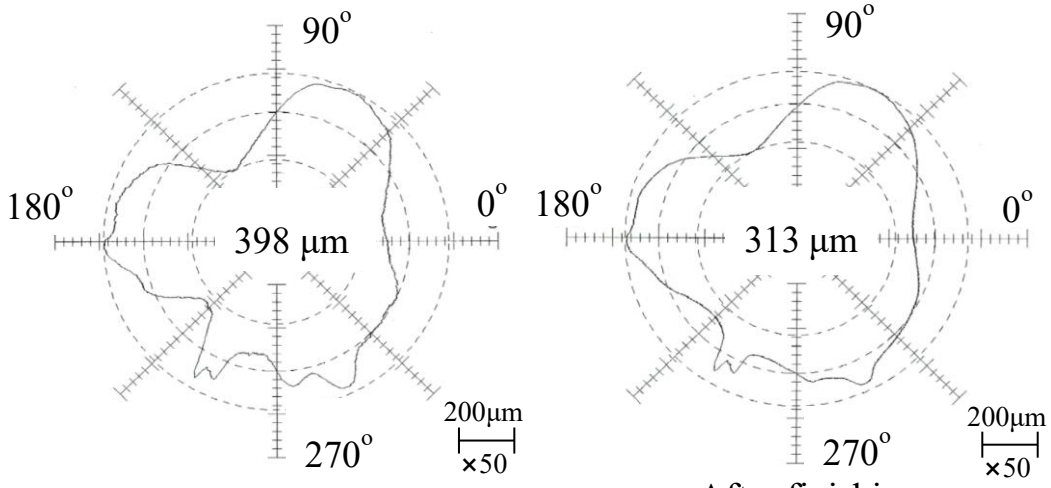

Before finishing After finishing

(a) Magnetic particles:12 g

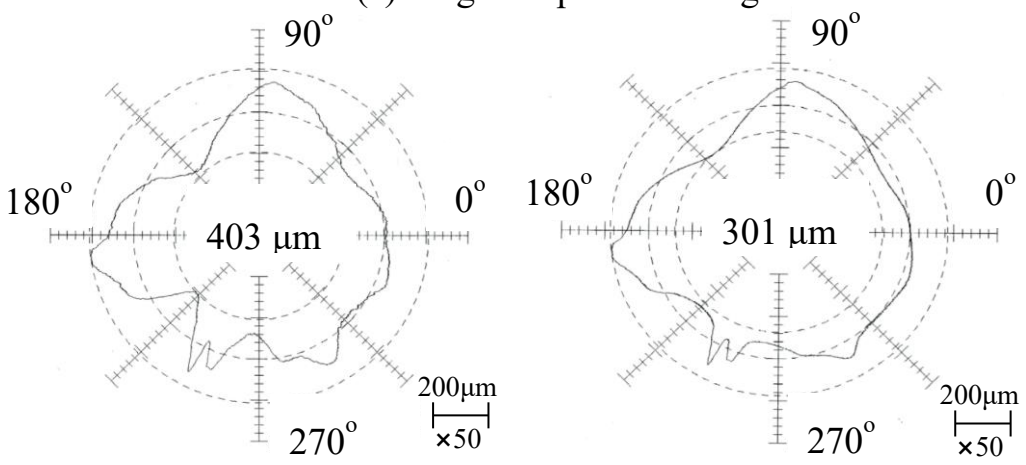

Before finishing After finishing

(b) Magnetic particles:13 g

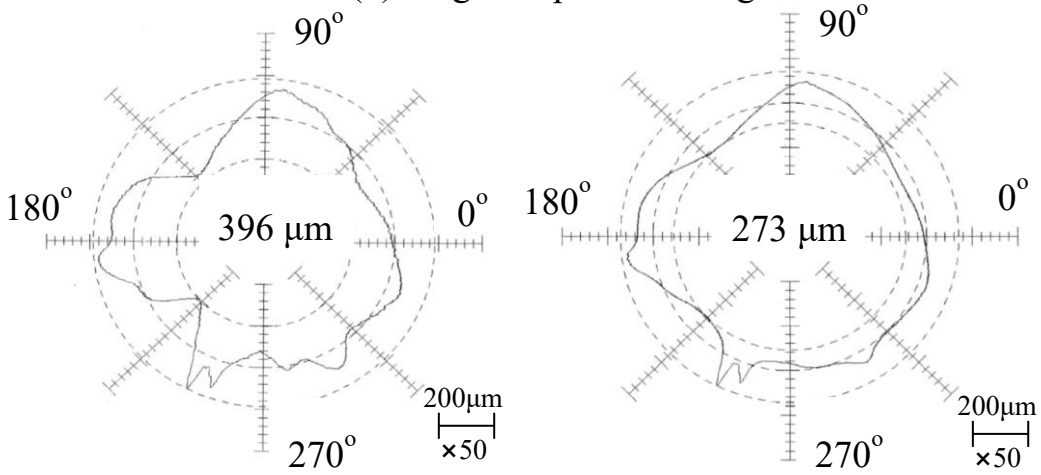

Before finishing After finishing

(c) Magnetic particles:14 g

Fig.5.9 Roundness profiles of the internal surface of the tube before and after finishing

5.4 Distributing magnetic particles on two areas and three areas

5.4.1 Experimental conditions and method

The experimental conditions are shown in Table 5.2. Fig.5.10 (a) shows the photographs of distribution of magnetic particles on the magnetic machining tool before finishing. In this part, in the experiment A placed 13 g electrolytic iron particles on the left area and right area respectively, in the experiment B placed 12 g electrolytic iron particles on the middle area and 13 g electrolytic iron particles on the right area, and in experiment C placed 12 g electrolytic iron particles on the middle area, 13 g electrolytic iron particles on the left area and right area respectively. And the thickness of magnetic particles in each area is 2.382 mm. The finishing time is 60 min, to understand the changes of roundness, surface roughness and material removal, each stage finishing time is 10 min.

Table 5.2 Experimental conditions

Workpiece	SUS304 stainless steel tube Ø89.1×79.1×200 mm Rotational speed: 80 rpm
Magnetic machining tool	Magnet: Nd-Fe-B permanent magnet Yoke: SS400 steel Molding material: Polymer
Magnetic pole unit	Magnet: Ferrite permanent magnet 50×35×26 mm Yoke: SS400 steel Rotational speed: 150 rpm Reciprocating speed: 25 mm/s

Magnetic particles	Electrolytic iron particles: 1680 μm in mean dia. Experiment A: On the left and right areas 13×2 g Experiment B: On the middle area 12 g and on the right area 13 g Experiment C: On the middle area 12 g, on the left and right areas 13×2 g
Abrasive particles	WA #400, 2.5 g
Grinding fluid	Water-soluble grinding fluid (SCP-23): 30 g
Working gap	10 mm
Finishing width	80 mm
Finishing time	60 min (each stage 10 min)

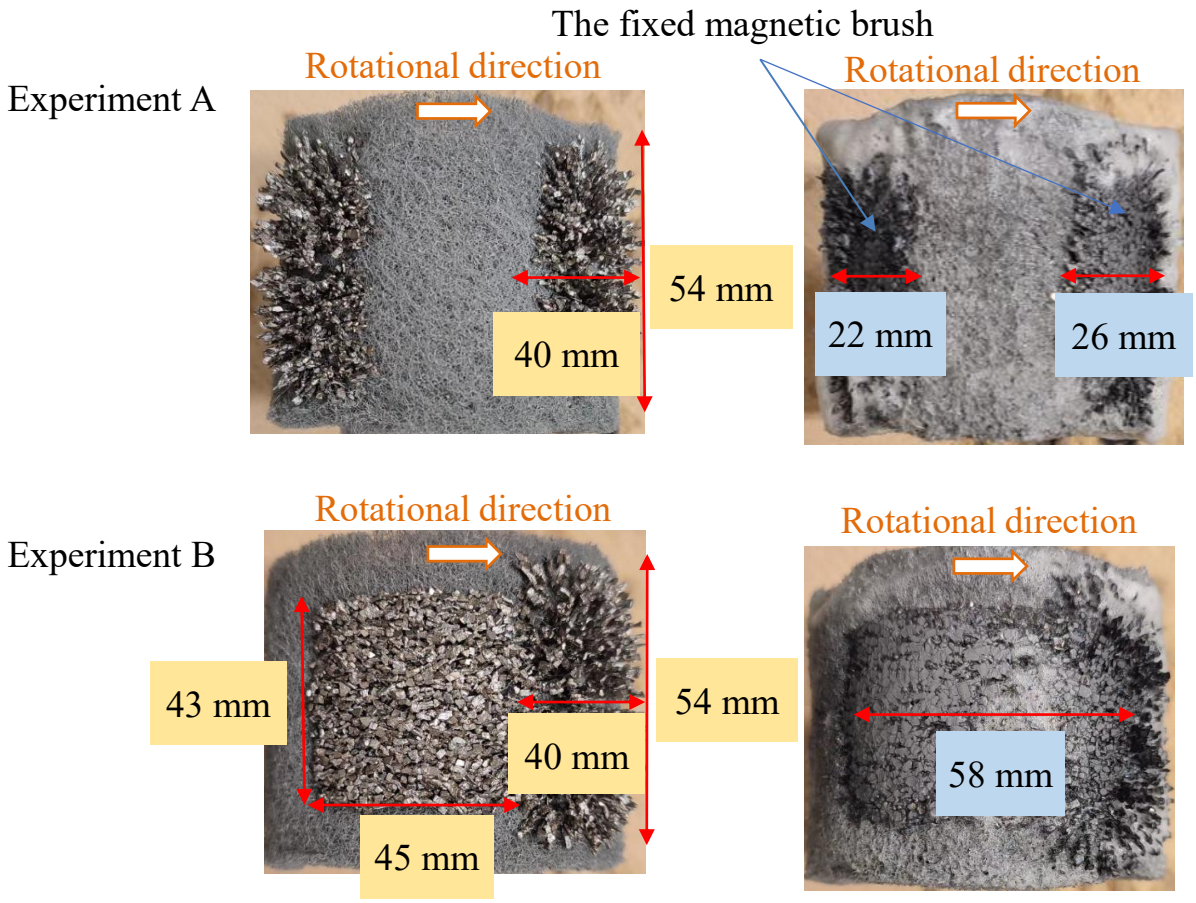

Fig.5.10 Photographs of magnetic machining tool before and after finishing

5.4.2 Experimental results and discussion

Fig.5.11 shows the changes in surface roughness and material removal with finishing time. It can be seen that in experiment C, the final surface roughness after finishing is the best and the amount of material removal is the largest.

Fig.5.12 shows the changes in roundness with finishing time. It can be seen that in experiment C, the value of roundness improvement is the largest. Fig.5.10 (b) shows the photographs of the magnetic machining tool after finishing. The magnetic particles on the left area and right area of the magnetic machining tool form magnetic brushes in the direction of the magnetic force line before finishing. After finishing, the pressure exerted by some magnetic particles on the magnetic force of the magnetic machining tool and the magnetic pole unit forms a fixed magnetic brush. It can be seen that in experiment A, the fixed magnetic brush is discontinuous in the circumferential direction, the left is 22 mm and the right is 26 mm, the total circumferential length of the fixed magnetic brush is 48 mm, in

experiment B, the circumferential length of the fixed magnetic brush is 58 mm, and in experiment C, the circumferential length of the fixed magnetic brush is 76 mm. Therefore, it can be concluded that as the circumferential length of the fixed magnetic brush increases, the roundness improvement increases. Because the fixed magnetic brush will only remove material at the peak of roundness curve during finishing, which is beneficial to the roundness improvement, regarding this part as productive particles. The magnetic particles of flexible magnetic brush remove material not only at the peak, but also at the trough of roundness curve, which is unbeneficial to the roundness improvement, and this part is regarded as unproductive particles. Moreover, if the arc of the fixed magnetic brush in contact with the circumferential direction of the inner surface of the workpiece is long, more peak materials will be removed, and it is more conducive to achieve the circular shape of the inner surface.

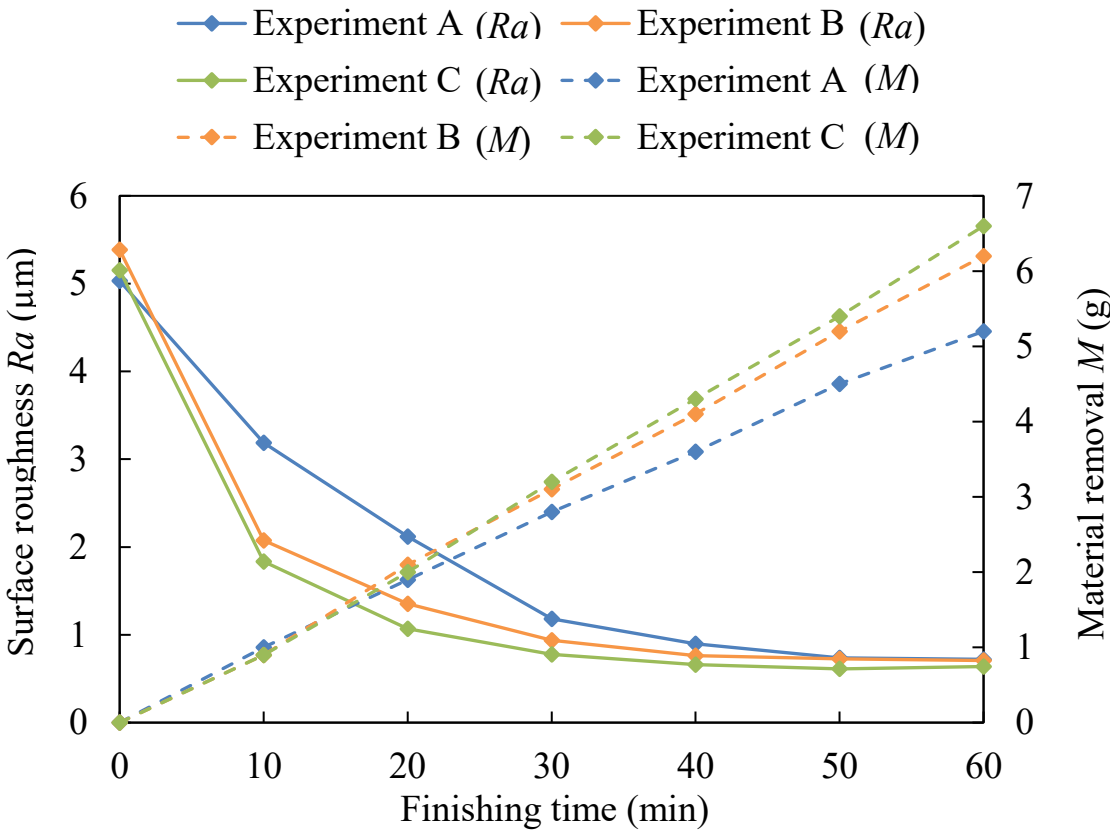

Fig.5.11 Changes in material removal and surface roughness with finishing time

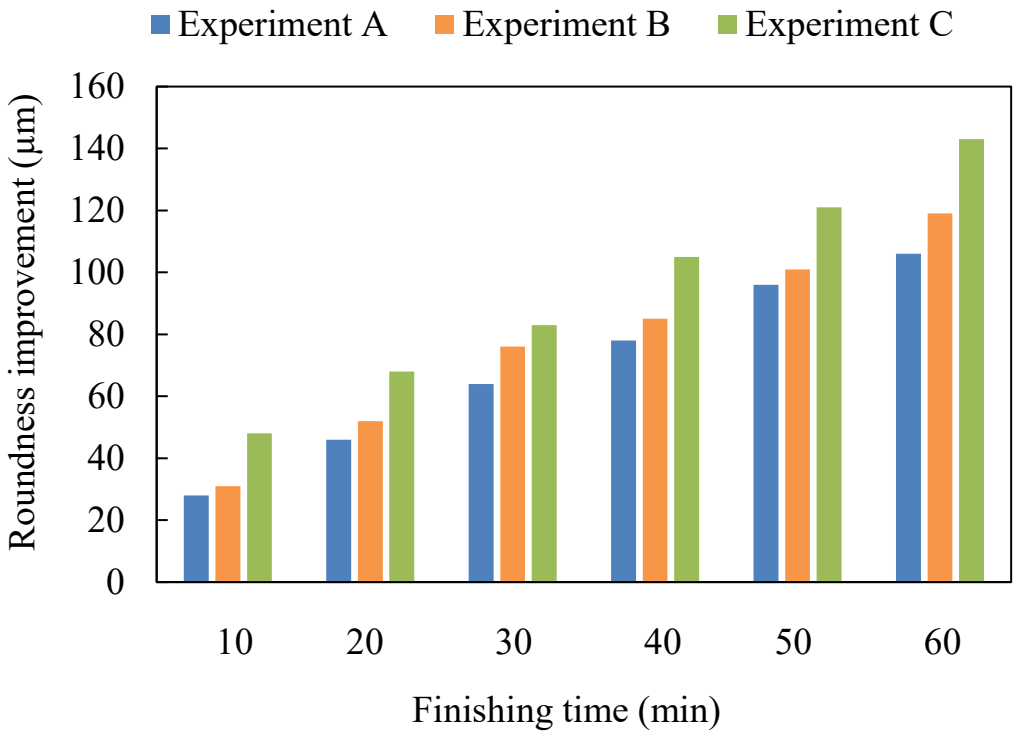

Fig.5.12 Roundness improvement with finishing time

Fig.5.13 shows the diagrams of straight-line expansion of roundness curve before and after finishing. The evaluation method of roundness measurement in this paper is the least square circle (LSC). According to the roundness evaluation method, the removal of wave trough is beneficial to the improvement of roundness. Taking 5 trough points on the roundness curve to discuss the influence of roundness improvement. The removal of point P is related to the evaluation of roundness. At point P, the roundness improvement values are 106 μm, 119 μm and 143 μm, respectively. And the sum of roundness improvements at the five trough points is 422 μm ,439 μm and 461 μm, respectively. Moreover, under condition C, the removal amount is the largest because the circumferential length of the fixed magnetic brush is the largest.

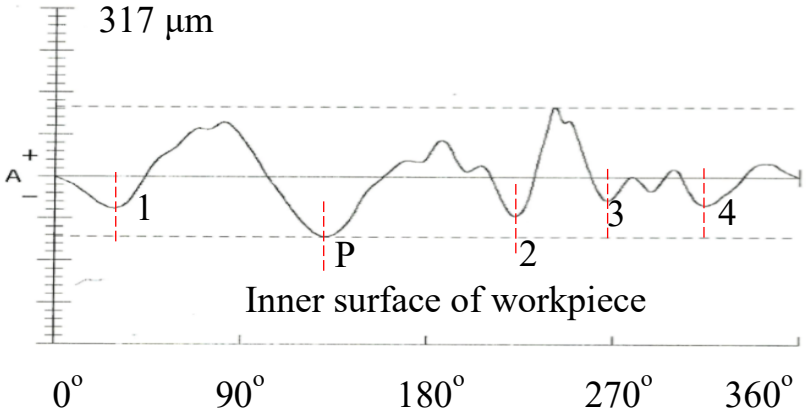

Before finishing

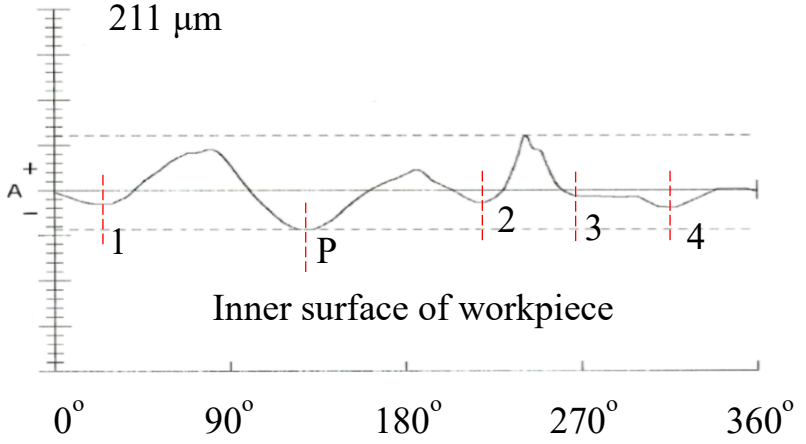

After finishing

(a) Experiment A

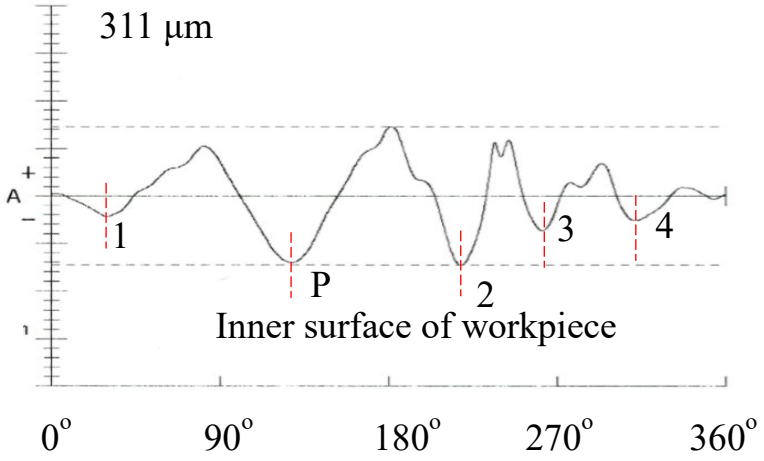

Before finishing

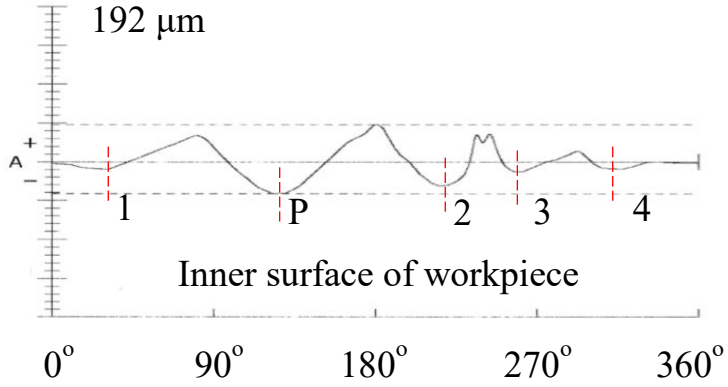

After finishing

(b) Experiment B

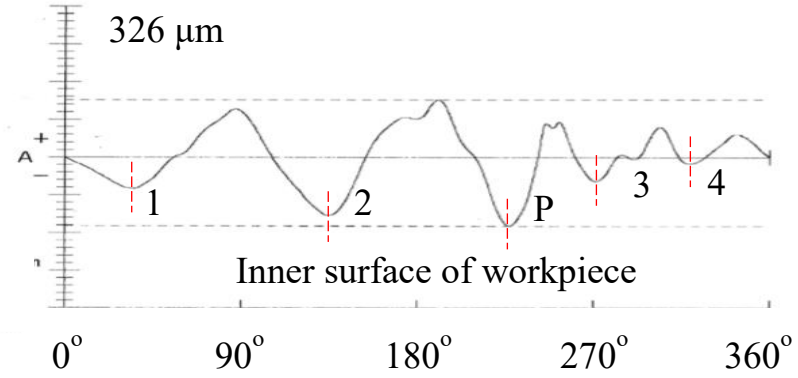

Before finishing

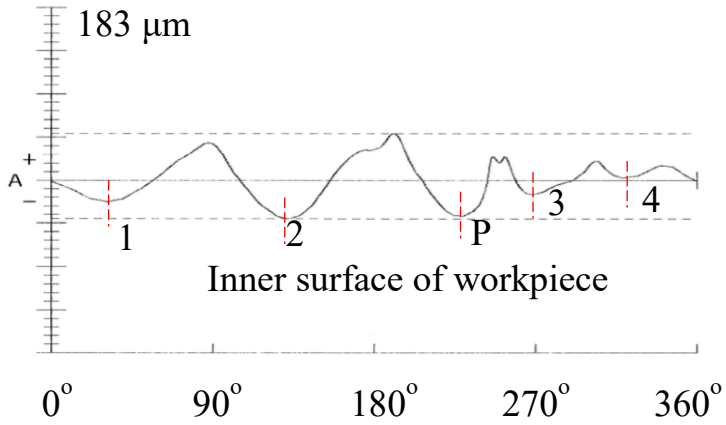

After finishing

(c) Experiment C

Fig.5.13 Diagrams of straight-line expansion of roundness curve before and after finishing

5.5 Conclusions

This chapter investigates the mechanism of roundness improvement by the internal magnetic abrasive finishing process using magnetic machining tool and the experiments were carried out on nonferromagnetic SUS 304 stainless steel tube. The main conclusions are summarized as follows:

The roundness improvement was discussed through the different distribution of magnetic particles on magnetic machining tool. In this process, the pressure exerted by some magnetic particles on the magnetic force of the magnetic machining tool and the magnetic pole unit forms a fixed form of magnetic brush. Therefore, it is concluded that when the distribution of magnetic particles on the magnetic processing tool can form a fixed magnetic brush with larger arc length in contact with the inner surface of tube, it is beneficial to the roundness improvement.

Chapter VI Industrial application of internal magnetic abrasive finishing process

6.1 Introduction

Furthermore, with the development of aerospace technology, higher precision products are also required. Therefore, in this chapter, we mainly discuss the realization of ultra-precision finishing of nonferromagnetic tube (SUS304 stainless steel tube) by the magnetic abrasive finishing process using a magnetic machining tool.

6.2 Ultra-precision finishing of SUS304 stainless steel tube

6.2.1 Experimental conditions and method

In this study, by adjusting the distance between the magnetic processing tool and the permanent magnet of the magnetic pole unit, the SUS304 stainless steel tube with a thickness of 10 mm was used as workpiece. The experimental conditions as shown in Table 6.1. The experiment includes three processes: rough machining, semi-precision finishing, and precision finishing. The magnetic particles and abrasive materials used in the rough machining are KMX1000 ~ 1680 μm and WA # 400 (average particle size is about 6 μm), respectively, while the magnetic particles and abrasive materials used from the second-stage to the seventh-stage are KMX1000 ~ 1680 μm and WA #1200 (average particle size is about 18 μm) respectively. Because the roundness improvement is affected by the material removal

(the increase of the radius of the inner surface of the workpiece), the initial weight of the tube is 2076.9 g, the weight of the tube after the first-stage machining is 2075.2 g, and the weight of the tube after the second-stage finishing is 2073.0 g, then the material removal of the first-stage machining is 1.7 g, and the material removal of the second-stage finishing is 2.2 g, so it can be seen that in the case of using magnetic particles with the same particle size, when using abrasive materials with small particle size, the material removal is relatively large, and the material removal of the eighth-stage finishing is 1.1 g. Therefore, in order to improve the roundness, KMX1000 ~ 1680 μm is used for magnetic particles in the second-stage finishing to seventh-stage finishing and use abrasive material WA # 1200 with smaller particle size. At the same time, it can also be concluded that under the condition of the same particle size of magnetic particles, using abrasive particles with smaller particle size can obtain larger material removal. In the case of the same particle size of abrasive particles, using magnetic particles with larger particle size can obtain larger material removal.

The reason for using abrasive materials with smaller particle size in the second-stage machining to seventh-stage finishing is to obtain large material removal, which not only affects the roundness improvement, but also affects the roughness of the inner surface of the tube. Because the initial inner surface of the SUS304 stainless steel tube used in this experiment is relatively rough, Fig.6.1 shows the roughness measurement curve before and after the first-stage machining of the tube.

Table 6.1 Experimental conditions

Workpiece		SUS304 stainless steel tube: Ø89.1×79.1×200 mm, Rotational speed:88 rpm	
Magnetic machining tool		Magnet: Nd-Fe-B permanent magnet, Yoke: SS400 steel, Molding material: Polymer	
Magnetic pole unit		Magnet: Ferrite permanent magnet 50×35×26 mm, Yoke: SS400 steel, Rotational speed of pole:254 rpm Reciprocating speed: 38 mm/s	
Process (The concentration of the abrasive slurry:7.5%wt, SCP-23, 40 mL)	Rough machining	1st-stage (15 min)	Magnet particles: KMX1000 ~ 1680 μm,12×2 g, Abrasive particles: WA #400,3.2 g
	Semi-precision finishing	2nd-stage ~ 7th-stage (15×6 min)	Magnet particles: KMX 1000 ~ 1680 μm, Abrasive particles: WA #1200,3.2 g
	Precision finishing	8th-stage (15 min)	Magnet particles: Electrolytic iron particles (510 μm in mean dia.), Abrasive particles: WA #1200,3.2 g
		9th-stage (15 min)	Magnet particles: Electrolytic iron particles (330 μm in mean dia.), Abrasive particles: WA #2000,3.2 g
		10th-stage (15 min)	Magnet particles: Electrolytic iron particles (149 μm in mean dia.), Abrasive particles: WA #4000,3.2 g
		11th-stage (15 min)	Magnet particles: Electrolytic iron particles (75 μm in mean dia.), Abrasive particles: WA #8000,3.2 g

Ra：4.958 μm　　Ra：0.720 μm

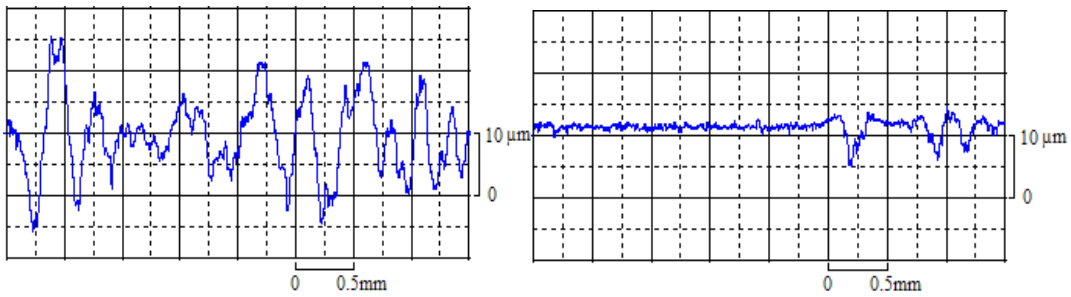

(a) Place a

Ra：5.120 μm　　Ra：2.041 μm

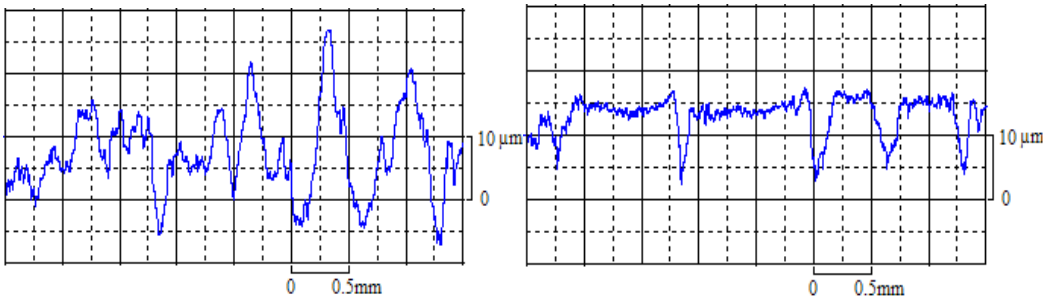

(b) Place b

Ra：4.584 μm　　Ra：0.289 μm

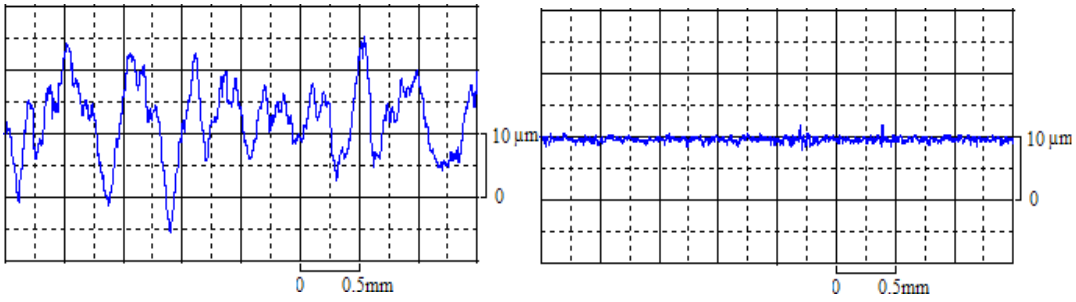

(c) Place c

Fig.6.1 The surface roughness curve of before finishing and after 1^{th}-stage finishing

Roughness measurement be carried out at place a, place b and place c after each stage of processing. As shown in Fig.6.2, the roughness at place a, place b and place c before processing are basically the same. However, by comparing the roughness measurement curves at a, b and c after the first-stage machining, it can be seen that the inner surface of the tube at this time is not uniformly processed, so it is necessary to remove the uneven parts through large material removal. At this time, the inner surface of the tube is basically processed evenly, and the removal of uneven points is also to better improve the roundness. Therefore, KMX1000~1680 μm and WA #1200 are used for magnetic particles and abrasive particles respectively in the second-stage finishing to seventh-stage finishing.

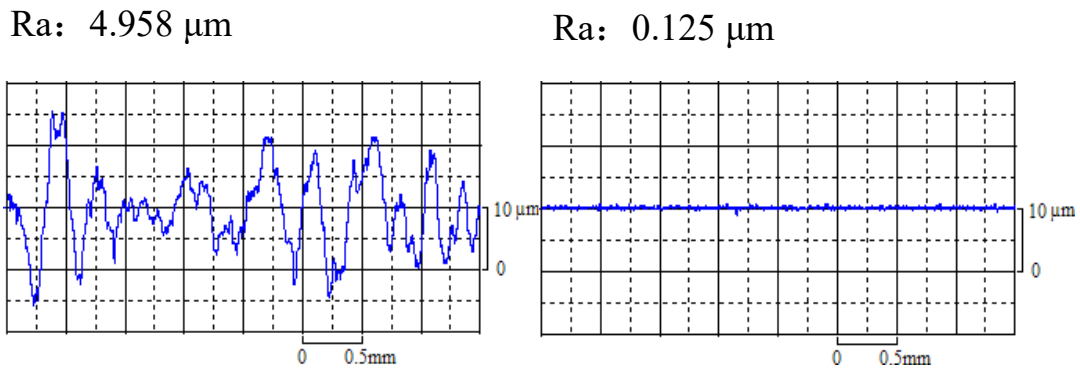

(a) Place a

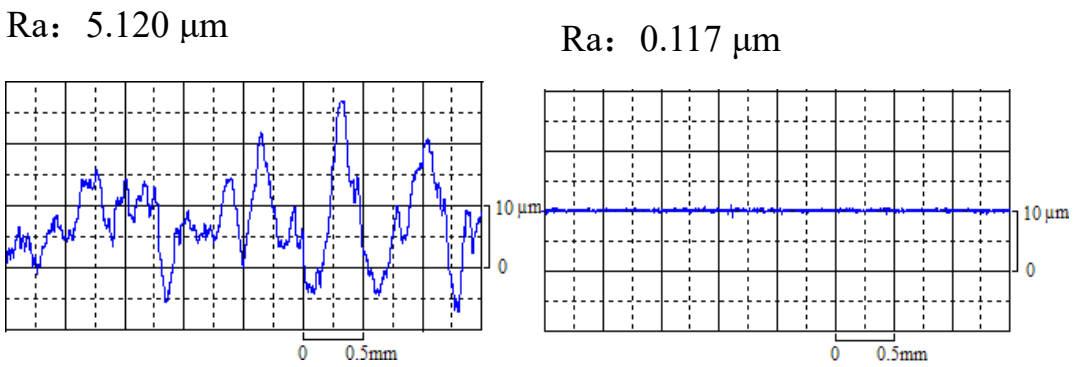

(b) Place b

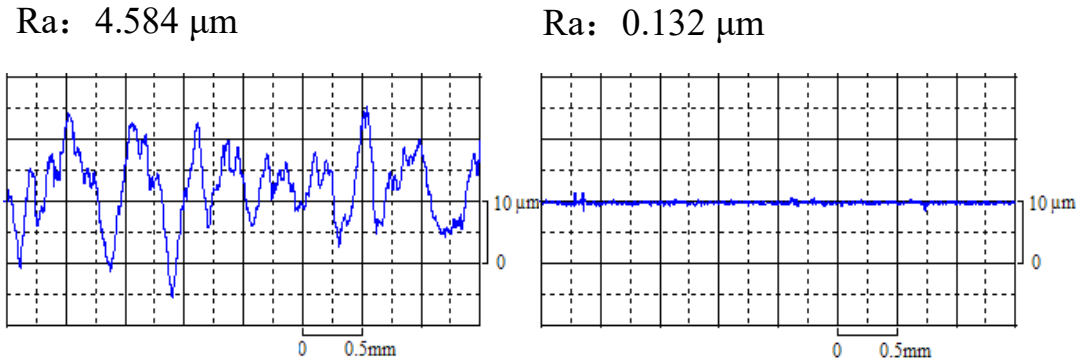

(c) Place c

Fig.6.2 The surface roughness curve of before finishing and after 7th-stage finishing

6.2.2 Experimental results and discussion

Fig.6.3 shows the curve of roughness change with time. The inner surface roughness Ra of the tube is improved from 4.887 μm to 0.011 μm. Fig.6.4 shows the changes of material removal with time, and the final material removal is 17.1 g.

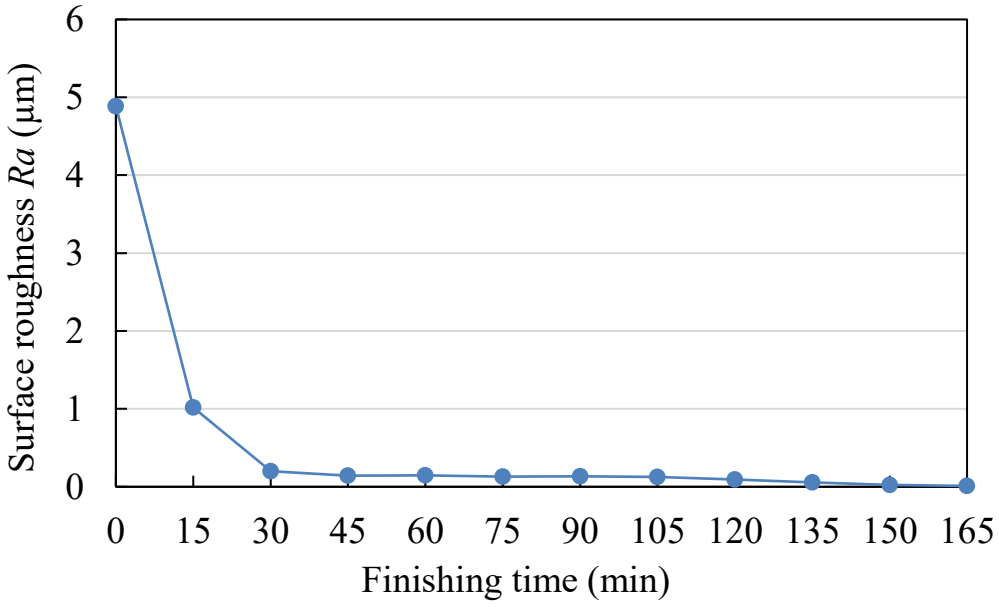

Fig.6.3 Changes in surface roughness with finishing time

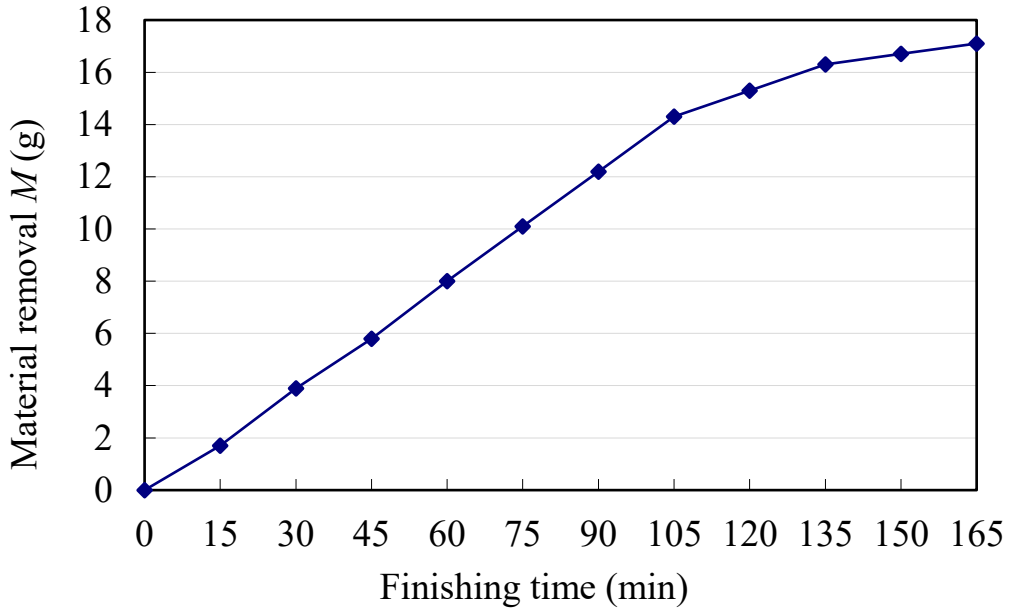

Fig.6.4 Changes in material removal with finishing time

It can be seen from Fig.6.3 and Fig.6.4 that although the material removal is constantly changing and increasing during the second-stage machining to seventh-stage machining, the roughness does not change much, and basically remains at the same value. The curve of the roundness improvement from the second-stage machining to seventh-stage machining is basically straight line. Therefore, it can be concluded that the material removal is constantly changing under the condition that the particle size of magnetic particles and abrasive materials is unchanged, that is, the roughness of the tube is related to the particle size of magnetic particles and abrasive materials.

Fig.6.5 shows the photos of the inner surface of the tube under the SEM (scanning electron microscope) before and after finishing.

Ra：4.887 μm

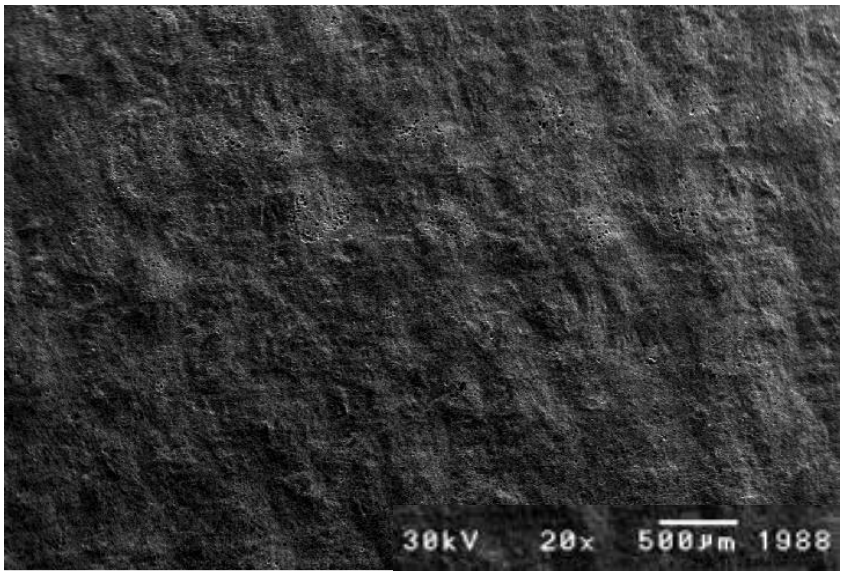

(a) Before finishing

Ra：0.011 μm

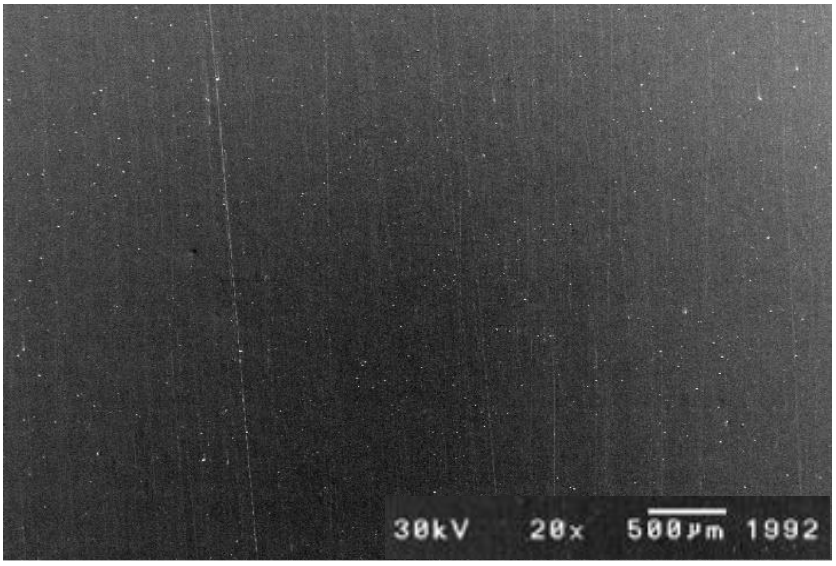

(b) After finishing

Fig.6.5 The SEM photos of before finishing and after finishing

As shown in Fig.6.6, the roundness of the tube is improved from 206 μm to 13 μm. It can be seen that this method is effective for the roundness improvement of the inner surface of the tube.

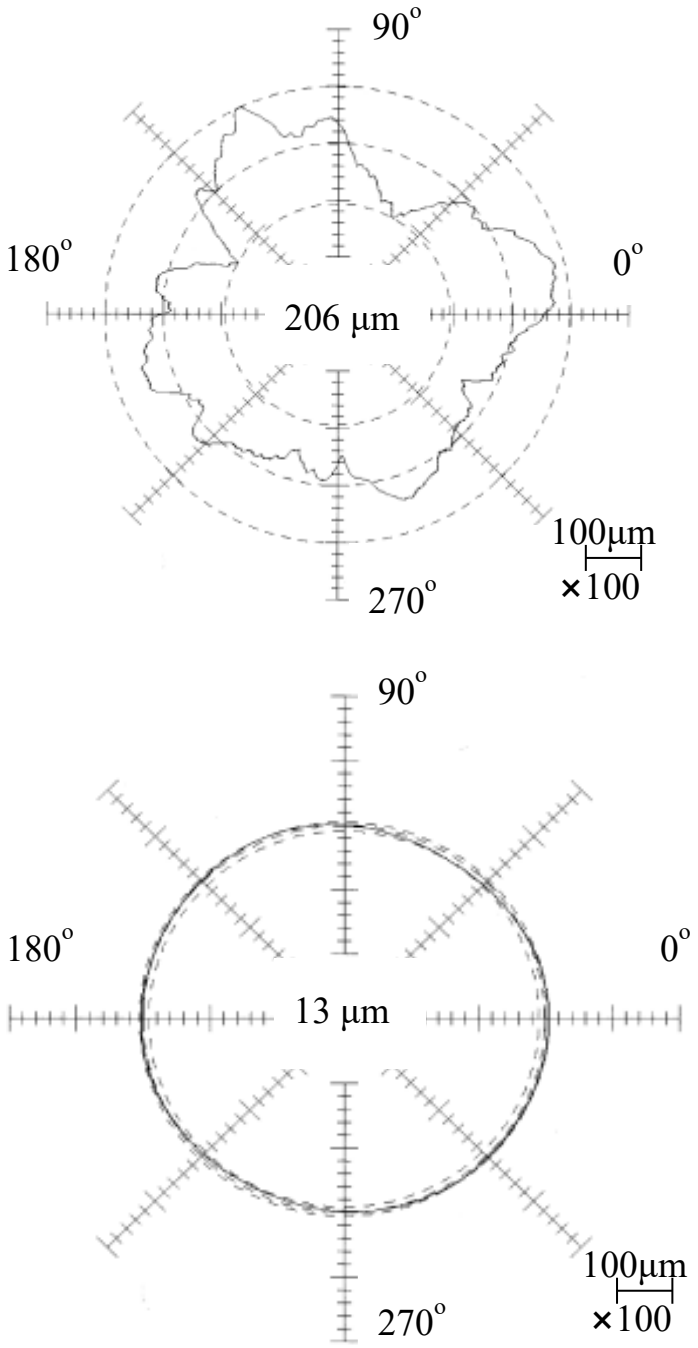

Fig.6.6 Roundness profiles of the internal surface of the tube before and after finishing

6.3 Conclusions

In this chapter, mainly investigating the industrial applicability of the inner surface magnetic abrasive finishing process using a magnetic machining tool, and conducted detailed verification experiments. By adjusting the distance between the magnetic processing tool and the permanent magnet of the magnetic pole unit, the SUS304 stainless steel tube with a thickness of 10 mm was used as the workpiece. Rough machining, semi-precision finishing, and precision finishing process were performed by selecting the size of the magnetic particles and abrasive particles. The inner surface roughness of SUS304 stainless steel tube can be improved from Ra 4.887 μm to Ra 0.011 μm and the roundness is improved from 206 μm to 13 μm by using three processes of rough machining, semi-precision finishing and precision finishing. It is hope for industrial application by this process.

Chapter VII Conclusions

Transport gas piping systems and clean gas cylinders used in semiconductor manufacturing and aerospace-related industries that required high inner surface accuracy to prevent the adhesion of contaminants. The magnetic field-assisted finishing process has been proposed for finishing high precision inner surfaces that are difficult to finish with ordinary tools and labor. Utilizing the penetrability of magnetic field lines, the application of magnetic force has great advantages for the finishing of inner surfaces.

In the previous study, the magnetic force generated by the magnetic particles and magnetic poles was used as the finishing force. It is effective to finish the tube with the thickness is less than 5 mm. But when the thickness of the tube is 5 mm or more, it is unable to finish due to insufficient magnetic force (finishing force). In order to increase the finishing force, the process using a magnetic machining tool has been proposed. It has been confirmed that the magnetic force can be enhanced several tens of times higher than that of the process using magnetic particles, and this process can finish inner surface of the tube with the thickness is 5~30 mm. And it also clarified that roundness can be improved while improving roughness.

However, the mechanism of roundness improvement is unclear, so this study mainly discussing the roundness improvement mechanism of the inner surface of a tube by magnetic abrasive finishing process.

Chapter 1

In chapter 1, the research background and some research on internal

magnetic abrasive finishing process are introduced. In addition, the research purpose of this thesis is explained and the content of each chapter is summarized.

Chapter 2

In chapter 2, the processing principle and experimental setup of the internal magnetic abrasive finishing using magnetic machining tool are explained. Moreover, in order to clarify the force that affects the roundness improvement, the finishing force is analyzed. In addition, in this process, the magnetic machining tool also rotates in the opposite direction to the workpiece, so its force is analyzed.

Chapter 3

In chapter 3, mainly studies the roundness improvement theoretically and discusses the factors influencing the roundness improvement of internal surfaces. Firstly, the roundness curve expression is derived using the principle of roundness measurement by the assumed center method, and the expression of roundness curve expanded by the Fourier series was obtained. Secondly, the process of roundness change is analyzed, and then the factors influencing the roundness improvement are discussed. Finally, the experiments were carried out on SUS304 stainless steel tube and by setting the distance between the magnetic machining tool and the magnetic pole of finishing unit, the thickness of the tube is equivalent to 10 mm, 20 mm and 30 mm, respectively.

Chapter 4

In chapter 4, mainly discussing the influence of finishing characteristics on internal surface roundness improvement. Firstly, the internal roundness improvement of thick SUS304 stainless steel tube was discussed through the dynamic and trajectory analysis. Because the roundness improvement is related to the material removal, and the material removal is related to the finishing force during finishing. The finishing characteristics affecting the internal roundness improvement of thick tube is investigated by discussing the reciprocating velocity of magnetic pole unit. Secondly, in order to discuss the influence of different structures of magnetic particles on roundness improvement, comparative experiments were carried out. Each experiment carried out five stages of processing, and in the first-stage, two different kinds of magnetic particles were used, the electrolytic iron particles (1680 μm in mean dia.) and the KMX magnetic particles (1000 ~ 1680 μm in mean dia.), respectively. Furthermore, in order to further clarify the influence of finishing characteristics on roundness improvement in this process, due to the magnetic machining tool and tube rotate in opposite directions, so discussing the influence of rotational speed of the magnetic machining tool by analyzing the finishing force and the influence of rotational speed of the tube on roundness improvement. And the influence of rotational speed is discussed comprehensively.

Chapter 5

In chapter 5, according to the distribution of magnetic force lines, the magnetic machining tool is divided into three areas, which are left area, middle area and right area, and the magnetic particles on the left area and right area of the magnetic machining tool form magnetic brushes in the direction of the magnetic force line before finishing. And after finishing,

the pressure exerted by some magnetic particles on the magnetic force of the magnetic machining tool and the magnetic pole unit forms a fixed magnetic brush, so mainly discusses the influence of the circumferential length of fixed magnetic brush on roundness improvement.

Chapter 6

In chapter 6, investigating the industrial applicability of the inner surface magnetic abrasive finishing process using a magnetic machining tool, and conducted detailed verification experiments. By adjusting the distance between the magnetic processing tool and the permanent magnet of the magnetic pole unit, the SUS304 stainless steel tube with a thickness of 10mm was used as the workpiece. Rough machining, semi-precision finishing, and precision finishing process were performed by selecting the size of the magnetic particles and abrasive particles, and the initial surface roughness of Ra 4.9 μm can be finished to a mirror surface of Ra 0.01 μm. And the roundness can be improved from 206 μm to 13 μm. It is hope for industrial application by this process.

Chapter 7

In chapter 7, the main conclusions of this research are summarized.

Reference

Chapter 1

[101] Zou YH, Shinmura T, Wang F (2009) Study on a magnetic deburring method by the application of the plane magnetic abrasive machining process. Adv. Mater. Res. 76–78, 276–281.

[102] Jain VK (2009) Magnetic field assisted abrasive based micro-/nano-finishing. J. Mater. Process. Technol. 209, 6022–6038.

[103] Yamaguchi H, Shinmura T (2004) Internal finishing process for alumina ceramic components by a magnetic field assisted fin-ishing process. Precis. Eng. 28, 135–142.

[104] Shinmura T, Takazawa K, Hatano E, Matsunaga M, Matsuo T (1990) Study on magnetic abrasive finishing. Ann. CIRP 39, 325–328.

[105] Shinmura T, Yamaguchi H (1995) Study on a new internal finishing process by the application of magnetic abrasive machining: Internal finishing of stainless steel tube and clean gas bomb. JSME Int. J. Ser. C 38, 798–804.

[106] Yamaguchi H, Shinmura T, Kobayashi A (2001) Development of an internal magnetic abrasive finishing process for nonferromagnetic complex shaped tubes. JSME Int. J. Ser. C 44, 275–281.

[107] Kang J, Yamaguchi H (2012) Internal finishing of capillary tubes by magnetic abrasive finishing using a multiple pole-tip sys-tem. Precis. Eng. 36, 510–516.

[108] Kang J, George A, Yamaguchi H (2012) High-speed internal finishing of capillary tubes by magnetic abrasive finishing. Proce-dia CIRP 1, 414–418.

[109] Jha S, Jain VK (2004) Design and development of the

magnetorheological abrasive flow finishing (MRAFF) process. Int. J. Mach. Tools Manuf. 44, 1019–1029.

[110] Jha S, Jain VK, Komanduri R (2007) Effect of extrusion pressure and number of finishing cycles on surface roughness in magnetorheological abrasive flow finishing (MRAFF) process. Int. J. Adv. Manuf. Technol. 33, 725–729.

[111] Das M, Jain VK, Ghoshdastidar PS (2007) Analysis of magnetorheological abrasive flow finishing (MRAFF) process. Int. J. Adv. Manuf. Technol. 38, 613–621.

[112] Kim J (2003) Polishing of ultra-clean inner surfaces using magnetic force. Int. J. Adv. Manuf. Technol. 21, 91–97.

[113] Kim J, Choi M (1995) Stochastic approach to experimental analysis of cylindrical lapping process. Int. J. Mach. Tools Manuf. 35, 51–59.

[114] Chen KY, Tu TY, Fan YH, Wang AC, Fu PK (2021) Study on the polishing characteristics of the rotating cylinder-based magnetic gel abrasive finishing. Processes 9, 1794.

[115] Cheng KC, Chen KY, Tsui HP, Wang AC (2021) Characteristics of the polishing effects for the stainless tubes in magnetic finishing with gel abrasive. Processes. 9, 1561.

[116] Zou YH, Shinmura T (2004) A study on the magnetic field assisted machining process for internal finishing using a magnetic machining jig. Key Eng. Mater. 257–258, 505–510.

[117] Muhamad MR, Zou YH, Sugiyama H (2015) Development of a new internal finishing of tube by magnetic abrasive finishing process combined with electrochemical machining. Int. J. Mech. Eng. Appl. 3, 22–29.

[118] González H, Calleja A, Pereira O, Ortega N, López de Lacalle LN, Barton M (2018) Super abrasive machining of integral rotary components using grinding flank tools. Metals 8, 24.

[119] Rodriguez A, López de Lacalle LN, Pereira1 O, Fernandez A, Ayesta

I (2020) Isotropic finishing of austempered iron casting cylindrical parts by roller burnishing. Int. J. Adv. Manuf. Technol. 110, 753–761.

[120] Shinmura T, Takazawa K, Hatano E (1990) Study on Magnetic Abrasive Process. Annals of the CIRP 39/1, 325.

[121] Fox M, Agrawal K, Shinmura T, Komanduri R (1994) Magnetic Abrasive Finishing of Rollers. Annals of the CIRP 43/1,181.

[122] Yamaguchi H, Shinmura T (2000) Study of an internal magnetic abrasive finishing using a pole rotation system: Discussion of the characteristic abrasive behavior. Precis. Eng. 24, 237–244.

[123] Zou YH, Shinmura T (2007) Mechanism of a magnetic field assisted finishing process using a magnetic machining jig. Key Eng. Mater. 339, 106–113.

[124] Zou YH, Shinmura T (2002) Development of magnetic field assisted machining process using magnetic machining jig. JSME Int. J. Ser. C 68, 233–239. (In Japanese)

Chapter 3

[301] Yamaguchi H, Shinmura T (2000) Study of an internal magnetic abrasive finishing using a pole rotation system: Discussion of the characteristic abrasive behavior. Precis. Eng. 24, 237–244.

[302] Zou YH, Shinmura T (2007) Mechanism of a magnetic field assisted finishing process using a magnetic machining jig. Key Eng. Mater. 339, 106–113.

[303] Zou YH, Shinmura T (2002) Development of magnetic field assisted machining process using magnetic machining jig. JSME Int. J. Ser. C 68, 233–239. (In Japanese)

[304] Nakata K (1972) Engineering Analysis: A Mathematical Approach for Engineers, 1st ed.; Ohm Press: Saitama, Japan, 79–84.

[305] Shinmura T, Takazawa K, Hatano E (1986) Study on magnetic abrasive finishing: Rounding condition and its confirmation by experiment. Bull. Jpn. Soc. Precis. Eng. 52, 1598–1603. (In Japanese)
[306] Shinmura T, Aizawa T (1989) Study on Internal Finishing of a Non-ferromagnetic Tubing by Magnetic Abrasive Machining Process. Bull. Jpn. Soc. Precis. Eng. 23, 37–41. (In Japanese)
[307] Nakano K (1992) Precision Shape Measurement Practice: Interpretation of Geometric Tolerances and Measurement of Geometric Deviations, 1st ed.; Kaibundo Publishing Co., Ltd.: Tokyo, Japan, 61–63.
[308] Yamaguchi H, Shinmura T (1996) Study on a new internal finishing process by the application of magnetic abrasive machining: Discussion of the roundness. Bull. Jpn. Soc. Precis. Eng. 62, 1617–1621. (In Japanese)

Chapter 4

[401] Zou YH, Shinmura T (2005) A New Internal Precise Finishing Process Using Magnetic Machining Jig，Bull. Jpn. Soc. Precis. Eng. 34, 1255–1256. (In Japanese)
[402] Shinmura T, Zou YH (2004) Study on Magnetic Field Assisted Machining Process Using Magnetic Machining Jig: Discussion on the Roundness of Inner Surface of Tubing，Bull. Jpn. Soc. Precis. Eng. 33, 649–650. (In Japanese)
[403] Zou YH, Shinmura T (2005) Study on Internal Magnetic Field Assisted Finishing Process Using a Magnetic Machining Jig. Key Engineering Materials 291-292, 281-286.
[404] Zou YH, Liu JN, Shinmura T (2011) Study on Internal Magnetic Field Assisted Finishing Process Using a Magnetic Machining Jig for Thick Non-Ferromagnetic Tube. Advanced Materials Research 325, 530-

535.

[405] Liu JN, Zou YH (2020) Discussion on Roundness of Non-Ferromagnetic Tube by Interior Magnetic Abrasive Finishing Using a Magnetic Machining Jig. Materials Science Forum 1018,105-110.

Chapter 5

[501] Shinmura T, Aizawa T (1989) Study on magnetic abrasive finishing process development of plane finishing apparatus using a stationary type electromagnet. Bull Jpn Soc Precis Eng 23(3), 236–239. (in Japanese)

[502] Shinmura T, Takazawa K, Hatano E, Aizawa T (1986) Study on magnetic-abrasive finishing (2nd report) finishing characteristics. J Jpn Soc Precis Eng 52 (10), 1761–1767. (in Japanese)

[503] Shinmura T, Aizawa T (1988) Development of plane magnetic abrasive finishing apparatus and its finishing performance (2nd report) finishing apparatus using a stationary type electromagnet. J Jpn Soc Precis Eng 54(5), 928–933. (in Japanese)

[504] Shinmura T, Hatano E, Takazawa K (1986) The development of magnetic-abrasive finishing and its equipment by applying a rotating magnetic field. Bulletin of JSME 29(258), 4437-4443.

[505] Yamaguchi H, Shinmura T, Kobayashi A (1986) Development of an internal magnetic abrasive finishing process for nonferromagnetic complex shaped tubes. JSME Int J Ser C 44, 275–281.

[506] Kang J, Yamaguchi H (2012) Internal finishing of capillary tubes by magnetic abrasive finishing using a multiple pole-tip system. Precis Eng 36, 510–516.

[507] Kang J, George A Yamaguchi H (2012) High-speed internal finishing of capillary tubes by magnetic abrasive finishing. Procedia CIRP 1, 414–418.

[508] Yin SH, Shinmura T (2012) A comparative study: Polishing characteristics and its mechanisms of three vibration modes in vibration-assisted magnetic abrasive polishing. Int J Mach Tool Manuf 44, 383–390.
[509] Yin SH, Shinmura T (2004) Vertical vibration-assisted magnetic abrasive finishing and deburring for magnesium alloy International Journal of Machine Tools Manufacture 44, 1297-1303.

List of main symbols

Symbols	Explanation
$\boldsymbol{F}_x$	The magnetic force generated by the magnetic machining tool and magnetic poles outside the tube in the direction of the equipotential line
$\boldsymbol{F}_y$	The magnetic attraction force generated by the magnetic machining tool and the magnetic poles outside the tube
$\boldsymbol{F}_c$	The centrifugal force generated by the rotation of the magnetic machining tool
$\boldsymbol{G}$	Gravity
$\boldsymbol{F}_f$	The frictional resistance generated during finishing
$\boldsymbol{F}$	Finishing force
$\boldsymbol{F}_n$	The normal component of finishing force
$\boldsymbol{F}_t$	The tangential component of finishing force
$\boldsymbol{F}_a$	The axial component of finishing force
$\boldsymbol{F}_{xy}$	Component of finishing force in the XOY plane
$\boldsymbol{F}_{xz}$	Component of finishing force in the XOZ plane
$\mathrm{A}_n, \mathrm{B}_m$	Amplitude
$\varphi_n,\ \beta_m$	Phase angle
$\Delta \mathrm{S}_0(\theta)$	The random variation of the rotation axis
$\varepsilon(\theta)$	The vibration amount
$\varepsilon_w(\theta)$	The vibration removal
$\Delta \mathrm{R}_\mathrm{N}(\theta)$	The roundness curve
P	The standard setting of finishing force
C_m	The processing quantity coefficient
K	The proportional coefficient between the finishing force and the change of roundness

L_N	The correction value of the reference circle (zero value)
L	The distance between the tube and the permanent magnet of the magnetic pole unit
D	The thickness of tube
$s(t)$	The trajectory
P	The pitch of the trajectory
$\boldsymbol{v}_r$	The tangential velocity of rotation
$\boldsymbol{v}_l$	The velocity of linear motion
$\boldsymbol{v}$	Velocity

Acknowledgement

I am grateful to those who have offered me encouragement and support over the past several years. It would be impossible to accomplish this work without the kindhearted help and full-hearted support of many people.

First and foremost, I would like to express my deepest gratitude to my advisor, Professor Yanhua Zou. His serious scientific attitude, rigorous academic spirit, and striving for perfection have deeply influenced and inspired me. In the process of my research, she gave me patient guidance and gave me many valuable suggestions, which made me learn a lot of valuable research experience and broaden my horizon.

I would like to express my heartfelt gratitude to Professor Yutaka Mabuchi, Associate Professor Ryunosuke Sato, Professor Yoshimasa Takayama and Associate Professor Atsushi Shirayori for their willingness to serve as members of my thesis defense committee.

The gratitude is also extended to some supports from Creative Department for Innovation (CDI) of Utsunomiya University and mechanical processing factories of Utsunomiya University for this research.

I also want to express my special gratitude to my husband (Mr. Youfa Gong), two daughters (Xianyue Gong and Tianjing Gong) and my parents. They are not only my family but also my best friends. Thanks to their support and encouragement, I can face every difficult moment with confidence to complete my study.

Last but not least, I also owe my sincere gratitude to my friends and classmates who give me their help and time in listening to me and helping me work out my problems when I meet difficulties in my thesis.

Contributed papers related to this study

Articles

1. Jiangnan Liu, Yanhua Zou, Discussion on Roundness of Non-Ferromagnetic Tube by Interior Magnetic Abrasive Finishing Using a Magnetic Machining Jig, Metal Materials Processes and Manufacturing, No.1018, pp.105-110, June, 2020.
2. Jiangnan Liu, Yanhua Zou, Study on Mechanism of Roundness Improvement by the Internal Magnetic Abrasive Finishing Process Using Magnetic Machining Tool, Machines, Vol.10, No.112, pp.1-15, February, 2022.
3. Jiangnan Liu, Yanhua Zou, Study on Elucidation of the Roundness Improvement Mechanism of the Internal Magnetic Abrasive Finishing Process Using a Magnetic Machining Tool, Journal of Manufacturing and Materials Processing, Vol.7, No.49, pp.1-22, February, 2023.

International conference

1. Jiangnan Liu, Yanhua Zou, Investigation of the Finishing Characteristics of Internal Magnetic Abrasive Finishing Process Using a Magnetic Machining Tool, The 5th International Conference on Surface and Interface Fabrication Technologies (ICSIF), Tokyo, 17 March, 2023.

Domestic conference

1. 劉 江楠，鄒 艶華，磁石工具を用いた内面磁気研磨法に関する研究（真円度改善の検討），2020 年度精密工学会秋季大会学術講演会講演論文集, pp.174-175, 9 月, 2020.

2. 劉 江楠，鄒 艷華，磁石工具を用いた内面磁気研磨法に関する研究（厚肉円管の形状精度の改善），日本機械学会 2021 年度茨城講演会講演論文集, No.210-2, pp.1-4, 8 月, 2021.

Awards

1. Best Paper Award, Awarded on the 3rd International Conference on Metal Material Processes and Manufacturing (ICMMPM2020), 2020.